MOLECULAR PHENOTYPE OF RIGHT VENTRICULAR HYPERTROPHY IN HUMAN TETRALOGY OF FALLOT

T.H.F. PETERS

Molecular phenotype of right ventricular hypertrophy in human tetralogy of Fallot.

Thesis, Erasmus Medical Center, Rotterdam.

ISBN 90-6734-038-3

Printed by Optima Grafische Communicatie, Rotterdam

MOLECULAR PHENOTYPE OF RIGHT VENTRICULAR HYPERTROPHY IN HUMAN TETRALOGY OF FALLOT

MOLECULAIR FENOTYPE VAN RECHTER VENTRIKEL HYPERTROFIE IN TETRALOGIE VAN FALLOT BIJ DE MENS

Proefschrift

ter verkrijging van de graad van doctor
aan de Erasmus Universiteit Rotterdam
op gezag van de Rector Magnificus
Prof. dr. ir. J.H. van Bemmel
en volgens het besluit van het College voor Promoties

De openbare verdediging zal plaatsvinden op
woensdag 26 november om 13.45 uur

door

Theodorus Hendrikus Franciscus Peters
geboren te Sambeek

Promotiecommissie

Promotoren:	Prof. dr. A.J.J.C. Bogers
	Prof. dr. P.R. Saxena
Overige leden:	Prof. dr. J.M.J. Lamers
	Prof. dr. R.E. Poelmann
	Prof. dr. W.A. Helbing
Co-promotor:	Dr. H.S. Sharma

The study described in this thesis was supported by a grant of the Netherlands Heart Foundation (NHS 96.082).
Financial support by the Netherlands Heart Foundation for the publication of this thesis is gratefully acknowledged.

Further financial support by Stichting Biomedical Engineering, Jacques H. de Jong Stichting and J.E. Jurriaanse Stichting for the publication of this thesis is gratefully acknowledged.

Voor mijn ouders

Table of Contents

Chapter 1

General introduction

Based on:

- *Bogers AJJC, Peters THF, Hokken RB, Saxena PR and Sharma HS. Myocardial phenotype of right ventricular hypertrophy in human tetralogy of Fallot. In: Imai Y, Momma K. eds: Proceedings of 2nd World Congress of PCCS 1998; 746-749: Futura, Armonk, New York, USA.*
- *Bogers AJJC, Peters THF, Jong de PL. Tetralogy of Fallot, surgical aspects. In: Bartelings MM, Wenink ACG eds: Congenital Heart Disease. suppl.: Boerhaave Committee for Postgraduate Medical Education. 1999; 59-65: Leiden, The Netherlands.*
- *Peters THF, Klompe L, Bogers AJJC and Sharma HS. Molecular phenotype of the developing heart with a congenital anomaly. In: Ostadal B, Nagano M and Dhalla NS eds.: Cardiac Development 2002; 195-212: Kluwer Academic Publishers, Boston, USA.*

1.1 Introduction

Tetralogy of Fallot

In 1888 the French physician Etienne-Louis Arthur Fallot described a "tetrad" of congenital anatomical defects in a heart, which are now collectively referred to as tetralogy of Fallot (TF). TF is characterized by a (sub)valvular pulmonary stenosis, a ventricular septal defect (VSD), dextroposition of the aorta (overriding the VSD) and concomitant right ventricular hypertrophy (RVH)[1,2] (Fig. 1.1). The right ventricular (RV) outflowtract obstruction can be more or less severe, depending on the degree of malformation as well as the extent of RVH. With an incidence of 1 per 2000 new-borns TF is a frequent cyanotic congenital heart malformation.

Anatomy

The pulmonary stenosis in TF originates from the anterior displacement of the outlet septum resulting in narrowing of the sub-pulmonary outlet, often accompanied by stenosis of the pulmonary valve and hypoplasia of both the pulmonary annulus and pulmonary trunk[3]. The pulmonary valve itself is often abnormal, dysplastic and immobile, causing an additional obstruction to pulmonary blood flow. The pulmonary valve may show fused valve leaflets giving dome-shaped, bicuspid, unicuspid, imperforate or atretic valves, with in some patients rudimentary or complete absent leaflets, with only a ridge of dysplastic valve tissue[4]. In more extreme forms, the aorta will be exclusively connected to the RV, representing TF with complete double outlet ventriculo-arterial connection[4,5].

In approximately 20-25% of the cases with TF the pulmonary stenosis is complete, the obliteration of the RV outflow tract results in pulmonary atresia with VSD (PA-VSD)[6]. This complicated form of TF is characterized by the extremely underdeveloped RV infundibulum with marked anterior and leftward displacement of the infundibular septum often fused with the anterior RV wall. Together with severe hypoplasia or absence of parts of the central pulmonary arteries, these patients depend on a patent ductus arteriosus or the presence of multiple systemic pulmonary collateral arteries (SPCAs) for their pulmonary circulation and survival[4,7].

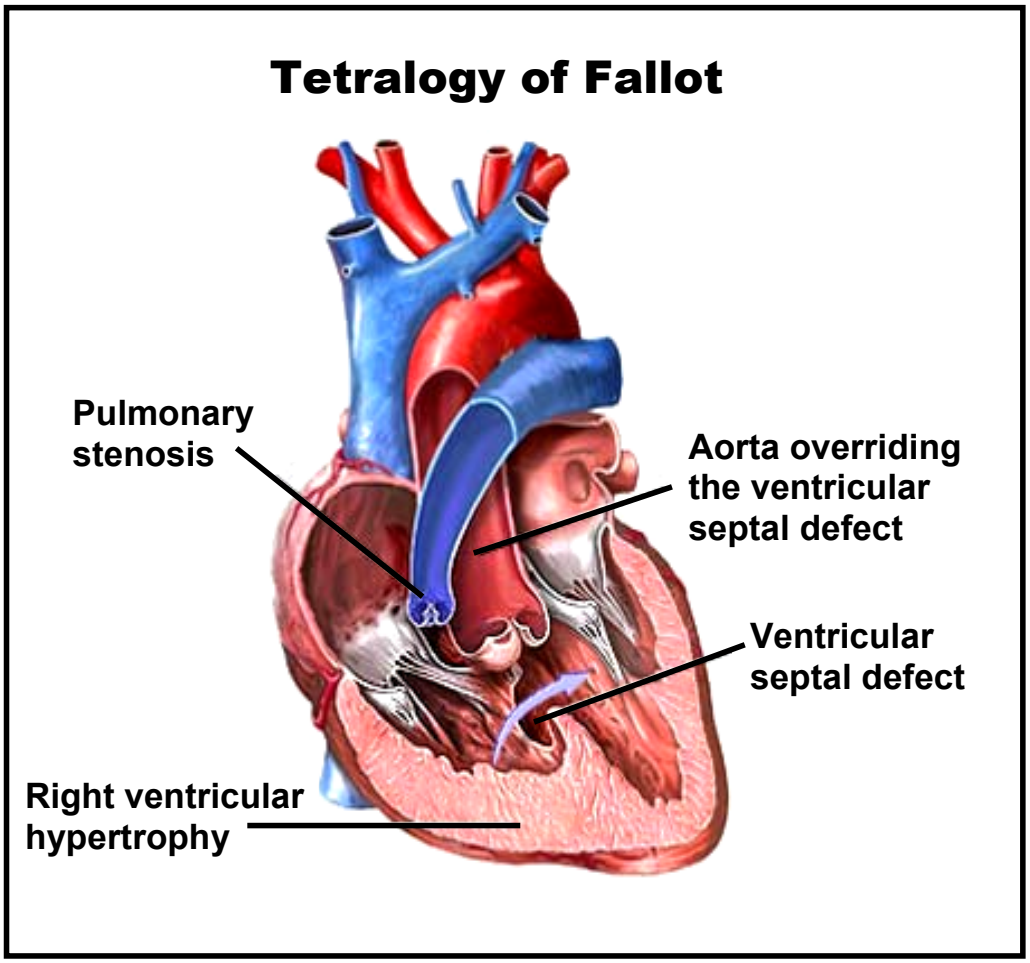

Figure 1.1. Diagrammatic representation of human tetralogy of Fallot
(*Modified from Stephenson et al.*[10])

The SPCAs are large and distinct arteries, highly variable in number that usually arise from the aortic arch or the subclavian, carotid or even the coronary arteries[8].

Pathophysiology

The RV outflow tract obstruction and the defect in the inter-ventricular septum lead to an equal systolic pressure in both ventricles and aorta, causing a varying degree of right to left shunting of the blood. Babies born with this congenital heart anomaly are usually referred to as blue babies as they have a diminished pulmonary flow and consequently insufficient blood oxygenation leading to hypoxemia, cyanosis and sometimes cyanotic spells[7,9]. Clinical findings associated with severe, longstanding cyanosis include polycythemia (abnormal increase of red blood cells), difficulty in feeding, failure to gain weight, retarded growth and physical development, dyspnoea

on exertion, and some times cerebral thrombosis[7,9]. Nowadays clubbing of the fingers and toes, pulmonary haemorrhage, stroke and infections of the brain and severe hypoxic spells rarely develop[10].

In response to the increased pressure overload caused by pulmonary stenosis in combination with the VSD, the RV undergoes hypertrophic growth. This is an adaptive process wherein an increase in RV mass caused by expanding myocytes attempts to normalize the wall stress. This adaptive response can further lead to a proportionate increase in coronary flow and growth of the coronary vasculature and to structural changes in the myocardial architecture (myocardial remodeling)[11-13].

1.2 Surgery of tetralogy of Fallot

Surgical strategies and timing

Without surgical treatment, TF ultimately results in cyanotic complications and cardiac failure. Approximately 30% of neonates with TF die within the first year of life if untreated, 90 % of the children would die before the age of 20 years and only 3 % will reach the age of 40 years[7]. Nearly 70% of patients with TF require an operation during their first year of life because of hypoxic spells or persistent hypoxemia defined as resting arterial oxygen saturation less than 70%[2,14].

Generally the surgical approach involves primary repair in the first year of life by means of closing the VSD and relieving the RV outflow tract obstruction[2,15-17]. Surgical repair thus aims at preventing complications due to long standing RVH such as ventricular dysfunction and arrhythmia. Surgical treatment can be corrective in infants at a very young age, provided that the pulmonary arterial system is complete and well developed. If not, palliative surgery may improve the clinical situation and prepare for later correction[6].

The aim of early corrective surgery is to relieve the hypoxemia, to eliminate the stimulus for the adaptive RVH as well as preserving RV function and electrical stability of the myocardium[11,12] and to encourage the normal development of the pulmonary vasculature[17]. The surgical strategy of primary repair of TF early in life

has given excellent early and late results and compares favorably with two-stage approaches. There is increasing evidence that early repair of congenital heart anomalies minimizes secondary damage to vital organs, particularly of the heart itself, the lungs, and the brain[2,14]. Furthermore, by establishing early antegrade pulmonary blood flow, postnatal pulmonary angiogenesis and alveologenesis may also be enhanced[2]. Finally, by eliminating cyanosis as early as possible, the adverse effects of cyanosis on the central nervous system might also be reduced[2].

Encouraged by the results of primary repair for symptomatic infants with TF, there is a tendency to operate electively on asymptomatic young infants with this abnormality. Although age less than 3 months was in some reports a risk factor for death after repair, this risk has lately decreased in neonates[2,14]. In this regard, neonatal hearts have less ability to adapt to sudden increases in stroke volume and neonates are more susceptible to the adverse effect of cardiopulmonary bypass. It is likely that results of early repair of TF in neonates will soon parallel those obtained in infants beyond the first month of life. As a result of the developments in extracorporeal circulation, improved anaesthetic management of neonates and infants, and advances in postoperative care, both mortality and morbidity after early one-stage repair of TF have decreased dramatically, and such repair is currently favored in many centres[2,14].

Despite adequate primary corrective surgery, on long-term follow up some patients however, suffer from pulmonary regurgitation, causing RV failure due to volume-overload. For these patients further secondary corrective surgery later in life is performed by implanting a pulmonary allograft heart valve between the RV and the pulmonary artery.

The actuarial survival rate, including hospital deaths, after corrective surgery for TF is reported to be 89-93% at 15 years[2,10,14,18,19]. Midterm re-operations are reported in 2-19% of the patients[2,14,19,20], mostly because of residual pulmonary stenosis and to a lesser extent due to residual VSD. Re-operation for pulmonary valve replacement is reported to be performed in about 9% of the TF patients[19]. The actuarial freedom from re-operation was 85-89% at 15 years[2,14].

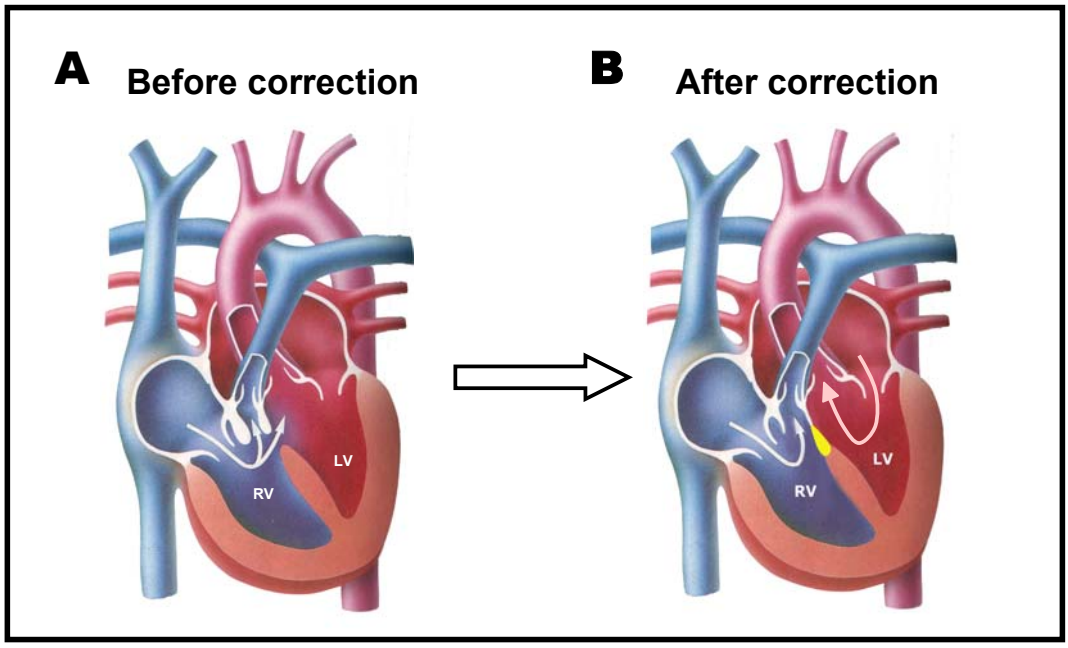

Figure 1.2. Blood flow before and after surgical correction of VSD and alleviation of pulmonary stenosis. (*Modified from Losekoot et al.*[18])

1.3 Myocardial hypertrophy

Growth of the heart

From the postnatal period to maturation the human heart undergoes a six-fold increase in heart mass[21]. The growth is most rapid in the first postnatal months, when the total number of myocytes double and remain relatively constant there after. In this period the myocyte diameter increases from 5 μm during infancy to 14-16 μm in adults[7,22]. Although the cardiac myocytes comprise one-third of the total cell number in the adult heart, they are responsible for 70 percent of the cardiac volume[21]. The growth of the heart becomes slower with the age, were the RV growth ceases at approximately 50 years of age while the left ventricle slowly continues to increases in volume[23]. The increase in myocardial mass is a result of myocyte hyperplasia (increase in cell number) and hypertrophy (increase in cell size). Myocyte hypertrophy can be either more eccentric, with longitudinal growth of the myocytes and normal wall thickness/dimension ratio, or concentric with increased wall thickness/heart dimension ratio[24]. The physiological increase in heart size by eccentric hypertrophy can be a result of isotonic athletic training like running, whereas isometric exercise such as weight

lifting stimulates concentric hypertrophy[24]. The diameter of long-distance runners can grow up to a 14% greater maximum diameter and 80% greater mass in the left ventricle[25]. The growth of the adult heart can be enhanced by the thyroid hormones, catecholamines and the renin-angiotensin system (RAS) hormones[23]. Under normal physiological conditions the adult human cardiac myocytes are believed to be terminally differentiated and have lost their ability to proliferate. Although some mild concentric hypertrophy may develop in the left ventricle as a consequence of age related decrease in sensibility of the peripheral vasculature[26]. However, under pathological conditions, such as pressure and volume overload and heart failure, there are some indications that cardiomyocytes re-initiate myocyte differentiation[23,27]. Under those circumstances the myocyte diameter can increase to more then 40 μm, depending on the degree of compensatory hypertrophy[7].

Pathological myocardial hypertrophy

In response to environmental and pathological conditions the heart may remodel to sustain the cardiac performance. Pathological myocardial cell hypertrophy is a physiological adaptive compensatory response, to increased haemodynamic overload, where the increase of cardiac mass serves to normalize wall stress and to permit normal cardiovascular function. Chronic haemodynamic overload will lead to cardiac remodeling with an increased risk of decompensated hypertrophy and finally result in cardiac failure[11,13,21,28]. The decompensated hypertrophy is a result from a number of intrinsic and extrinsic mechanisms of the cardiac myocytes, including changes in cardiomyocytes contractility, in regulatory-calcium-cycling and structural proteins together with apoptosis, necrosis, inadequate growth secondary to altered signal transduction pathways and extracellular matrix remodeling[29,30]. The myocyte dropout, due to myocardial cell death and hypertrophy, of the remaining viable myocytes has been proposed to account for impaired function and failure during ageing and hypertension[21,31-33]. At the same time apoptosis is also of importance in contributing to the remodeling of the cardiac chambers and vascular geometry in response to pathologic stimuli[34,35].

Pathological conditions such as ventricular outflow tract obstruction, systemic or pulmonary arterial hypertension or aortic coarctation, may cause pressure overload

and cardiac hypertrophy. This will increase the wall stress and result in concentric hypertrophy, with characteristic wall thickening. Pressure overload hypertrophy will activate early oncogenes and angiotensin II, mediated by the RAS-system and the responses of the cardiomyocytes to strech[23]. Volume overload, occurring during mitral or aortic regurgitation, however, may cause increased either diastolic wall stress or both systolic and diastolic wall stress and result in (left) ventricular hypertrophy[21].

Molecular markers of cardiac hypertrophy

Alterations in gene expression play an important role in the myocardial adaptation in response to increased work load[36]. A battery of genes including immediate early genes (like proto-oncogenes, c-fos, c-jun and c-myc) and genes from the fetal period (like ANF, ß-MHC and α-skeletal actin) have been implicated in the cellular alterations leading to ventricular hypertrophy[37-39]. The altered and increased cardiac protein synthesis, resulting in a hypertrophic phenotype, can be triggered by dynamic or static stretch of neonatal or adult cardiomyocytes[40]. Increased stretch of myocytes activates the transcription of the early genes c-fos, c-jun and c-myc stimulating hyperplasia and (fetal) myocyte growth within minutes[41]. Angiotensin II, growth factors and noradrenaline are known to activate these early genes[23].

Mechanotransducers (e.g. tyrosine kinase-containing receptors and stretch-activated sarcolemmal ion channels) activate the process of mechanotransduction that in turn stimulates the intracellular growth pathways[42]. Via this cytosolic pathway the expression of specific "hypertrophic" genes are upregulated[43]. Insulin like growth factor (IGF), acidic and basic fibroblast growth factor (FGF-1 and FGF-2), platelet-derived growth factor (PDGF) and epidermal growth factor (EGF) are all growth factors that interact with those tyrosine-kinase receptors[21]. Transforming growth factor β (TGF-β) however, is one of the factors that has a myocyte proliferation and growth inhibitory activity and is suppressed during myocyte hypertrophy, allowing myocytes to grow[44]. Angiotensin II originated by the RAS-system, activates several protein kinases involved in cell growth and particularly in structural remodeling in cardiac hypertrophy and early postnatal development[21,45,46]. Other hormones known

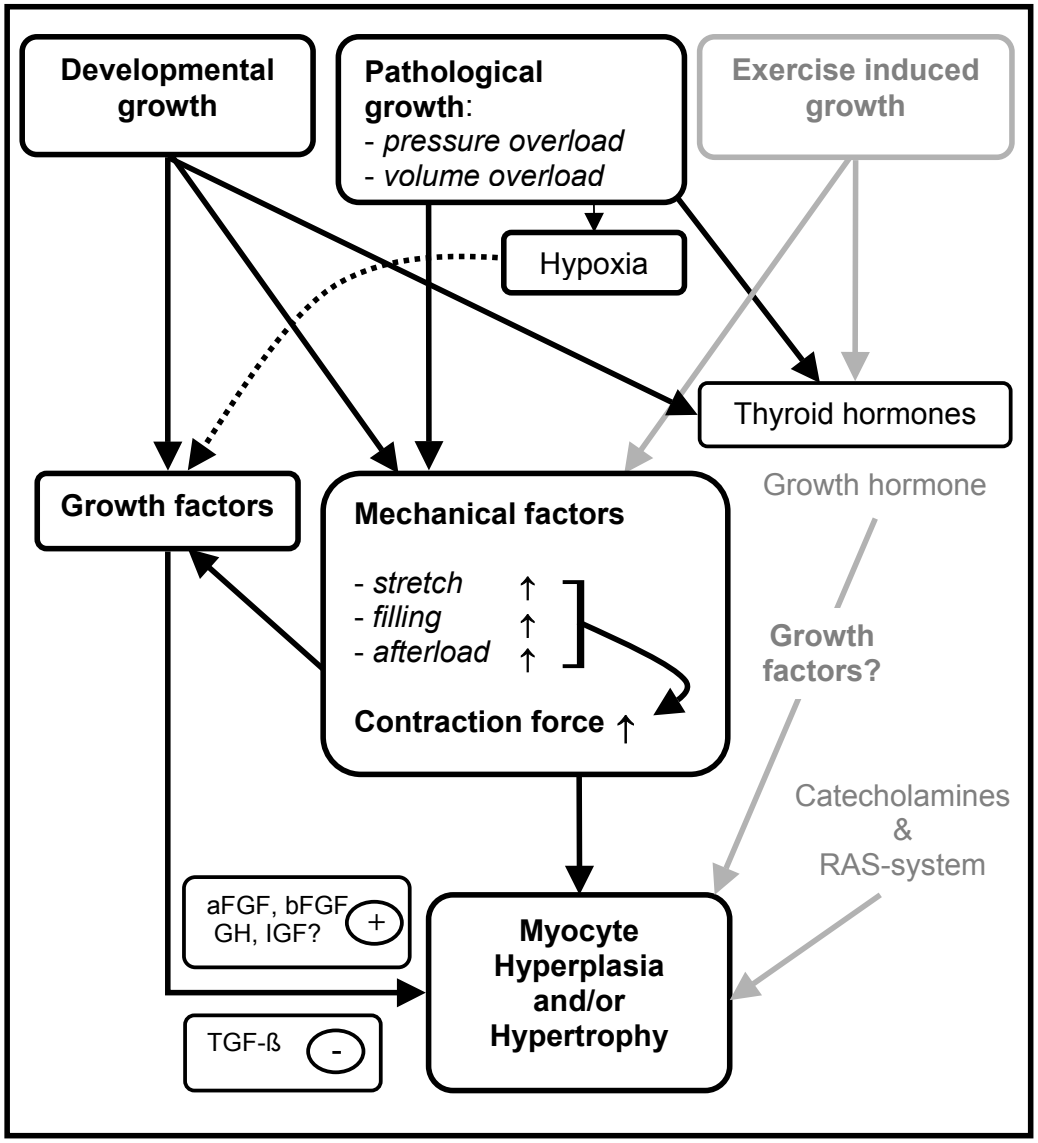

Figure 1.3. Factors involved in myocardial hyperplasia and hypertrophy
(adapted from Hudlicka et al.[23])

to contribute to hypertrophy are; growth hormone which is involved in the myosin α to β-isoform shift[47] and thyroid hormone, induced during increased oxygen consumption and augmented cardiac workload, and considered to be an endocrine mediator of cardiac hypertrophy[21,23]. The sympathetic nervous system is also thought to have a supporting regulatory role during pressure overload hypertrophy[48]. Besides the net increased protein synthesis there is also a modestly increase of protein degradation in cardiac hypertrophy. This increased degradation, involves the lysosomal and cytosolic protease activation, which may play a crucial role in the

variably altered geometry of the ventricles in response to pressure overload or volume overload, hypertrophy, regression, and atrophy[49,50]. Normally the average half live of cardiac proteins is 5 days, regenerating the composition of the adult heart approximately every 3 weeks[51,52]. During cardiac hypertrophy there is an net increase in protein synthesis accounting for the hypertrophic myocardial phenotype and increased mass[51,52].

Both myosin and myofibrillar ATPase activity are depressed in the hypertrophied myocardium. The loss of contractile protein may contribute to the impaired function as observed in cardiac muscle from failing human hearts[53]. In small mammals there is a transcriptionally mediated shift from α- to β-myosin heavy chain (MHC) and from cardiac to skeletal actin isoform in response to pressure overload[54,55]. Some studies report that this MHC shift[56,57] is caused by significant loss of α-MHC expression rather then β-MHC up regulation[12,58]. Because the α-form has a three to seven fold greater ATPase activity than β-myosin, it is believed that the abundance in β-MHC increases the efficiency of force development by producing the same absolute muscle tension at a slower rate[59]. In higher mammals and humans, decreased myosin ATPase activity of the hypertrophied heart is believed to be due to alterations in troponin isoform composition or post-translational generation of a lower molecular variant of β-MHC[21,60].

Myocardial hypertrophy in tetralogy of Fallot

The characteristic pulmonary stenosis with VSD in TF, will lead to increased RV pressure overload. In an adaptive response to normalize the wall stress, the RV will hypertrophy with expansion of the cardiomyocytes. This will lead to RV remodeling and the development of myocardial fibrosis[11,12,61]. Histopathological studies on TF myocardium report that the myocardial cell diameter in postoperative patients was reduced as compared to preoperative patients with TF, but postoperative cellular diameter was still larger than that in the age matched normal subjects[62,63]. These findings suggest that RVH after corrective surgery of TF can regress to some extent provided that residual pulmonary stenosis can be avoided.

1.4 Myocardial fibrosis

Interstitial fibrosis

The normal myocardial cellular architecture consists of nicely arrayed cardiac myocytes comprising cardiac fibroblasts and endothelial cells in the interstitial space. In-between the myocytes there is a fibrous protein structure, the extracellular matrix, that contributes to the myocardial organization and architecture, supports transmission of the contractile force generated by cardiac myocytes, contributes to the passive stretch and serves to restore the ventricular myocytes to precontraction length. The extracellular matrix composition exists of collagenous proteins that account for proteins, for example collagen, fibronectin, glycoproteins, proteoglycans and elastin[64].

Throughout normal physiological myocardial growth there is a balance of hyperplasia of cardiac fibroblasts and connective tissue distribution[37,65]. The collagen network, in the extra-cellular space of the myocardium, consists of collagen fibers, which provide the mechanical strength and stiffness of the myocardium[66,67]. When the balance is disturbed, in case of pressure overload, the network gets damaged. As a result to the increased wall stress, the myocyte support is compromized allowing myocardial tissue expansion with disarray of myocytes[68]. This, together with the increased tension on the fibers leads to a compensating excessive production of connective tissue, the development of fibrosis. This process may continue until the extracellular matrix fibers together with the hypertrophied myocytes counterbalance the pressure overload and prevent (further) dilatation[11-13,69]. Disproportionate accumulation of collagen, either reactive or reparative, has been observed during myocardial fibrosis. The increased accumulation of extracellular matrix proteins during myocardial fibrosis results in a decrease of compliance and declining contractile performance[12,70,71].

Fibronectin and collagen type I and III are major components of the interstitial fibrillar network. They are predominantly synthesized by cardiac and vascular fibroblasts with a little expression by myocytes[72]. The RAS-system, activated during pressure overload hypertrophy, activates fibroblast cell division enlarging the synthesis[23], where transcriptional upregulation of the encoding collagenous genes contribute to the myocardial fibrosis[12]. Experimental[73] and clinical data[74] show that

both fibronectin and collagen I and III are up-regulated during RVH[75]. The TGF-β expression is also up-regulated during pressure overload cardiac hypertrophy. It is believed to be involved in the mechanisms that activate fibrosis by the stimulation of fibronectin and collagen expression in a variety of cell types and their incorporation in the extracellular matrix[12,76]. Other factors that are thought to effect the collagenous synthesis by fibroblasts are PDGF, angiotensin and endothelin, although the exact mechanisms remains to be elucidated[77]. Pressure overload hypertrophy, induced by aortic banding, showed a high increase of collagen I syntheses already after 2 days, followed by collagen III after one week, suggesting differential expression regulation[77]. The higher collagen concentration is a result of a decreased collagen destruction and a higher collagen synthesis rate. The mRNA levels for collagen as well as for fibronectin were found to be increased in cardiac pressure-overload hypertrophy[75].

Under normal conditions there is a continuous expression and degradation of collagens by the adult cardiofibroblast[77]. There is a rapid collagen turnover in the heart, were daily 5% of the collagen fibers are renewed. Most mature cross-linked collagens are degraded extracellularly by members of the family of matrix metalloproteases (MMPs), whereas already a large fraction (60%) of the newly synthesized collagens is degraded rapidly within 8 minutes intracellularly, in the lysosomes and endoplasmic reticulum[78,79]. MMPs may play an important role in the tissue remodeling in both normal and pathological conditions. They belong to three main groups, classified on their substrate specificity. The MMPs involved in the myocardial remodeling are: the type IV collegenases (MMP-9 and MMP-2), the stromelysins (MMP-3) and the interstitial collegenases (MMP-1)[80]. The MMPs are secreted as a proenzyme (zymogen) by a number of cells including fibroblasts, endothelial cells, smooth muscle cells and cardiomyocytes and can be activated by plasmin[80,81]. The activity can be regulated by different cytokines and tissue inhibitors of MMPs (TIMPs)[81] but the extracellular matrix turn over is mainly regulated by MMPs and the TIMPs[82]. TIMPs can bind the active sites of the MMPs thereby blocking access to the collagen substrate[80]. An increase of the expression or activation of the MMPs or an decrease in of TIMPs leads to increased proteolytic activity in the extracellular space and increased extracellular remodeling including disregulated

fibrillar collagen degradation, myofibril disarray and progressive myocyte loss[82]. Increased levels of catecholamines, angiotensin II and endothelin may cause increased myocardial MMP levels in the remodeling heart whereas tumor necrosis factor-α (TNF-α) and ischemia are believed to increase the TIMP-1 and TIMP-4 levels respectively[80]. From the four TIMPs known, TIMP-4 is the most cardiac specific one, although all 4 are active in the myocardium[83]. An second role of TIMP 1 and 2 might be a fibroblast growth stimulation effect[80,84,85].

Peri-vascular fibrosis

During embryonic development, smooth muscle cells, endothelial cells and fibroblasts secrete extracellular matrix proteins in the peri-vascular area to form a supportive structure for the vascular wall. Under normal conditions, after birth, the vascular smooth muscle cells do not proliferate or develop contractile fibers but are kept in an quiescent state. When the smooth muscle cells are exposed to increased haemodynamic load, arterial injury, or physiological stress they will get activated, stimulate vascular remodeling, resulting in smooth muscle cell growth (due to hypertrophy) or mesenteric medial thickening (due to hyperplasia). Factors such as FGF, EGF and VEGF are known to stimulate the vascular smooth muscle hyperplasia[21].

Extracellular matrix proteins

In the myocardium the myocytes represent only one-third of the number of cells, but over two-third of their volume, whereas the number of fibroblasts, which produces most of the collagen fibers represent as much as two-third of the cells[86]. Four from the five collagen subtypes in the heart, type I, III, V and VI are produced by cardiac fibroblasts and type IV by other cell types including cardiac myocytes[87-89]. Collagen type I represents 80% of the total cardiac collagen content and is the major collagenous product of cardiac fibroblasts[87,90], which is important for the cardiac mechanical strength and stiffness[66]. Collagen type III, important for tissue elasticity, represents about 12% of total cardiac collagen content[91]. Collagen type I and III are widely distributed in-between myocytes and among muscle fibers[90,92]. Collagen types IV, V and VI constitute approximately 10-12% of total cardiac collagen content[64].

The collagen fibers have several functions, (i) one is to provide a scaffolding that supports muscle cells and blood vessels[67,93], (ii) to act as a lateral connection between cells and muscle bundles to control architecture while co-ordinating the delivery of force from the myocytes to the ventricle[67,93,94], (iii) to provide myocardial stiffness by tensile properties and resilience to resist myocardial deformation, maintain shape and wall thickness, and to prevent ventricular aneurysm and rupture[95,96].

Fibronectin, a glycoprotein located in the extracellular matrix of most tissue, serves as a bridge between cardiac myocytes and interstitial collagen mesh network[64,97]. It influences diverse processes including cell growth, adhesion, migration, and wound repair[91]. During the development of cardiac hypertrophy due to pressure overload, fetal fibronectin has been shown to accumulate in rats[75]. Fibronectin binds collagen and modulates the collagen fibrillogenesis, resulting in higher collagen type I concentration and a lower collagen type III concentration[98]. The fibronectin mRNA-splicing variant encoding the EIIIA segment is an isoform, expressed during wound healing[99], embryogenesis[100] and pressure-overload hypertrophy[101]. The structural properties of the EIIIA isoform of fibronectin are not well understood but it is postulated that this isoform may be important in the deposition of the extracellular matrix[99-101].

Fibrosis in tetralogy of Fallot

Progressive myocardial fibrosis due to cardiac hypertrophy is an important cause of myocardial dysfunction, clinical deterioration and cardiac death. Morphometrical studies on TF revealed that the RV is affected with enhanced fibrosis associated with increased myocytes diameter and myocardial disarray[69,102]. A post mortem analysis study of myocardium of TF patients showed normal fibrosis levels in the left ventricle and abnormal increased levels in the RV of patients older then 1 year with an increase in outflow tract and subendocardium[102]. The collagen concentration of the RV is about 30% higher than the left ventricle, because the RV myocytes are smaller[103]. Within the RV the highest concentrations are found in the outflow tract and subendocardium[11]. Changes in the cardiac extracellular matrix proteins composition have also been observed in other congenital heart disease, however in most of the types they where relatively small[37,72,95].

1.5 Myocardial angiogenesis

Vasculogenesis and angiogenesis

Angiogenesis is generally used to describe the formation of new blood vessels from pre-existing vessels. This involves not only the formation of capillaries, but also the formation of small and large blood vessels. The central physiological role of angiogenesis is to ensure a proper blood flow through the tissue. It is a multi-step process involving endothelial cell activation, migration, proliferation, tube formation and maturation. In contrast, vasculogenesis concerns the differentiation of a primitive network of new vessels during embryogenesis. The tissue glucose and oxygen concentrations are important environmental factors as pro-angiogenic stimuli. Besides endothelial cells several other cell types like vascular smooth muscle cells, pericytes and fibroblasts and non-cellular structures, such as the basal lamina and the extracellular matrix are involved[104,105].

Development of pre-mature vasculature

During embryogenesis when the number of cells is increasing within an avascular tissue, there is an increased demand for oxygen which can not be met by the oxygen diffusion. The hypoxic state, will trigger vessel formation by a process referred to as vasculogenesis. Undifferentiated precursor cells (angioblasts) will differentiate to endothelial cells that assemble into a vascular labyrinth. The endothelial cells will differentiate and proliferate to form a premature tubular network[106]. This network includes some of the major vessels in the embryo, such as the aorta and major veins, as well as a honey comb-like plexus connecting these major vessels. Vascular endothelial growth factor (VEGF) is one of the first growth factors to be induced in this process. It stimulates the formation of an unstable immature primary vasculature.
In the next process, referred to as angiogenic remodeling, the initial primitive network of premature vessel is modified, through both sprouting and vessel enlargement, to form the interconnecting branching patterns characteristic for a stable mature complex vascular network. During this process, vessel walls, premature as well as mature, and endothelial cells integrate tightly with supporting cells (such as smooth muscle cells and pericytes) and surrounding matrix, influenced by VEGF, Angiopoietin 1 (Ang-1) and ephrin B2. The endothelial cells are kept in a quiescence state by Ang-1. Once the

endothelial cells become quiescent they can survive for years. Expression of Ang-2 (like in pathological conditions) can destabilize the vessels and bring them in regression. If at the same time VEGF is co-expressed, VEGF can induce angiogenic sprouting in the destabilized vessel[105,107].

During angiogenic sprouting, new vessels (sprouts) from existing vessels are formed into a previously avascular tissue. In some cases it seems as if mature vessels must first be destabilized to allow subsequent sprouting. Angiogenic sprouting is responsible for the vascularization of certain tissues during normal development, such as the neural tube or the retina, and for most new vessel formation in the adult[106,107]. To supply all rapidly growing myocytes of oxygen after birth, the capillary length and surface increases 23 times faster than the myocardial mass, however the capillary diameter decreases, limiting the increasing capillary volume[23].

Destabilization of the vessel can apparently lead to vascular regression. The survival of the established vasculature, in the adults, depends on the quiescent state of the endothelial cells which have prolonged life times (several years). A continuous quantity of stabilizing factors is needed to keep the endothelial and smooth muscle cells in a quiescent state. An imbalance of survival and apoptotic factors could contribute to the regression of terminal myocardial vessels in pathological conditions of hypertension and diabetes. The formation of new vessels in adults will only occur by angiogenesis[104]. Under pathological conditions or during wound healing, when the quiescent vascular equilibrium is disrupted, autocrine induction or up-regulation of Ang-2, can reinitiate (angiogenic) vascular remodeling and angiogenic sprouting. In the presence of VEGF new vessels will be formed, but without VEGF vessels destabilize and go into regression[105]. Although sometimes also adult vasculogenesis occurs, it only leads to immature poorly functional vasculature[107].

Angiogenic stimuli and mechanisms

Angiogenesis is a complex process regulated and maintained by multiple endogenous pro-angiogenic and anti-angiogenic factors. In many cases, the activity of factors depends on their local concentration and/or the microenvironment[104,105]. The different angiogenic factors must be expressed in perfect harmony, on a complementary and

co-ordinated manner to form functional vessels and to overcome vascular regression[108]. Besides, many other non-vascular endothelium-specific growth factors like PDGF, TGF-β and many other gene products ranging from transcription factors to members of the Notch family have been shown to be crucial for proper vessel formation[107,109,110].

Among the angiogenic growth factors acting on the vascular endothelium, are the 5 members of the VEGF family, four members of the angiopoietin family and at least one family of the large ephrin family[105]. VEGF is the most critical and specific vascular growth factor in the vascular formation, required for the initiation of immature vessels by vasculogenesis or angiogenic sprouting. During hypoxia its half-life is prolonged from 30 minutes to 8 hours[23]. Ang-1 and ephrin B2 are needed for the further remodeling and maturation of the immature vasculature. In this process epherin B2 is important in the distinction to develop arterial or venous vessels. Ang-1 is important to maintain the quiescence and stable state of the vasculature. Disruption of the stabilizing Ang-1 signal will reinitiate vascular remodeling in the adult (e.g. in tumor)[105]. Autocrine production of Ang-2 (the Ang-1 natural antagonist) by endothelium cells will destabilize the vessels. VEGFs, angiopoietins and ephrin B2 apparently are not capable to trigger the entire process of vascular remodeling in adults individually[105].

Many of the angiogenic factors involved in the remodeling and establishment of functional blood vessels are regulated by paracrine signals from the receptor tyrosine kinases family[106] as listed in table 1.1.

Table 1.1. Overview of tyrosine kinase receptors and their ligands, involved in angiogenesis

VEGF Receptor family			Tie Receptor family		Epherin Receptor family			
Receptor:								
VEGFR-1 (Flt-1)	VEGFR-2 (KDR/Flk-1)	VEGFR-3 (Flt-4)	Tie1	Tie2	EphB2	EphB3	EphB4	EphA2
Ligand:								
VEGF-A VEGF-B PlGF	VEGF-A VEGF-C VEGF-D	VEGF-C VEGF-D	?	Ang-1 Ang-2 Ang-3 Ang-4	Ephrin-B1 Ephrin-B2	Ephrin-B1 Ephrin-B2	Ephrin-B2	Ephrin-A1

Other factor involved in angiogenesis are the acidic (FGF-1) and basic (FGF-2) fibroblast growth factors which stimulate the endothelial cell growth. They are expressed by fibroblasts in response to hypoxia. FGF-1 stimulates the branching of the myocardial arteries and stimulates the formation of functional vessels by preventing the regression[23,107]. In combination with vasoconstricting growth promoters, FGF-2 is an important endogenous activator of collateral vessel development in ischemic myocardium. During ischemia VEGF expression is up-regulated and triggers the release of stored FGF-2. The vasoconstricting growth promoters, such as angiotensin II, thrombin, thromboxane, prostaglandins, serotonin and endothelin, are less potent then peptide growth factors and they are believed to enhance other stimulators of vascular smooth muscle cell growth. In quiescent vasculature they are found to stimulate FGF-2 expression. TGF-β is one of the regulators that inhibit vascular smooth muscle cell growth but stimulates the synthesis of the extracellular matrix[21]. At low concentrations TGF-β still can stimulate vascular growth, by increasing autocrine PDGF synthesis, however higher concentrations reduces the PDGF receptor expression, interrupting the autocrine effect[111]. Thyroid hormones are involved in the capillary elongation or splitting of pre-existing vessels, increasing the capillary supply[23].

Besides hypoxia, capillary growth in the heart can be stimulated by moderate athletic training, as found in normal young but not in adult animal hearts, leading to growth of the arterioles and coronary vessels[23]. The increased blood flow is stimulating mechanical factors like shear stress and wall tension, which are stimuli that initiate vessel growth[23]. Increased shear stress leads to endothelial release of angiogenic prostaglandins and nitric oxide, whereas increased wall tension initiate smooth muscle cell and endothelial cell proliferation with the release of growth factors. Shear stress is also one of the factors known to be involved in vascular remodeling, where it can disrupt the peri-vascular matrix and releases plasminogen activator and MMPs activating a process that enables cell migration and proliferation[23]. In the same manner, a lower heart rate is believed to enhance capillary growth. During the diastole, the capillary diameter is larger than during systole increasing the wall tension. A lower heart rate will enhance the diastolic period thereby increasing the capillary wall stress and tension. Besides higher blood pressures and velocity, shear stress can also be increased by increased haematocrit[23,112].

Angiogenic factors

VEGF is known to be a critical vascular regulator. Although hypoxia can induce VEGF, it is not necessarily inducing a useful angiogenic response. A very precise concentration of other factors is needed to avoid vascular disorganization and induction of immature and leaky vessels[105]. Alliterations in VEGF expression during embryonic development can lead to profound abnormalities or early postnatal death[113,114]. The VEGF-family consists of the 4 VEGF homologues (VEGF-A, VEGF-B, VEGF-C or VEGF-related protein (VRP) and VEGF-D) and placental growth factor (PlGF)[115]. The different members of the VEGF family have overlapping abilities to interact with a set of cell-surface receptors such as VEGFR-1 (also known as flt-1), VEGFR-2 (also known as Flk-1 or KDR) and VEGFR-3 (also known as Flt-4). The VEGF receptors are closely related to receptor tyrosine kinase. Angiogenesis and the initiation of the permeability of blood vessels are regulated by VEGF via its receptors VEGFR-1 and VEGFR-2[105]. VEGF-A, one of the most potent and crucial regulatory factors during myocardial angiogenesis[105], is induced in a wide range of cells under conditions of hypoxia[116] and hypo-glycemia[117] and in the presence of some (growth) factors[118] like phorbol ester, adenosine, TGF-β, PDGF and TNF-α[105]. It is a ligand for the endothelial cell surface receptors, flt-1 and KDR[119]. VEGF-KDR binding activates a cascade that promote angiogenesis by promoting vascular endothelium cell proliferation, inducing vascular leaking and permeability but also by enhancing the glucose transport[120]. Although several isoforms ($VEGF_{120,}$ $VEGF_{121}$ and $VEGF_{165}$) of this member are known, the exact functions still have to be elucidated[107]. It is known that VEGF-A is involved in the formation of the vascular lumen, when the endothelial cells assemble to solid cords. Intercalation or thinning of endothelial cells and fusion of pre-existing vessels, influenced by VEGF-A, allow vessels to increase their diameter and length[107]. VEGF-B is believed to play a role in the in the coronary vascularization and growth. Loss of VEGF-B during embryogenesis reduces the heart size[121], whereas VEGF-C, a ligand for VEGFR3, is involved in embryonic and adult pathological angiogenesis. VEGFR-3 is also expressed on lymphatic vessels where it regulates, via VEGF-C, the lymphangiogenic activity[122-125]. Hardly anything is know about the physiological role of VEGF-D[107]. Also from the growth factor PlGF only a little is known, although there are some indications that it might have a limiting role in adult vascular remodeling[107].

From the VEGF receptors, VEGFR-2 seems to mediate the major growth and permeability whereas VEGFR-1 has a negative role by acting as a decoy receptor or by suppressing signaling through VEGFR-2. VEGF affects embryonic, neonatal and pathological angiogenesis via its receptor VEGFR-2[126]. The exact involvement of VEGFR-1 signaling during (pathological) angiogenesis remains undetermined[127]. Although VEGF does not seem necessary for the vascular maintenance in adults, disruption of VEGF expression mimics VEGFR-2 knock out, resulting in only a very few proliferated endothelial cells and complete absence of vasculature[126,128,129].

Angiopoietins are the ligands for the Tie receptors (Tie1 and Tie2) which are like the VEGF receptors expressed within the vascular endothelium[105]. The 4 members of the angiopoietin family (based on their homology with Ang-1) all bind primarily to Tie 2 receptor[105,130]. Tie2 is widely expressed in cardiovascular tissue[131,132]. There is some evidence that the Tie2 cascade regulates the extracellular recruitment of stromal cells required to encase and thereby stabilize primitive endothelial tubes[133,134]. Ang-1 binding to endothelial Tie2 receptor is necessary to maintain the quiescence state in adult vasculature, via a maximum stimulation of the interaction between endothelial and peri endothelial cells, their surrounding support cells and matrix[105]. It further protects the vasculature against vascular permeability and leakage induced by VEGF or inflammatory agents[105]. Ang-1 alone fails to induce endothelial proliferation[105,108,135], however in presence of VEGF unprecedented hyper-vascularization will occur resulting in an increased number and size of the vessels[136]. Further Ang-1 is believed to be a chemotactic for endothelial cells. Ang-2 binding to the Tie2 receptor can either activate or antagonize the Tie2 receptor[137]. At least in presence of VEGF, Ang-2 will enhanced the sprouting of capillary vessels by antagonizing the stabilization effect of Ang-1. Ang-2 itself cannot induce angiogenesis but is indirectly involved in Angiotensin II-mediated angiogenesis by enhancing the angiogenic activity of VEGF[138]. Angiotensin II can stimulate the remodeling of the heart and vessels via cell growth-promoting effects[139]. By binding to Angiotensin II receptors AT1 and AT2 , which are expressed in large amounts on the vascular endothelial cells in the myocardium[140], Angiotensin II can selectively induce and up-regulate VEGF and Ang-2 expression in cardiac vascular endothelial cells[141].

The ephrin receptors tyrosine kinases belong to the largest known family of growth factor receptors[108]. Ephrin-B2 and its EphB4 receptor are believed to play a key role during vascular development, especially in establishing arterial venous identity and in fusing arterial and venous vessels at their junctions[105]. During adult angiogenic sprouting the expression of ephrin-B2 is found to be strongly up-regulated in the endothelium of new vessels. Ephrin-B2 is not only required during the earliest stages of arterial/venous determination, but may also be important during the development of arteries by regulating interactions between endothelial and smooth muscle cells involved in the formation of the arterial muscular walls[105].

Angiogenesis in tetralogy of Fallot

In TF patients the RV myocytes hypertrophy as an adaptive response to the (sub)pulmonary stenosis in combination with the VSD, to normalize RV wall tension. This will trigger a response to improve myocardial perfusion by the formation of new capillaries and by the enlargement of pre-existing collateral vessels to reduce the increased capillary-myocyte diffusion distance, to prevent hypoxia and decreased nutrient delivery[12,13,142]. But also the mechanical factors such as stretch, shear stress, and increased wall tension, which occur in TF due RV pressure and volume overload may be stimuli for angiogenesis during cardiac hypertrophy[12,13,142]. Experimental animal studies with induced RVH due to pressure overload, revealed increased blood flow per unit myocardial mass at rest, without an increase in minimum coronary resistance[143]. During volume overload RVH however, normal flow values per unit myocardial mass at rest are measured, with normal or mild increases minimum coronary resistance and normal or mildly decreased coronary reserve[144].

From previous studies on the myocardial vascularization in TF patients it is known that the overall myocardial capillary density in the infundibulum of the right ventricular outflow tract of (1-7 years old) TF patients was reported to be similar to normal capillary density (1648±123 *vs.* 1782±203 capillaries/mm^2)[145]. Also the capillary domain (cross-sectional tissue area nearest to that capillary) and the capillary tissue supply volume are not affected in TF. However the capillary segment length (distance between two branching points) was found to be increased[145] whereas the capillary radius was decreases, from 2.8 to 2.4 μm[146]. There are also some indications

that the capillary supply per myocyte is proportional to the increased myocyte size, keeping the capillary per myocyte ratio similar[147]. The elimination of the hypertrophic stimuli in TF are believed to reverse the RVH and the associated coronary circulatory abnormalities[148].

1.6 Aims of the thesis

Different surgical interventions nowadays are applied to TF patients already at an early age to correct the cardiac malformations. It is, however, not yet established whether early intervention will result in (complete) regression of RVH and restore normal cardiac performance.

The underlying molecular mechanisms in the development and regression of RVH at different stages in the treatment of human TF still remains to be elucidated. The molecular and cellular characteristics of the RV myocardium at corrective and redo surgery are thought to correlate with the clinical condition of the patient and with cardiac prognosis. When experimental data and clinical parameters can be correlated more information will become available to enhance our knowledge in assessing the timing for surgery and eventually postoperative cardiac prognosis. Our working hypothesis is that molecular and cellular characteristics of the RV myocardium at corrective or redo surgery may provide information, relevant for the assessment of the clinical condition of the patient and important for cardiac prognosis.

Hence, aims of this thesis were to elucidate the changes in the RV phenotype (at mRNA and protein level) of patients with TF as compared to the normal myocardial phenotype by studying:

(i) the myocardial cellular organization and the degree of hypertrophy,
(ii) the degree of fibrosis (e.g. collagens and fibronectin),
(iii) the myocardial vascularization (e.g. VEGF expression and vascular density).

The obtained molecular biological data and clinical parameters (medical history, echocardiography and cardiac catheterization) of the different forms and stages of the disease will be analyzed to enhance our knowledge about the myocardial remodeling and RVH regression after surgery.

In the first part of the thesis our hypothesis was that the pressure overload and resulting RVH in patients with TF will go along with increased fibrosis represented by the enhanced expression of collagens and fibronectin. To elucidate the degree of myocardial fibrosis, we studied the localization of total collagen and fibronectin with light microscopy, assessed the expression by visual scoring in RV biopsies of TF and compared the data to autograft root replacement patients (control group), as described in ***chapter 2***. After computerized video image analysis of the same sections together with sections of post mortem controls, the autograft control biopsies appeared to include fibrotic changes as well (***chapter 3***) and thus could not be used as a proper control. In order to assess the degree of fibrosis and myocyte hypertrophy in TF patients and appropriate control groups, we analyzed the expression patterns of fibronectin and the collagen subtypes I and III at protein and mRNA level in an extended study. The results are described in ***chapter 4***, together with mRNA expression data of other factors known to be involved in myocardial fibrosis achieved by DNA micro-array chip analysis. In a similar fashion the degree of myocardial fibrosis in the PA-VSD patients has been analyzed in as described in ***chapter 5***.

In the second part of the thesis the hypothesis was that the remodeling of the heart in TF patients, apart from RVH, also concerns myocardial angiogenesis, triggered by the increased capillary-myocyte oxygen diffusion distance. VEGF, a ligand for the *flk-1* receptor, is one of the key players during angiogenesis. In the ***chapters 6 and 7*** the results are described of the assessment of angiogenic factor such as VEGF and the resulting increase in vascular density.

In ***chapter 8*** the observations of the studies as described in this thesis are discussed together with the implications for possible treatment and future research.

References

1. Bogers AJJC, van der Laarse A, Vliegen HW, et al. Assessment of hypertrophy in myocardial biopsies taken during correction of congenital heart disease. *Thorac Cardiovasc Surgeon*. 1988;36:137-140.
2. Castaneda AR, Jonas RA, Mayer JE, et al. *Cardiac surgery of neonate and infant*. Philadelphia, USA: Saunders; 1994.
3. Soto B, Pacifico AD, Ceballos R, et al. Tetralogy of Fallot: an angiographic-pathologic correlative study. *Circulation*. 1981;64:558-66.
4. Bartelings MM. Morphology of tetralogy of Fallot. In: Bartelings MM, Wenink ACG, eds. *Congenital Heart Disease*. Leiden: Boerhaave Committee; 1999:49-56.
5. Anderson RH, Tynan M. Tetralogy of Fallot--a centennial review. *Int J Cardiol*. 1988;21:219-32.
6. Ottenkamp J. Clinical presentation-introduction: What is tetralogy of Fallot? In: Bartelings MM, Wenink ACG, eds. *Congenital Heart Disease*. Leiden: Boerhaave Committee; 1999:41-46.
7. Schoen F. The Heart. In: Cotran R, Robbins S, Kumar V, eds. *Pathologic basis of disease*. 5th ed. Philadelphia: W.B. Saunders Company; 1994:560.
8. Jacobs ML. Congenital Heart Surgery Nomenclature and Database Project: tetralogy of Fallot. *Ann Thorac Surg*. 2000;69:S77-82.
9. Enersen O. Fallot. In: www.whonamedit.com. Oslo; 2001.
10. Stephenson L, Rodengen J. *State of the heart*. 1 ed. Fort Launderdale: Write Stuff Enterprises Inc; 1999.
11. van Bilsen M, Chien KR. Growth and hypertrophy of the heart: towards an understanding of cardiac specific and inducible gene expression. *Cardiovasc Res*. 1993;27:1140-1149.
12. Boluyt MO, L. O, Meredith AL, et al. Alterations in cardiac gene expression during the transition from stable hypertrophy to heart failure. Marked upregulation of genes encoding extracellular matrix components. *Circ Res*. 1994;75:23-32.
13. Schwartz K, Carrier L, Mercadier JJ, et al. Molecular phenotype of hypertrophied and failing myocardium. *Circulation*. 1993;87:VII 5-10.
14. Kirklin JW, Barrat-Boyes BG. *Ventricular septal defect and pulmonary stenosis or atresia*. 2nd ed. ed. New York: Churchill-Livingstone: Churchill-Livingstone; 1993.
15. Starnes VA, Luciani GB, Latter DA, et al. Current surgical management of tetralogy of Fallot. *Ann Thorac Surg*. 1994;58:211-215.
16. Van Arsdell GS, Maharaj GS, Tom J, et al. What is the optimal age for repair of tetralogy of Fallot? *Circulation*. 2000;102:III123-9.
17. Pozzi M, Trivedi DB, Kitchiner D, et al. Tetralogy of Fallot: what operation, at which age. *Eur J Cardiothorac Surg*. 2000;17:631-636.
18. Losekoot G, Kamphuis R. *Kinderen met een hartafwijking*. meppel: Boom; 1988.
19. de Ruijter FT, Weenink I, Hitchcock FJ, et al. Right ventricular dysfunction and pulmonary valve replacement after correction of tetralogy of Fallot. *Ann Thorac Surg*. 2002;73:1794-800; discussion 1800.
20. Pacifico AD. Reoperations after repair of tetralogy of Fallot. In: Stark J, Pacifico AD, eds. *Reoperations in cardiac surgery*: Springer; 1989:171-86.

21. Walsh R, Dorn G. Growth and hypertrophy of the heart and blood vessels. In: Alexander W, Schlant R, Fuster V, eds. *Hurst's The Heart, arteries and veins*. 9th edition: The McGraw-Hill Companies; 1998:155-168.
22. Rakusan K. Cardiac growth, maturation and ageing. In: Zak R, ed. *Growth of the heart in health and disease*. New York: Raven press; 1984:131-164.
23. Hudlicka O, Brown MD. Postnatal growth of the heart and its blood vessels. *J Vasc Res*. 1996;33:266-87.
24. Ford LE. Heart size. *Circ Res*. 1976;39:297-303.
25. Schaible T, Scheuer J. Response of heart to exercise training. In: Zak R, ed. *Growth of the heart in health and disease*. New York: Raven press; 1984:381-419.
26. Walsh R. Cardiovascular effects of the aging process. *Am J Med*. 1987;82:34-40.
27. Field LJ. Atrial natriuretic factor-SV40 T antigen transgenes produce tumours and cardiac arrhythmias in mice. *Science*. 1988;239:1029-33.
28. Grossman W. Cardiac hypertrophy; useful adaptation or pathological process? *Am J Med*. 1980;69:576-584.
29. Teiger E, Than VD, Richard L, et al. Apoptosis in pressure overload-induced heart hypertrophy in the rat. *J Clin Invest*. 1996;97:2891-7.
30. Cheng W, Li B, Kajstura J, et al. Stretch-induced programmed myocyte cell death. *J Clin Invest*. 1995;96:2247-59.
31. Anversa P, Hiler B, Ricci R, et al. Myocyte cell loss and myocyte hypertrophy in the ageing rat heart. *J Am Coll Cardiol*. 1986;8:1441-1448.
32. Engelmann GL, Vitullo JC, Gerrity RG. Morphometric analysis of cardiac hypertrophy during development, maturation, and senescence in spontaneously hypertensive rats. *Circ Res*. 1987;60:487-494.
33. Capasso JM, Palackal T, Olivetti G, et al. Left ventricular failure induced by long-term hypertension in rats. *Circ Res*. 1990;86:1400-1412.
34. Thompson CB. Apoptosis in the pathogenesis and treatment of disease. *Science*. 1995;267:1456-62.
35. Vaux DL, Strasser A. The molecular biology of apoptosis. *Proc Nat Acad Sci U S A*. 1996;93:2239-44.
36. Brilla CG, Janicki JS, Weber KT. Impaired diastolic function and coronary reserve in genetic hypertension. Role of interstitial fibrosis and medial thickening of intramyocardial coronary arteries. *Circ Res*. 1991;69:107-115.
37. Bishop SP. Structural alterations in the hypertrophied and failing myocardium. In: Abel FL, Hewman WH, eds. *Functional aspects of the normal hypertrophied and failing heart.* The Hague: Martinus Nijhoff Publishing; 1984:278-300.
38. Boheler KR, Dillmann WH. Cardiac response to pressure overload in the rat: the selective alteration of in vitro directed RNA translation products. *Circulation Res*. 1988;63:448-456.
39. Brand T, Sharma HS, Fleischmann KE, et al. Proto-oncogene expression in porcine myocardium subjected to ischemia and reperfusion. *Circ Res*. 1992;71:1351-1360.
40. Cooper Gt. Cardiocyte adaptation to chronically altered load. *Ann Rev Physiol*. 1987;49:501-18.
41. Lompre AM, Mercadier JJ, Schwartz K. Changes in gene expression during cardiac growth. *Int Rev Cytol*. 1991;124:137-86.

42. watson P. Mechanical activation of signalling pathways in cardiovascular system. *Trends Cardiovasc Med*. 1996;6:73-79.
43. Sugden PH, Bogoyevitch MA. Intracellular signalling through protein kinases in the heart. *Cardiovasc Res*. 1995;30:478-92.
44. Engelmann GL, Boehm KD, Birchenall-Roberts MC, et al. Transforming growth factor-beta 1 in heart development. *Mech Dev*. 1992;38:85-97.
45. Beinlich CJ, Baker KM, White GJ, et al. Control of growth in the neonatal pig heart. *Am J Physiol*. 1991;261:3-7.
46. Falkenhahn M, Gohlke P, Paul M, et al. The renin-angiotensin system in the heart and vascular wall: new therapeutic aspects. *J Cardiovasc Pharmacol*. 1994;24 Suppl 2:S6-13.
47. Sacca L, Cittadini A, Fazio S. Growth hormone and the heart. *Endocr Rev*. 1994;15:555-73.
48. Strauer BE. [Progression and regression of heart hypertrophy in arterial hypertension: pathophysiology and clinical aspects]. *Z Kardiol*. 1985;74 Suppl 7:171-8.
49. Parker TG, Packer SE, Schneider MD. Peptide growth factors can provoke "fetal" contractile protein gene expression in rat cardiac myocytes. *J Clin Invest*. 1990;85:507-14.
50. Samarel AM. Hemodynamic overload and the regulation of myofibrillar protein degradation. *Circulation*. 1993;87:1418-20.
51. Morgan HE, Gordon EE, Kira Y, et al. Biochemical mechanisms of cardiac hypertrophy. *Ann Rev Physiol*. 1987;49:533-43.
52. Hannan RD, Luyken J, Rothblum LI. Regulation of ribosomal DNA transcription during contraction-induced hypertrophy of neonatal cardiomyocytes. *J Biol Chem*. 1996;271:3213-20.
53. Pagani ED, Alousi AA, Grant AM, et al. Changes in myofibrillar content and Mg-ATPase activity in ventricular tissues from patients with heart failure caused by coronary artery. *Circ Res*. 1998;63(2):380-385.
54. Morkin E. Regulation of myosin heavy chain genes in the heart. *Circulation*. 1993;87:1451-60.
55. Boheler KR, Chassagne C, Martin X, et al. Cardiac expressions of alpha- and beta-myosin heavy chains and sarcomeric alpha-actins are regulated through transcriptional mechanisms. Results from nuclear run-on assays in isolated rat cardiac nuclei. *J Biol Chem*. 1992;267:12979-85.
56. Bing OH, W. BW, Conrad CH, et al. Intracellular calcium transients in myocardium from spontaneously hypertensive rats during the transition to heart failure. *Circ Res*. 1991;68(5):1390-1400.
57. Conrad CH, W. BW, G. RK, et al. Impaired myocardial function in spontaneously hypertensive rats with heart failure. *Am J Physiol*. 1991;260 (1 Pt 2):H136-145.
58. Lowes BD, Minobe W, Abraham WT, et al. Changes in gene expression in the intact human heart. Down regulation of alpha-myosin heavy chain in hypertrophied, failing ventricular myocardium. *J Clin Invest*. 1997;100:2315-24.
59. Cooper Gt. Load and length regulation of cardiac energetics. *Ann Rev Physiol*. 1990;52:505-22.
60. Anderson PA, Greig A, Mark TM, et al. Molecular basis of human cardiac troponin T isoforms expressed in the developing, adult, and failing heart. *Circ Res*. 1995;76:681-6.

61. Schwartz SM, Gordon D, Mosca RS, et al. Collagen content in normal, pressure, and pressure-volume overloaded developing human hearts. *Am J Cardiol*. 1996;77:734-738.
62. Mitsuno M, Nakano S, Shimazaki Y, et al. Fate of right ventricular hypertrophy in tetralogy of Fallot after corrective surgery. *Am J Cardiol*. 1993;72:694-698.
63. Seliem MA, Wu YT, Glenwright K. Relation between age at surgery and regression of right ventricular hypertrophy in tetralogy of Fallot. *Ped Cardiol*. 1995;16:53-55.
64. Pelouch V, Dixon IM, Golfman L, et al. Role of extracellular matrix proteins in heart function. *Mol Cell Biochem*. 1994;129:101-120.
65. Medugorac I. Myocardial collagen in different forms of the heart hypeortrophy in the rat. *Res Exp Med*. 1980;177:201-211.
66. Weber KT, Sun Y, Tyagi SC, et al. Collagen network of the myocardium: function, structural remodelling and regulatory mechanisms. *J Mol Cell Cardiol*. 1994;26:279-292.
67. Bishop JE, Rhodes S, Laurent GJ, et al. Increased collagen synthesis and decreased collagen degradation in right ventricular hypertrophy induced by pressure overload. *Cardiovasc Res*. 1994;28:1581-1585.
68. Whittaker P. Collagen and ventricular remodelling after acute myocardial infarction: concepts and hypotheses. *Basic Res Cardiol*. 1997;92:79-81.
69. Kawai S, Okada R, Kitamura K, et al. A morphometrical study of myocardial disarray associated with right ventricular outflow tract obstruction. *Jpn Circ J*. 1984;48:445-456.
70. Conrad CH, Brooks WW, Sen S, et al. Increased collagen content may contribute to increased myocardial stiffness and heart failure in spontaneously hypertensive rat. *J Am Coll Cardiol*. 1990;15:48A.
71. Weber KT, Brilla CG. Pathological hypertrophy and cardiac interstitium. Fibrosis and renin-angiotensin-aldosterone system. *Circulation*. 1991;83(6):1849-1865.
72. Bishop JE, Greenbaum M, Gibson DG, et al. Enhanced deposition of predominantly type I collagen in myocardial disease. *J Mol Cell Cardiol*. 1990;22:1157-1165.
73. Jalil JE, Doering CW, Janicki JS, et al. Fibrillar collagen and myocardial stiffness in the intact hypertrophied rat left ventricle. *Circ Res* 1989;64:1041-1050.
74. McLenachan JM, Dargie HJ. Ventricular arrhythmias in hypertensive left ventricular hypertrophy. Relationship to coronary artery disease, left ventricular dysfunction, and myocardial fibrosis. *Am J Hypertens*. 1990;3:735-740.
75. Samuel JL, Barrieux A, Dufour S, et al. Accumulation of fetal fibronectin mRNAs during the development of rat cardiac hypertrophy induced by pressure overload. *J Clin Invest*. 1991;88:1737-1746.
76. Ignotz RA, Massague J. Transforming growth factor-beta stimulates the expression of fibronectin and collagen and their incorporation into the extracellular matrix. *J Biol Chem*. 1986;261(9):4337-4345.
77. Bishop JE, Rhodes S, Laurent GJ, et al. The regulation of collagen deposition in the hypertrophying heart. *Ann N Y Acad Sci*. 1995;752:236-9.

78. Laurent GJ. Dynamic state of collagen: pathways of collagen degradation in vivo and their possible role in regulation of collagen mass. *Am J Physiol*. 1987;252:C1-9.
79. Bienkowski RS, Cowan MJ, McDonald JA, et al. Degradation of newly synthesized collagen. *J Biol Chem*. 1978;253:4356-63.
80. Mann DL, Spinale FG. Activation of matrix metalloproteinases in the failing human heart: breaking the tie that binds. *Circulation*. 1998;98:1699-702.
81. Galis ZS, Muszynski M, Sukhova GK, et al. Cytokine-stimulated human vascular smooth muscle cells synthesize a complement of enzymes required for extracellular matrix digestion. *Circ Res*. 1994;75:181-9.
82. Li YY, Feldman AM, Sun Y, et al. Differential expression of tissue inhibitors of metalloproteinases in the failing human heart. *Circulation*. 1998;98:1728-34.
83. Greene J, Wang M, Liu YE, et al. Molecular cloning and characterization of human tissue inhibitor of metalloproteinase 4. *J Biol Chem*. 1996;271:30375-80.
84. Dollery CM, McEwan JR, Henney AM. Matrix metalloproteinases and cardiovascular disease. *Circ Res*. 1995;77:863-8.
85. Birkedal-Hansen H, Moore WG, Bodden MK, et al. Matrix metalloproteinases: a review. *Crit Rev Oral Biol Med*. 1993;4:197-250.
86. Zak R. Cell proliferation during cardiac growth. *Am J Cardiol*. 1973;31:211-219.
87. Chapman D, Weber KT, Eghbali M. Regulation of fibrillar collagen types I and III and basement membrane type IV collagen gene expression in pressure overloaded rat myocardium. *Circ Res*. 1990;67:787-794.
88. Weber KT. Cardiac interstitium in health and disease: The fibrillar collagen network. *J Am Coll Cardiol*. 1989;13:1637-1652.
89. Speiser B, Riess CF, Schaper J. The extracellular matrix in human myocardium: part 1: Collagens I, II, IV and VI. *Cardioscience*. 1991;2:225-232.
90. Bashey RI, Martinez-Hernandez A, Jiminez SA. Isolation, characterization, and localization of cardiac collagen type VI. Associations with other extracellular matrix components. *Circ Res 70*. 1992;70:1006-1017.
91. Farhadian F, Contard F, Corbier A, et al. Fibronectin expression during physiological and pathological cardiac growth. *J Mol Cell Cardiol*. 1995;27:981-990.
92. Weber KT, Pick R, Jalil JE, et al. Patterns of myocardial fibrosis. *J Mol Cell Cardiol*. 1989;21 (Suppl V):121-131.
93. Borg TK, Caulfield JB. The collagen matrix of the heart. *Fed Proc*. 1981;20:2037-2041.
94. Weber KT, Janicki JS, Pick R, et al. Collagen in the hypertrophied pressure-overloaded myocardium. *Circulation*. 1987;75 (Suppl. I):I-40-7.
95. Dawson R, Milne G, Williams RB. Changes in the collagen or rat heart in copper-deficiency-induced cardiac hypertrophy. *Cardiovasc Res*. 1982;16:559-65.
96. Factor SM, Robinson TF, Dominitz R, et al. Alterations of the myocardial skeletal framework in acute myocardial infarction with and without ventricular rupture. *Am J Cardiovasc Pathol*. 1986;1:91-97.

97. Wayner E, Carter W, Piotrowitz R, et al. The function of multiple extracellular matrix receptors mediating cell adhesion to extracellular matrix: Preparation of monoclonal antibodies to the fibronectin receptor that specifically inhibit cell adhesion to fibronectin and react with platelet glycoproteins. *J Cell Biol*. 1988;107:1881-1891.
98. Kucharz E. *The collagens: biochemistry and pathophysiology*. Berlin: Springer Verlag; 1992.
99. Ffrench-Constant C, van de Water L, Dvorak HF, et al. Reappearance of an embriotic pattern of fibronectin splicing during wound healing in adult heart. *J Cell Biol*. 1989;109:903-914.
100. Norton PA, Hynes RO. Alternative splicing of chicken fibronectin in embryos and in normal and transformed cells. *Mol Cell Biol*. 1987;7(12):4297-4307.
101. Villareal FJ, Dillman WH. cardiac hypertrophy induced changes in mRNA levels for TGF-b, fibronectin and collagen. *Am J Physiol*. 1992;31:H1861-H1866.
102. Hegerty A, Anderson RH, Deanfield JE. Myocardial fibrosis in tetralogy of Fallot: effect of surgery or a part of the natural history? *Br. Heart J.* 1988;59:123 (abstract).
103. Caspari PG, Gibson K, Harris P. Changes in myocardial collagen in normal development and after b-blockade. *Rec Adv Card Struct Metab*. 1976;7:99-104.
104. Huminiecki LB, R. Angiogenesis. In: Bikfalvi A, ed. *Encyclopedic reference of vascular biology & pathology*. Berlin Heidelberg: Springer Verlag; 2000:2-8.
105. Yancopoulos GD, Davis S, Gale NW, et al. Vascular-specific growth factors and blood vessel formation. *Nature*. 2000;407:242-8.
106. Risau W. Mechanisms of angiogenesis. *Nature*. 1997;386:671-4.
107. Carmeliet P. Mechanisms of angiogenesis and arteriogenesis. *Nat Med*. 2000;6:389-395.
108. Gale NW, Yancopoulos GD. Growth factors acting via endothelial cell-specific receptor tyrosine kinases: VEGFs, angiopoietins, and ephrins in vascular development. *Genes Dev*. 1999;13:1055-66.
109. Hellstrom M, Kalen M, Lindahl P, et al. Role of PDGF-B and PDGFR-beta in recruitment of vascular smooth muscle cells and pericytes during embryonic blood vessel formation in the mouse. *Development*. 1999;126:3047-55.
110. Hirschi KK, Rohovsky SA, Beck LH, et al. Endothelial cells modulate the proliferation of mural cell precursors via platelet-derived growth factor-BB and heterotypic cell contact. *Circ Res*. 1999;84:298-305.
111. Stouffer GA, Owens GK. TGF-beta promotes proliferation of cultured SMC via both PDGF-AA-dependent and PDGF-AA-independent mechanisms. *J Clin Invest*. 1994;93:2048-55.
112. Hudlicka O, Brown MD, Walter H, et al. Factors involved in capillary growth in the heart. *Mol Cell Biochem*. 1995;147:57-68.
113. Miquerol L, Langille BL, Nagy A. Embryonic development is disrupted by modest increases in vascular endothelial growth factor gene expression. *Development*. 2000;127:3941-6.

114. Carmeliet P, Ng YS, Nuyens D, et al. Impaired myocardial angiogenesis and ischemic cardiomyopathy in mice lacking the vascular endothelial growth factor isoforms VEGF164 and VEGF188. *Nat Med*. 1999;5:495-502.
115. Eriksson U, Alitalo K. Structure, expression and receptor-binding properties of novel vascular endothelial growth factors. *Curr Top Microbiol Immunol*. 1999;237:41-57.
116. Shweiki D, Itin A, Soffer D, et al. Vascular endothelial growth factor induced by hypoxia may mediate hypoxia-initiated angiogenesis. *Nature*. 1992;359:843-845.
117. Shweiki D, Neeman M, Itin A, et al. Induction of vascular endothelial growth factor expression by hypoxia and by glucose deficiency in multicell spheroids: implications for tumour angiogenesis. *Proc Nat Acad Sci U S A*. 1995;92:768-772.
118. Horiuchi T, Weller PF. Expression of vascular endothelial growth factor by human eosinophils: upregulation by granulocyte macrophage colony-stimulating factor and interleukin-5. *Am J Respir Cell Mol Biol*. 1997;17:70-77.
119. Detmar M, Brown LF, Berse B, et al. Hypoxia regulates the expression of vascular permeability factor/vascular endothelial growth factor (VPF/VEGF) and its receptors in human skin. *J Invest Dermatol*. 1997;108:263-268.
120. Waltenberger J, Mayr U, Pentz S, et al. Functional upregulation of the vascular endothelial growth factor receptor KDR by hypoxia. *Circulation*. 1996;94:1647-1654.
121. Bellomo D, Headrick JP, Silins GU, et al. Mice lacking the vascular endothelial growth factor-B gene (VEGF-B) have smaller hearts, dysfunctional coronary vasculature, and impaired recovery from cardiac ischemia. *Circ Res*. 2000;86:E29-35.
122. Dumont DJ, Jussila L, Taipale J, et al. Cardiovascular failure in mouse embryos deficient in VEGF receptor-3. *Science*. 1998;282:946-9.
123. Ferrara N, Alitalo K. Clinical applications of angiogenic growth factors and their inhibitors. *Nat Med*. 1999;5:1359-64.
124. Taipale J, Makinen T, Arighi E, et al. Vascular endothelial growth factor receptor-3. *Curr Top Microbiol Immunol*. 1999;237:85-96.
125. Olofsson B, Jeltsch M, Eriksson U, et al. Current biology of VEGF-B and VEGF-C. *Curr Opin Biotechnol*. 1999;10:528-35.
126. Carmeliet P, Ferreira V, Breier G, et al. Abnormal blood vessel development and lethality in embryos lacking a single VEGF allele. *Nature*. 1996;380:435-9.
127. Hiratsuka S, Minowa O, Kuno J, et al. Flt-1 lacking the tyrosine kinase domain is sufficient for normal development and angiogenesis in mice. *Proc Nat Acad Sci U S A*. 1998;95:9349-54.
128. Ferrara N, Chen H, Davis-Smyth T, et al. Vascular endothelial growth factor is essential for corpus luteum angiogenesis. *Nat Med*. 1998;4:336-40.
129. Shalaby F, Rossant J, Yamaguchi TP, et al. Failure of blood-island formation and vasculogenesis in Flk-1-deficient mice. *Nature*. 1995;376:62-6.
130. Maisonpierre PC, Suri C, Jones PF, et al. Angiopoietin-2, a natural antagonist for Tie2 that disrupts in vivo angiogenesis. *Science*. 1997;277:55-60.
131. Wong AL, Haroon ZA, Werner S, et al. Tie2 expression and phosphorylation in angiogenic and quiescent adult tissues. *Circ Res*. 1997;81:567-74.

132. Witzenbichler B, Maisonpierre PC, Jones P, et al. Chemotactic properties of angiopoietin-1 and -2, ligands for the endothelial-specific receptor tyrosine kinase Tie2. *J Biol Chem*. 1998;273:18514-21.
133. Dumont DJ, Gradwohl G, Fong GH, et al. Dominant-negative and targeted null mutations in the endothelial receptor tyrosine kinase, tek, reveal a critical role in vasculogenesis of the embryo. *Genes Dev*. 1994;8:1897-909.
134. Vikkula M, Boon LM, Carraway KL, 3rd, et al. Vascular dysmorphogenesis caused by an activating mutation in the receptor tyrosine kinase Tie2. *Cell*. 1996;87:1181-90.
135. Suri C, McClain J, Thurston G, et al. Increased vascularization in mice overexpressing angiopoietin-1. *Science*. 1998;282:468-71.
136. Thurston G, Suri C, Smith K, et al. Leakage-resistant blood vessels in mice transgenically overexpressing angiopoietin-1. *Science*. 1999;286:2511-4.
137. Carmeliet P. Developmental biology. Controlling the cellular brakes. *Nature*. 1999;401:657-8.
138. Fujiyama S, Matsubara H, Nozawa Y, et al. Angiotensin AT(1) and AT(2) receptors differentially regulate angiopoietin-2 and vascular endothelial growth factor expression and angiogenesis by modulating heparin binding-epidermal growth factor (EGF)-mediated EGF receptor transactivation. *Circ Res*. 2001;88:22-9.
139. Baker KM, Booz GW, Dostal DE. Cardiac actions of angiotensin II: Role of an intracardiac renin-angiotensin system. *Ann Rev Physiol*. 1992;54:227-41.
140. Stoll M, Steckelings UM, Paul M, et al. The angiotensin AT2-receptor mediates inhibition of cell proliferation in coronary endothelial cells. *J Clin Invest*. 1995;95:651-7.
141. Chua CC, Hamdy RC, Chua BH. Upregulation of vascular endothelial growth factor by H2O2 in rat heart endothelial cells. *Free Radic Biol Med*. 1998;25:891-7.
142. van Bilsen M, Chien KR. Growth and hypertrophy of the heart: towards an understanding of cardiac specific and inducible gene expression. *Cardiovasc Res*. 1993;27:1140-1149.
143. Murray PA, Vatner SF. Reduction of maximal coronary vasodilator capacity in conscious dogs with severe right ventricular hypertrophy. *Circ Res*. 1981;48:25-33.
144. Hultgren PB, Bove AA. Myocardial blood flow and mechanics in volume overload-induced left ventricular hypertrophy in dogs. *Cardiovasc Res*. 1981;15:522-528.
145. Rakusan K, Cicutti N, Spatenka J, et al. Geometry of the capillary net in human hearts. *Int J Microcirc Clin Exp*. 1997;17:29-32.
146. Turek Z, Rakusan K. Lognormal distribution of intercapillary distance in normal and hypertrophic rat heart as estimated by the method of concentric circles: its effect on tissue oxygenation. *Pflugers Arch*. 1981;391:17-21.
147. Rakusan K, Flanagan MF, Geva T, et al. Morphometry of human coronary capillaries during normal growth and the effect of age in left ventricular pressure-overload hypertrophy. *Circulation*. 1992;86:38-46.
148. Isoyama S, Ito N, Kuroha M, et al. Complete reversibility of physiological coronary vascular abnormalities in hypertrophied hearts produced by pressure overload in the rat. *J Clin Invest*. 1989;84:288-294.

Chapter 2

Quantitative analysis of collagens and fibronectin expression in human right ventricular hypertrophy

Based on:
T.H.F. Peters, H.S. Sharma, E. Yilmaz and A.J.J.C. Bogers. Quantitative analysis of collagens and fibronectin expression in human right ventricular hypertrophy. Ann N Y Acad Sci 1999; 874:278-285.

Abstract

One of the main features in human Tetralogy of Fallot (TF) is right ventricular hypertrophy (RVH) due to pressure (sub-pulmonary stenosis) and volume overload (ventricular septal defect). Currently, primary correction at a young age is the treatment of choice. To unravel the role of extracellular matrix in RVH, we examined myocardial expression of collagens and fibronectin in TF patients; primary correction (TF-1, mean age 0.7 ± 0.2 years), secondary surgery (TF-2, mean age 36.9 ± 4.6 years) and in age matched control patients. Picro-sirius red staining quantified by video imaging showed significantly increased interstitial staining for collagens in both TF-1 and TF-2 groups as compared to respective controls. Fibronectin was expressed in extracellular spaces, peri-vascular regions and in some cardiomyocytes. Quantitative analysis of fibronectin revealed increased expression in only TF-1 group as compared to respective control. Our results indicate an increased amount of myocardial extracellular matrix deposition as a sign of fibrosis during RVH in patients with TF.

Introduction

Tetralogy of Fallot (TF) is a common form of cyanotic congenital heart disease, with an incidence rate of 1 out of 2000 new borns. TF is characterized by overriding of the aorta, a ventricular septal defect, (sub) valvular pulmonary stenosis and right ventricular hypertrophy (RVH) resulting in hypoxemia due to diminished pulmonary flow[1]. The RVH in human TF is an adaptive response of cardiomyocytes to increased pressure as well as volume overload caused by (sub) pulmonary stenosis and by ventricular septal defect, respectively. The adaptive response requires proportionate increase of coronary flow or growth of the coronary vasculature, leading to myocardial remodeling as well as development of fibrosis and, without treatment, ultimately results in cardiac failure[2-5].

In myocardial fibrosis, collagens and fibronectin play a prominent role. Damage of the collagen structure compromises the myocyte support, decreases myocardial strength and stiffness and allows expansion of the tissue[6]. Collagen fibers are organized in the collagen network, which is found in the extracellular space of the myocardium[7-10]. In myocardial fibrosis a disproportionate accumulation, either reactive or reparative, of collagen has been observed. Experimental[11] and clinical data[12,13] show that a rise in collagen content increases myocardial stiffness and promotes abnormalities of cardiac function during hypertrophy. In a morphometrical study, an increase in fibrosis in TF was associated with an increased diameter of myocytes and an increase of myocardial disarray[14]. In addition, the peri-vascular accumulation of collagen fibers may impair the vasodilator capacity of intramyocardial coronary arteries and may contribute to the decrease in coronary reserve[15].

Fibronectin is found in the extracellular matrix of most tissue, serving as a bridge between cells and interstitial collagen mesh network and influencing diverse processes including cell growth, adhesion, migration, and wound repair[16]. In rats, fetal fibronectin was shown to be accumulated during development of cardiac hypertrophy by pressure overload[17]. The hypertrophied heart exhibits significant qualitative as well as quantitative changes in gene expression. The altered expression patterns in hypertrophy, include transient expression of proto-oncogenes[18]. It is thought that those changes in cardiac hypertrophy reflect a change toward an embryonic program of gene expression[19].

However, it is still not clarified whether those altered expression patterns are general markers of cardiac hypertrophy or markers of a specific parallel pathogenic process such as TF. Animal studies have shown that the levels of mRNA for fibronectin and collagens were elevated in cardiac hypertrophy[17].

Most attention in research on human TF so far is focused on clinical treatment and surgical methods to limit the myocardial injury. TF patients are usually operated during their first years of life. The aim of early primary repair is to close the ventricular septal defect and to remove the right ventricular outflow tract obstruction, thus relieving the hypoxemia and eliminating the stimulus for the adaptive RVH as well as preserving right ventricular function[1,20]. However, after corrective surgery some patients develop right ventricular failure due to volume-overload caused by pulmonary regurgitation and may for this reason require further secondary corrective surgery later in life[21,22]. Histopathological studies on TF myocardial tissue reported that the myocardial cell diameter was reduced in patients after corrective surgery, indicating regression of RVH. Nevertheless, it is not yet known to what extent the RVH in TF patients regresses. Only little attention has been paid to the molecular component of the disease. In this study, we examined the degree of fibrosis in human TF by measuring the expression of myocardial fibrosis markers such as fibronectin and collagen in right ventricular biopsies obtained during corrective surgery for TF and compared the data with that of age matched patients with normal right ventricle.

Materials and Methods

Biopsies

The present study was approved by the Medical Ethical Committee of the University Hospital, Erasmus University, Rotterdam. Myocardial tissue biopsies were obtained from patients who underwent primary corrective surgery (TF-1, mean age 0.7 ± 0.2 years, n=11), secondary surgery (TF-2, mean age 36.9 ± 4.6 years, n=6) and age matched control patients. All control patients had clinically normal right ventricle and underwent autograft aortic root replacement (C-1, mean age 1.5 ± 0.2 years, n=6 and C-2, mean age 31.7 ± 4.2, n=12). Myocardial tissue was fixed in 4% paraformaldehyde in

PBS for minimal 24 hours and further processed for dehydration and embedding in paraffin for histological and immunohistochemical studies[23].

Picro-sirius red staining

The total collagen in myocardial tissue specimens was stained with Picro-sirius red F3BA[24]. Tissue sections of 6 μm thickness, were treated with 0.2% aqueous phosphomolybdic acid and incubated in 0.1% Picro-sirius red. Before dehydration, the slides were treated with 0.01N HCl and mounted. The Picro-sirius red stained area was determined as percentage of total tissue area using a Kontron-KS 400 (Kontron Electronik/Zeiss, Eching, Germany) computerized image analysis system. Distribution of collagen fibers in the interstitial space as well as in the peri-vascular region was measured as Picro-sirius red positive area. 12 different images from each section were analyzed to calculate the mean of percentage stained tissue area and statistically significant values were accepted at $p \leq 0.05$.

Immunohistochemistry

After fixation and dehydration, the cardiac tissue was embedded in paraffin. Sections of 6 μm thickness were cut and mounted on poly-L-lysin coated microscope slides, followed by immunohistochemistry using avidin-biotin complex (ABC) method (BioGenex, San Ramon, CA). The sections were deparaffinized and quenched for endogenous peroxidase by 2% hydrogen peroxide in methanol. Non-specific binding sites were blocked by 10% normal goat serum. Human serum pre-absorbed polyclonal antibodies, against human fibronectin in 1:1000 dilution (Life Technologies, Breda, The Netherlands), were applied as primary antiserum and the sections were incubated at room temperature for 30 min. Negative controls were performed by omission of the primary antibody. After washing in 0.5% tween-20 in PBS solution, the sections were incubated with mouse biotinylated anti-rabbit IgG (BioGenex, San Ramon, CA) for 30 min. and subsequently, with peroxidase conjugated streptavidin. Color was developed using 3,3'-diaminobenzidine tetrahydrochloride dehydrate (DAB) and then sections were counter stained with hematoxylin. Sections were mounted and visualized under the light microscope and photographed. A semi-quantitative analysis of the sections was done by 2 independent observers using a staining score ranging from 0 (no staining) to 4 (very

strong, dark brown, staining) to asses the level of fibronectin expression in the myocardial tissue obtained from TF patients and age matched controls.

Results and discussion

Picro-sirius red staining was performed for the total collagens in order to assess the degree of myocardial fibrosis. The red staining was quantified by video imaging and showed a significantly increased interstitial and peri-vascular staining for total collagens in TF-1 (1.4 ± 0.2 fold) (Fig. 2.1B and D) and TF-2 (1.6 ± 0.2 fold) (Fig. 2.1C and D) as compared to their respective controls (Fig. 2.1A and D). The immunolocalization of fibronectin showed that fibronectin was expressed in the interstitium, in the peri-vascular area, as well as in some cardiomyocytes. Semiquantitative analysis using a staining score ranging from 0-4, revealed that the fibronectin expression was significantly increased in TF-1 (Fig. 2.2B and D) as compared to control (3.0 ± 0.2 *vs.* 2.6 ± 0.2)(Fig. 2.2B and D). There were no differences in fibronectin expression in patients from TF-2 (Fig. 2.2B and D) as compared with age-matched controls. Our results indicate an increased amount of myocardial extracellular matrix deposition in RVH in patients with TF, with an apparent increase of total collagen and a slight increase in fibronectin at young age.

The apparent development of cardiac hypertrophy is induced by changes in cardiac gene expression that provide the heart means of compensation for increased haemodynamic load[25]. In this regard, our data are in agreement with the histopathologic findings from the right ventricular myocardium in preoperative TF that show interstitial fibrosis, myofibrillar disorganization, disarray and degenerative changes in addition to myocardial cell hypertrophy[18,26,27]. The changes as found in our study for expression of collagens and fibronectin could be attributed to altered structure or function of the myocardium. It is believed that changes in gene expression accompanying cardiac hypertrophy are the result of a multifactorial process and the observed changes may therefore be concomitant a phenomena. The alteration in ventricular gene expression might be an indicator of cardiac hypertrophy and may result from a number of different stimuli. We assume that the changes in the right ventricular fibronectin and collagen

expression in TF patients could be as a result of increased haemodynamic load as it has been often found to be parallel with the increase in ventricular mass[19].

In case of TF patients, the early increase of collagen and fibronectin deposition in the right ventricle may occur because the original myocardial extracellular matrix has been expanded and weakened due to the haemodynamic overload. The myocardium will compensate until enough new collagen has been produced to restore tensile strength and to resist the distending forces. Our findings in the TF-1 and TF-2 group fit into this

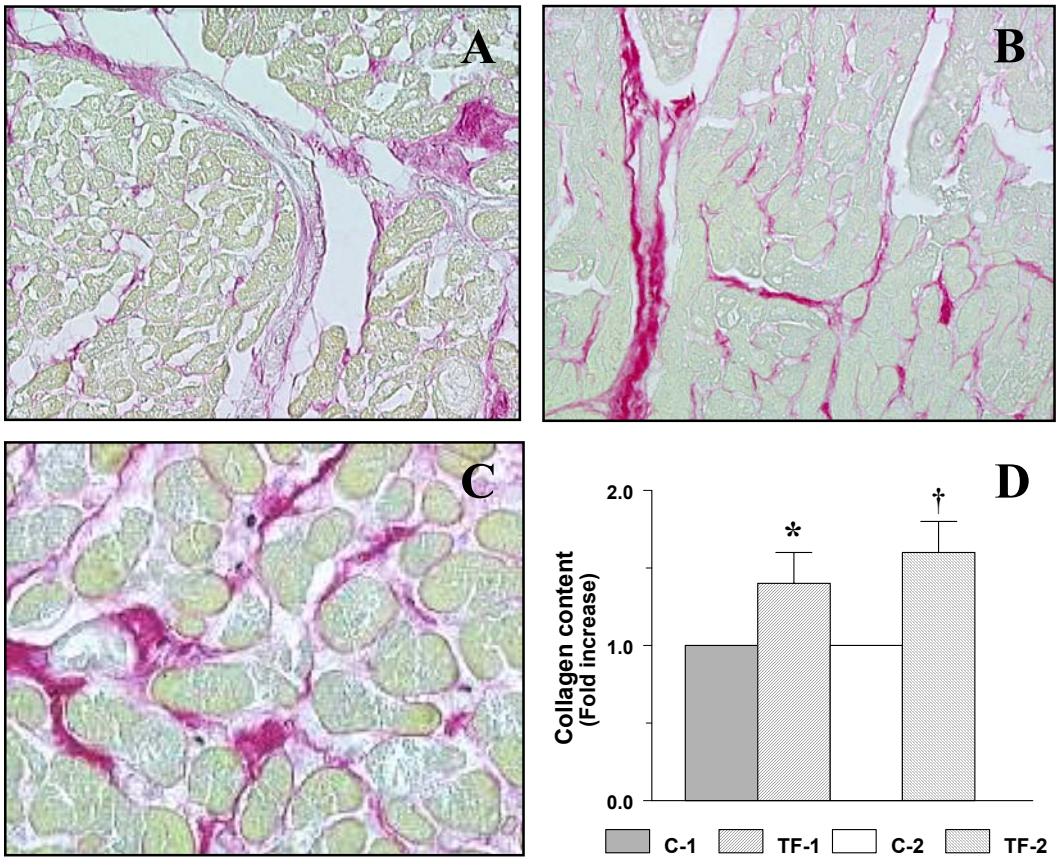

Figure 2.1. Right ventricular total collagen content in patients with tetralogy of Fallot. Micro-photographs of the human right ventricular tissue obtained from patients undergoing surgery; panel **A:** for autograft aortic root replacement (Control), panel **B:** for primary repair due to tetralogy of Fallot (TF-1) and panel **C:** for secondary surgery (TF-2). Tissue sections were prepared and stained with collagen specific stain, Picro-sirius red. Collagen fibers appear red and are localized in interstitial and peri-vascular areas. Note the interstitial fibrosis in the case of TF patients. Panel **D:** Bar diagram depicting significantly enhanced interstitial collagen content in both TF-1 and TF-2 group as compared to the control. Distribution of collagen fibers in tissue was visualized under normal and polarized light and quantified using video imaging software. Values are fold induction and shown as mean ± SEM of Picro-sirius red positive interstitial/total tissue area.

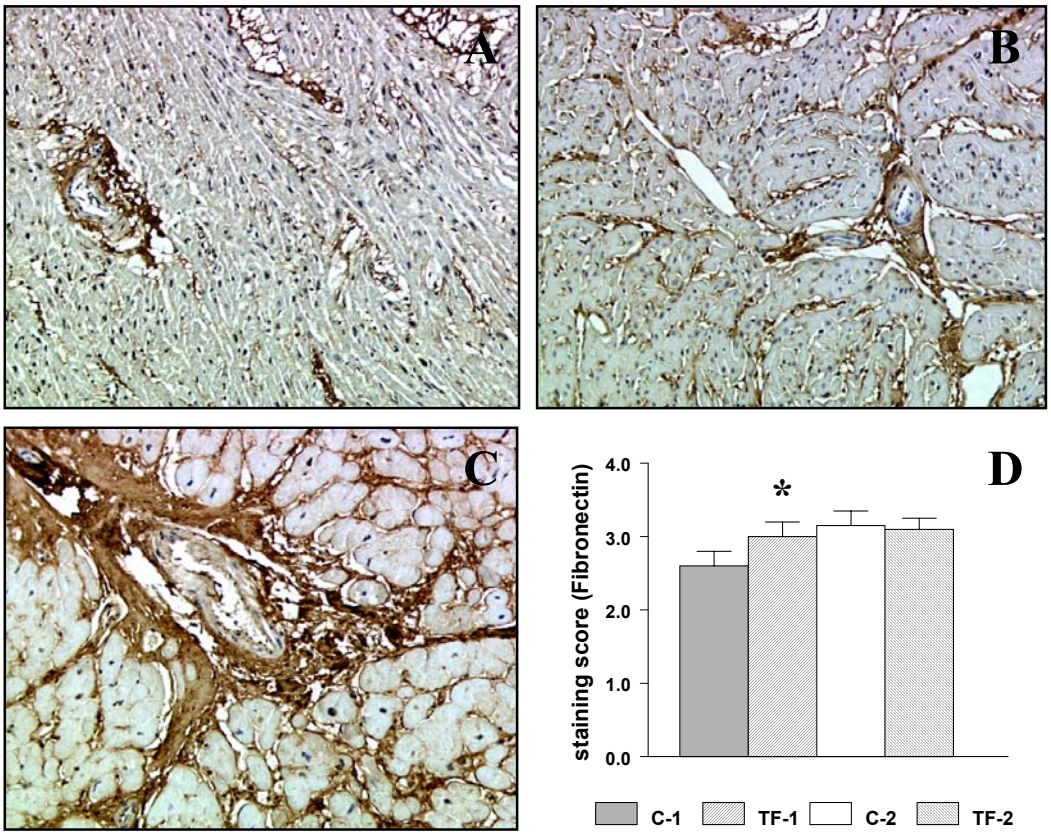

Figure 2.2. Immunohistochemical localization of fibronectin in right ventricular tissue of patients with tetralogy of Fallot. Micro-photographs showing human right ventricular tissue stained with rabbit-anti-human fibronectin polyclonal antibodies(as described in materials and methods) from patients undergoing surgery; panel **A:** for autograft aortic root replacement (Control), panel **B:** for primary repair for tetralogy of Fallot (TF-1) and panel **C:** for secondary surgery (TF-2). Panel **D:** Bar diagram depicting significantly enhanced interstitial fibronectin staining in the TF-1 group as compared to the respective controls. A semiquantitative analysis of the section was done by 2 independent observers using a staining score ranging from 0 (no staining) to 4 (very strong, dark brown, staining) to assess the levels of fibronectin staining. Values are shown as mean ± SEM.

concept as the TF-2 shows a more prominent increase in the amount of collagen as compared to TF-1. Corrective surgery limit the myocardial overload and may therefore limits the amount of damage to the myocardial collagen matrix[6]. Our study provide further evidence that myocardial architecture in patients with TF depicts fibrosis as the expression levels of extracellular matrix components like collagens and fibronectin were elevated. However, further research at the mRNA level would add to the notion that the gene expression of a number of proteins involved in fibrosis was transcriptionally altered.

Summary and conclusions

In the present study the degree of myocardial fibrosis at protein level in patients with tetralogy of Fallot was examined by assessing quantitatively the expression of total collagens and fibronectin. We found a significant increase in staining for interstitial and total collagens at primary correction as well as at secondary corrective surgery as compared to the age matched control patients. However, immuno-histochemical localization of fibronectin revealed significant increase in this protein levels at primary correction only. Our results clearly demonstrate an increased amount of myocardial extracellular matrix deposition resulting in tissue fibrosis in TF patients with right ventricular hypertrophy. This vital information could be of great help in assessing the timing of surgery as well as post-operative prognosis.

Acknowledgements

Financial support from the Netherlands Heart Foundation (NHS 96.082) is gratefully acknowledged.

References

1. Castaneda AR, Jonas RA, Mayer JE, et al. *Cardiac surgery of neonate and infant*. Philadelphia, USA: Saunders; 1994.
2. Arai M, Matsui H, Periasamy M. Sarcoplasmic reticulum gene expression in cardiac hypertrophy and heart failure. *Circ Res*. 1994;74:555-564.
3. Boluyt MO, L. O, Meredith AL, et al. Alterations in cardiac gene expression during the transition from stable hypertrophy to heart failure. Marked upregulation of genes encoding extracellular matrix components. *Circ Res*. 1994;75:23-32.
4. van Bilsen M, Chien KR. Growth and hypertrophy of the heart: towards an understanding of cardiac specific and inducible gene expression. *Cardiovasc Res*. 1993;27:1140-1149.
5. Schwartz K, Carrier L, Mercadier JJ, et al. Molecular phenotype of the hypertrophied and failing myocardium. *Circulation*. 1993;87:VII 5-10.
6. Whittaker P. Collagen and ventricular remodelling after acute myocardial infarction: concepts and hypotheses. *Basic Res Cardiol*. 1997;92:79-81.
7. Weber KT, Sun Y, Tyagi SC, et al. Collagen network of the myocardium: function, structural remodelling and regulatory mechanisms. *J Mol Cell Cardiol*. 1994;26:279-292.

8. Bishop JE, Rhodes S, Laurent GJ, et al. Increased collagen synthesis and decreased collagen degradation in right ventricular hypertrophy induced by pressure overload. *Cardiovasc Res*. 1994;28:1581-1585.
9. Brilla CG, Janicki JS, Weber KT. Impaired diastolic function and coronary reserve in genetic hypertension. Role of interstitial fibrosis and medial thickening of intramyocardial coronary arteries. *Circ Res*. 1991;69:107-15.
10. Chapman D, Weber KT, Eghbali M. Regulation of fibrillar collagen types I and III and basement membrane type IV collagen gene expression in pressure overloaded rat myocardium. *Circ Res*. 1990;67:787-794.
11. Jalil JE, Doering CW, Janicki JS, et al. Fibrillar collagen and myocardial stiffness in the intact hypertrophied rat left ventricle. *Circ. Res*. 1989;64:1041-1050.
12. Hess OM, Schneider J, Koch R, et al. Diastolic function and myocardial structure in patients with myocardial hypertrophy. Special reference to normalized viscoelastic data. *Circulation*. 1981;63:360-371.
13. McLenachan JM, Dargie HJ. Ventricular arrhythmias in hypertensive left ventricular hypertrophy. Relationship to coronary artery disease, left ventricular dysfunction, and myocardial fibrosis. *Am J Hypertens*. 1990;3:735-740.
14. Kawai S, Okada R, Kitamura K, et al. A morphometrical study of myocardial disarray associated with right ventricular outflow tract obstruction. *Jpn Circ J*. 1984;48:445-456.
15. Strauer BE. The significance of coronary reserve in clinical heart disease. *J Am Coll Cardiol*. 1990;15:775-783.
16. Farhadian F, Contard F, Corbier A, et al. Fibronectin expression during physiological and pathological cardiac growth. *J Mol Cell Cardiol*. 1995;27:981-990.
17. Samuel JL, Barrieux A, Dufour S, et al. Accumulation of fetal fibronectin mRNAs during the development of rat cardiac hypertrophy induced by pressure overload. *J Clin Invest*. 1991;88:1737-1746.
18. Brand T, Sharma HS, Fleischmann KE, et al. Proto-oncogene expression in porcine myocardium subjected to ischemia and reperfusion. *Circ Res*. 1992;71:1351-1360.
19. Vikstrom KL, Bohlmeyer T, Factor SM, et al. Hypertrophy, pathology, and molecular markers of cardiac pathogenesis. *Circ Res*. 1998;82:773-778.
20. Starnes VA, Luciani GB, Latter DA, et al. Current surgical management of tetralogy of Fallot. *Ann Thorac Surg*. 1994;58:211-215.
21. Murphy JG, Gersh BJ, Mair DD, et al. Long-term outcome in patients undergoing surgical repair of tetralogy of Fallot. *N Engl J Med*. 1993;329:593-599.
22. Warner KG, Anderson JE, Fulton DR, et al. Restoration of the pulmonary valve reduces right ventricular volume overload after previous repair of tetralogy of Fallot. *Circulation*. 1993;88:II189-197.
23. Sharma HS, Tang ZH. Expression and immunohistochemical localization of vascular endothelial growth factor during ischemia induced ventricular dysfunction in pigs. *Circulation*. 1994;90:I-522.
24. Takahashi T, Schunkert H, Isoyama S, et al. Age-related differences in the expression of proto-oncogene and contractile protein genes in response to pressure overload in the rat myocardium. *J Clin Invest*. 1992;89:939-946.
25. Katz AM. Cardiomyopathy of overload. A major determinant of prognosis in congestive heart failure. *N. Engl. J. Med*. 1990;322:100-110.

26. Brand T, Sharma HS, Schaper W. Expression of nuclear proto-oncogenes in isoproterenol-induced cardiac hypertrophy. *J Mol Cell Cardiol*. 1993;25:1325-1337.
27. Mitsuno M, Nakano S, Shimazaki Y, et al. Fate of right ventricular hypertrophy in tetralogy of Fallot after corrective surgery. *Am J Cardiol*. 1993;72:694-698.

Chapter 3

Computerized image analysis in the quantitative assessment of interstitial fibrosis late after correction of tetralogy of Fallot

Based on:
Peters THF, Sharma HS and Bogers AJJC. Computerized image analysis in the quantitative assessment of interstitial fibrosis late after correction of tetralogy of Fallot. Cardiovasc Eng 2003; 8:114-120.

Abstract

Objective: To explore the possibilities of computerized image analysis in determining the extent of right ventricular (RV) fibrosis in tetralogy of Fallot (TF) by evaluating the expression pattern of collagen and fibronectin in myocardial biopsies.

Methods: RV biopsies were obtained from 12 patients at corrective surgery (TF-1, mean age 0.8 ± 0.1 years) and 10 patients at reoperation for pulmonary regurgitation after correction of TF (TF-2, mean age 30.1 ± 2.4 years). Comparison was made with 10 mean age matched patients operated for pulmonary autograft root replacement (PAG) (age 27.4 ± 0.9 years) and 5 normal hearts (NL) from heart valve donors (age 29.8 ± 3.9 years). Expression patterns of collagen and fibronectin were analyzed using the Leica Qwin standard Y2.2b image analysis software.

Results: Total collagen expression was significantly higher in TF-2 than in TF-1 (TF-1 12.5±0.7% *vs.* TF-2 19.2±2.4%, $p<0.05$), but not different from NL, while PAG showed higher levels than NL (TF-2 19.2±2.4% *vs.* PAG 22.5 ± 2.7% *vs*. NL 16.9 ± 1.7%, $p<0.05$). Interstitial collagen was also higher in TF-2 (TF-1 11.2 ± 0.7% *vs.* TF-2 18.6 ± 2.3%, $p<0.05$). TF-2 and PAG did not differ, but PAG differed from NL (TF-2 18.6 ± 2.3% *vs*. PAG 21.8 ± 2.7% *vs.* NL 16.1 ± 1.5%, $p<0.05$). Peri-vascular collagen, corrected for vascular lumen area, was higher in TF-1 (TF-1 ratio 17.8 ± 1.9 *vs.* TF-2 ratio 9.8 ± 1.2, $p<0.05$) but also increased in PAG (TF-2 ratio 9.8 ± 1.2 *vs.* PAG ratio 14.6 ± 2.2 *vs.* NL ratio 8.9 ± 1.6, $p<0.05$).

Total fibronectin expression showed no difference in TF-1 and TF-2, but lower values of TF-2 comparing with PAG and NL (TF-2 14.7 ± 1.5% *vs.* PAG 20.2 ± 3.6% *vs.* NL 20.3 ± 1.5%, $p<0.05$). There were lower values of interstitial fibronectin in TF-2 comparing with PAG and NL (TF-2 14.1 ± 1.4% *vs.* PAG 19.8 ± 3.6% *vs.* NL 20.0 ± 1.5%, $p<0.05$). Peri-vascular fibronectin, corrected for vascular lumen area, in TF-2 was higher than in PAG and NL (TF-2 ratio 7.1 ± 1.2 *vs*. PAG ratio 4.9 ± 0.9 *vs.* NL ratio 3.7 ± 0.5, $p<0.05$).

Conclusion: Computerized image analysis is a useful and effective adjunct in the analysis of RV hypertrophy in TF. Using this technique we found a higher content of total and interstitial collagen, but a lower peri-vascular collagen ratio in older patients who got re-do surgery. This was accompanied by a lower amount of total and interstitial fibronectin and an increased fibronectin peri-vascular ratio. Using this technique we also found that RV biopsies from pulmonary autograft patients can not be regarded as normal, despite clinically normal RV function. Our findings leave room for improvement of contemporary clinical treatment of patients with TF by allowing an assessment of the adequacy of timing for surgery.

Introduction

Nowadays most patients with tetralogy of Fallot (TF) are operated in their first year of live by primary repair. The aim of early primary repair is to relieve the hypoxemia and to eliminate the stimulus for the adaptive right ventricular hypertrophy (RVH) as well as to preserve right ventricular (RV) function[1]. On long-term follow up however, a number of patients suffer from pulmonary regurgitation after primary correction, causing RV dilatation and failure due to volume-overload. For these patients further secondary corrective surgery later in life is performed by implanting a pulmonary allograft heart valve between the RV and the pulmonary artery[2,3]. At these different stages of disease, there is a different and evoluating response of the RV myocardium, leading to remodeling of the myocardium and to the development of fibrosis[4-6]. Collagen and fibronectin both play an important part in myocardial fibrosis. The collagen network in the extracellular space of the myocardium, consists of collagen fibers, which provide the myocardial strength[7-9]. Experimental[10] and clinical data[11] show that a rise in the collagen content increases the myocardial stiffness and promotes abnormalities of cardiac function during hypertrophy. An increase in fibrosis in TF was associated with an increased diameter of myocytes and an increase of myocardial disarray[12]. In this regard, fibronectin, located in the extracellular matrix of most tissues, serves as a bridge between cells and interstitial collagen mesh network. It further influences diverse processes including cell growth, adhesion, migration, and wound repair[13].

Most attention in research on human TF so far is focused on clinical treatment and surgical methods. In addition, histopathological data on TF myocardial tissue showed a reduction of the myocardial cell diameter in patients after corrective surgery[14]. This would indicate a diminishing degree of RVH. Hardly any research has been done in TF at molecular level. In this study, we examined the degree of fibrosis at protein level in human TF by evaluating the expression of collagen and fibronectin in RV biopsies obtained during redo surgery and compared the data with that of age matched patients with a normal RV.

Material and Methods

Patients

Our study was approved by the Medical Ethical Committee of the University Hospital Rotterdam (MEC153.268/1996/119). The group of patients operated upon for primary correction of TF (TF-1) consisted of 12 patients. The mean age of the TF-1 group at the time of operation was 0.8 ± 0.1 years. The group of patients operated upon for pulmonary allograft implantation late after correction of TF (TF-2) consisted of 10 patients, with a mean age of 30.1 ± 2.4 years. They were compared with an age-matched control group consisting of 10 patients who were operated upon for a pulmonary autograft root replacement (PAG) with a mean age of 27.4 ± 0.9 years and with a group of 5 normal hearts (NL) from heart valve donors (mean age 29.8 ± 3.9 years). All patients operated upon for a pulmonary autograft procedure showed clinically normal RV function.

All operations were done with the use of cardiopulmonary bypass with moderate hypothermia using bicaval cannulation. In selected cases of both PAG and TF-2, single right atrial cannulation was used. St.Thomas hospital cardioplegic solution was applied except in some of the TF-2 patients, in whom the pulmonary allograft was implanted in the beating heart. In TF-1 pulmonary valve function was preserved in 7 patients, a transannular patch was necessary in the remaining 5 patients. In patients with preserved pulmonary valve function the biopsies consisted of removed endomyocardial tissue from the RV outflow tract. In patients with a transannular patch the biopsies consisted of a transmural sample from the incision in the anterior RV wall. In TF-2 pulmonary allografts were implanted as previously described[15,16]. Biopsies consisted of tissue from the anterior free wall of the right ventriculotomy. All PAG procedures were done as previously described[17,18]. In harvesting the pulmonary autograft, the main pulmonary artery was transsected just proximal to its bifurcation and excision was done from the right RV outflow tract leaving a ridge of supporting myocardial cuff. From the area of the free RV wall of this cuff the PAG biopsies were taken as a transmural sample. Five biopsies were obtained from normal hearts from the Heart Valve Bank Rotterdam (Heart Valve Bank Rotterdam, Rotterdam, The Netherlands)

The myocardial biopsies were fixed in 4% paraformaldehyde in PBS for at least 24 hours and further processed for dehydration and embedding in paraffin for histological and immunohistochemical studies.

There was no operative or other early mortality. There were no complications that could be attributed to taking the biopsies.

Picro-sirius red staining

The total collagen in myocardial tissue specimens was stained with Picro-sirius red F3BA[19]. Tissue sections (5 μm thickness) were treated with 0.2% aqueous phosphomolybdic acid and incubated in 0.1% Picro-sirius red. Before dehydration, the slides were treated with 0.01N HCl and mounted. Slides were visualized under light microscope and eventually collagen contents were quantified.

Immunohistochemistry

Paraffin sections (5 μm thickness) of the myocardial tissues were cut and mounted on 3-amino-propyl-trioxysilane (Sigma, St Louis, MO, USA) coated glass slides. Immunohistochemistry using a multiple step avidin-biotin complex (ABC) method was performed essentially following suppliers instructions. In brief, after deparaffinization in xylene and rehydration through graded alcohol the slides were rinsed with water and phosphate buffered saline and quenched for endogenous peroxidase by 2 % hydrogen peroxide in methanol. The slides were placed in a Sequeza Immunostaining Workstation (Shandon Scientific, Astmoor, UK). Slides were pre-incubated for 15 minutes with 10% normal goat serum to block non-specific binding. Specific human-preabsorbed polyclonal antibodies, against human fibronectin in 1:1000 dilution (Life Technologies, Breda, The Netherlands), were applied as primary antiserum and the sections were incubated at room temperature for 30 min. The supra optimal dilution was obtained by examining the intensity of staining obtained with a series of dilutions of the antisera from 1:100 to 1:2500 and selecting the dilution that gave specific but easily visible signals. Negative controls were performed by omission of the primary antibody. After washing in 0.5% tween-20 in PBS solution, the sections were incubated with mouse biotinylated anti-rabbit IgG (BioGenex, San Ramon, CA, USA) for 30 min and subsequently with peroxidase conjugated streptavidin. Color was developed using DAB (3,3'-diaminobenzidine tetrahydrochloride dehydrate) and the

sections were counterstained with hematoxylin. Sections were mounted and visualized under the light microscope and fibronectin was quantified.

Video image analysis

Expression of collagen as well as fibronectin was quantitatively analyzed using a video image analysis system. For video image analysis, all the myocardial tissue specimens were stained at the same time to prevent variations in staining conditions. After staining, the sections were mounted and visualized under a Leica DM RBE light

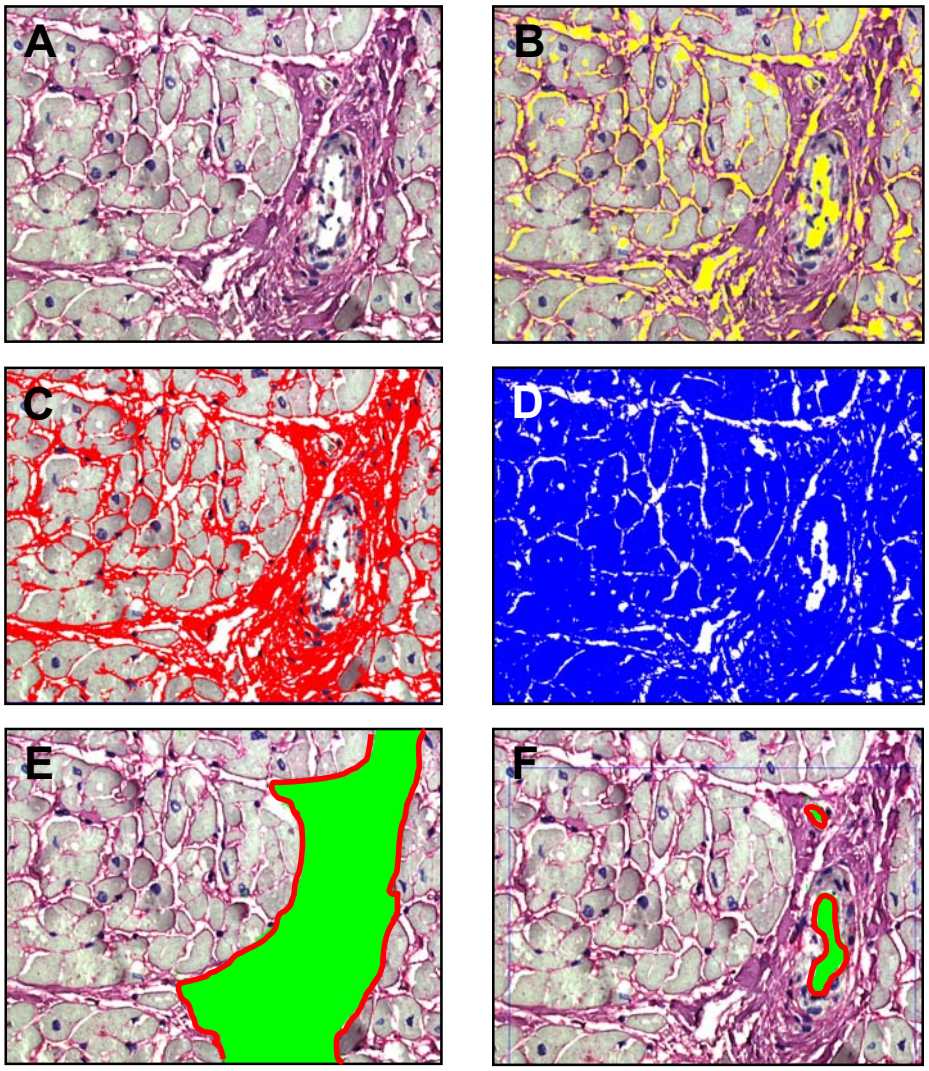

Figure 3.1. Video image analysis cycles.
A: Image. **B:** Binary 1, background in yellow. **C:** Binary 2, total staining in red. **D:** Binary 3, total tissue area in blue. **E:** Binary 4, peri-vascular area in green lined with red. **F:** Binary 7, lumen area in green lined with red.

microscope (Leica, Wetzlar, Germany) using a 20x lens. The microscopic light was optimized with a standard grey filter, a N16 neutralizing filter and a daylight filter. From each section a series of 12 digital color images (736x574 pixels) were taken from a representative area of the myocardium with a Sony DXC-950 3 CCD Power HAD color video camera (Sony, Tokyo, Japan) after auto white balancing. The camera contains a 0.5 inch tree-chip powered hole-accumulated (HAD) charge-coupled device (CCD) light sensitive (2000 lux, F8.5, 3200K) chip with a resolution of 752x582 effective picture elements (horizontal resolution of 750 TV lines) and a scanning frequency of 15.625 kHz horizontal and 50 Hz vertical. All sections were photographed in the same session, using the same settings for the microscope and the Dell dimension XPS D266 computer with 64 RAM, connected to a 19.6 inch high resolution Dell D2128-TCO screen with 1024x768 pixel setting, powered by a Mantrox Millennium II AGP graphics card and software (Dell, Amsterdam, The Netherlands). The digital images were analyzed for the staining of interest with a special designed analysis program (macro) for the Leica Qwin standard image analysis software (Y2.2b) (Leica Imaging Systems, Cambridge, UK) operating under Microsoft windows 95 (Microsoft, Redmond, WA, USA). After optimalization, the staining detection levels for hue, saturation and intensity in the computer were set and used for analysis of all images derived from one staining session. The analysis macro is designed to reduce the staining background by eroding and dilating each pixel followed by creating binary files for the detected color intervals. Binary files are created for white background (Binary1), total stained area (Binary2), tissue area (Binary3 = total image - Binary1), peri-vascular area (Binary4; drawn manually), peri-vascular staining (Binary5; overlap of Binary2 and Binary4), interstitial staining (Binary6 = Binary2 - Binary5) and vessel lumen area (Binary7; drawn manually)(Fig. 3.1). Results are expressed as the ratio of staining area per analyzed total tissue area. Interstitial staining is expressed as percentage stained tissue area excluding peri-vascular area per analyzed total tissue area. Peri-vascular staining is expressed as percentage peri-vascular staining per analyzed total tissue area. Peri-vascular staining was normalized to its vascular lumen area, to correct for the vessel size, and expressed as the ratio of peri-vascular stained area divided by vascular lumen area[20].

Statistical analysis

The collagen and fibronectin staining scores were calculated percentually for the different groups in our study. The results are expressed as mean ± standard error of mean. Scoring values were compared by Student's t-test. Results were accepted as statistically significant with $p \leq 0.05$.

Results

Collagen expression

Picro-sirius red staining for collagen depicted a myocardial collagen localization pattern predominantly in the interstitium as well as limited in peri-vascular areas in all patients. Analysis of total collagen expression showed a significant higher level in TF-2 as compared with TF-1 (TF-1 12.5 ± 0.7% *vs*. TF-2 19.2 ± 2.4%, $p<0.05$). There was no significant difference with NL, but PAG showed a significantly higher level compared to NL (TF-2 19.2 ± 2.4% *vs*. PAG 22.5 ± 2.7% *vs*. NL 16.9 ± 1.7%, $p<0.05$). This difference was also found comparing interstitial collagen in TF-1 and TF-2 (11.2 ± 0.7% *vs*. 18.6 ± 2.3%, $p<0.05$). Interstitial collagen in PAG was higher compared to NL (TF-2 18.6 ± 2.3% *vs*. PAG 21.8 ± 2.7% *vs*. NL 16.1 ± 1.5%, $p<0.05$). No differences were found in peri-vascular collagen percentages. Peri-vascular collagen,

Table 3.1. Data on expression of total collagen and fibronectin.

	TF-1	TF-2	PAG	NL
Collagen				
Total (%)	12.5±0.7	19.2±2.4[1]	22.5±2.7[2]	16.9±1.7
Interstitial (%)	11.2±0.7	18.6±2.3[1]	21.8±2.7[2]	16.1±1.5
Peri-vascular (%)	1.2±0.1	0.6±0.2[1]	0.7±0.1	0.8±0.1
Peri-vascular ratio	17.8±1.9	9.8±1.2[1]	14.6±2.2[3]	8.9±1.6
Fibronectin				
Total (%)	12.8±1.8	14.7±1.5[4]	20.2±3.6	20.3±1.5
Interstitial (%)	12.4±1.8	14.1±1.4[4]	19.8±3.6	20.0±1.5
Peri-vascular (%)	0.4±0.1	0.6±0.1	0.4±0.1	0.3±0.1
Peri-vascular ratio	5.7±0.6	7.1±1.2[4]	4.9±0.9	3.7±0.5

[1]$p<0.05$ compared to TF-1, [2]$p<0.05$ compared to NL, [3]$p<0.05$ compared to TF-1, TF-2 and NL, [4]$p<0.05$ compared to PAG and NL

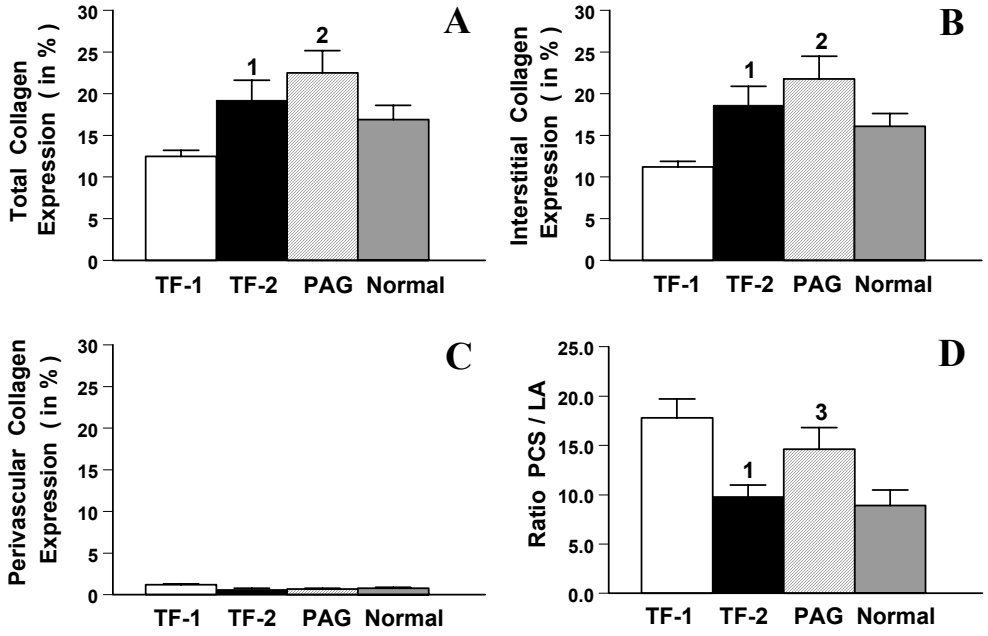

Figure 3.2. Right ventricular collagen content in tetralogy of Fallot.
TF-1: right ventricular biopsies from correction of tetralogy of Fallot at young age. TF-2: right ventricular biopsies from redo operation with allograft insertion in the pulmonary position late after correction for tetralogy of Fallot. PAG: right ventricular biopsies harvested from the pulmonary autograft procedure. Normal: right ventricular biopsies from normal hearts from heart valve donors. PCS: perivascular collagen staining. LA: lumen area. [1]$p<0.05$ compared to TF-1. [2] $p<0.05$ compared to NL. [3] $p<0.005$ compared to TF-1, TF-2, and NL

corrected for vascular lumen area, showed a higher value in TF-1 (TF-1 ratio 17.8 ± 1.9 *vs.* TF-2 ratio 9.8 ± 1.2, $p<0.05$). TF-2 showed comparable levels to NL, but PAG was significantly higher than NL (TF-2 ratio 9.8 ± 1.2 *vs.* PAG ratio 14.6 ± 2.2 *vs.* NL ratio 8.9 ±1 .6, $p<0.05$) (see table 3.1 and Fig. 3).

Fibronectin expression

Myocardial localization of fibronectin showed that the expression is confined predominantly to the interstitial and limited to the peri-vascular regions, as well as to the cytoplasm of some cardiomyocytes in all groups.

Fibronectin expression analysis showed no difference when TF-1 was compared with TF-2 (TF-1 12.8 ± 1.8% *vs.* TF-2 14.7 ± 1.5%, p=ns) and a lower value for TF-2 compared with PAG and NL was found (TF-2 14.7 ± 1.5% *vs.* PAG 20.2 ± 3.6% *vs.* NL 20.3 ± 1.5%, $p<0.05$). This was also found comparing interstitial fibronectin in TF (TF-1 12.4 ± 1.8% *vs.* TF-2 14.1 ± 1.4%, p=ns). Interstitial fibronectin was

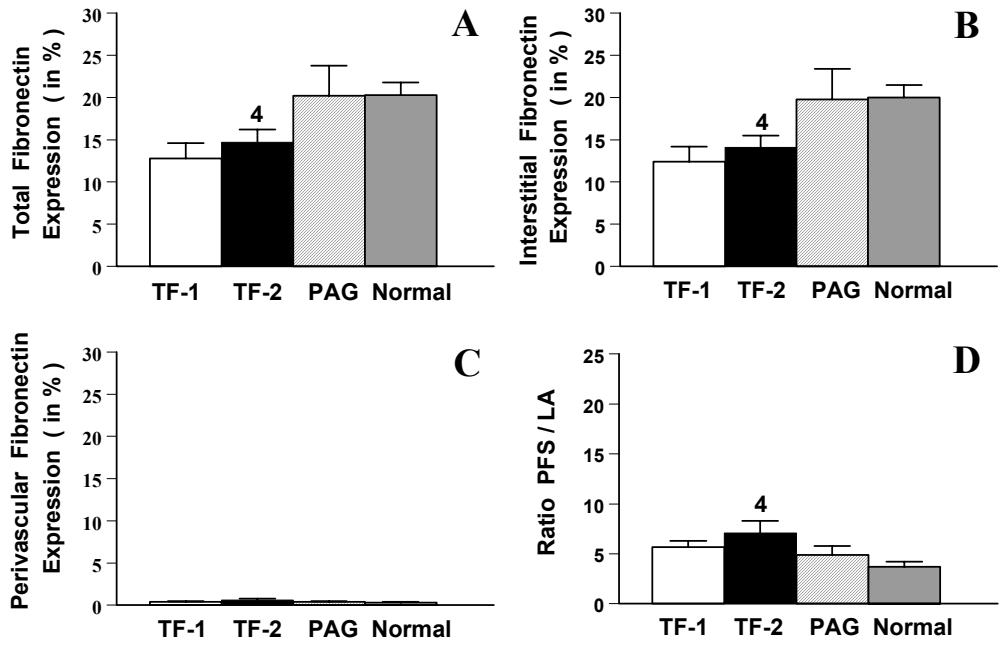

Figure 3.3. Right ventricular fibronectin content in tetralogy of Fallot.
TF-1: right ventricular biopsies from correction of tetralogy of Fallot at young age. TF-2: right ventricular biopsies from redo operation with allograft insertion in the pulmonary position late after correction for tetralogy of Fallot. PAG: right ventricular biopsies harvested from the pulmonary autograft procedure. Normal: right ventricular biopsies from normal hearts from heart valve donors. PFS: perivascular fibronectin staining. LA: lumen area. [4]$p<0.05$ compared PAG and NL

significantly lower in TF-2 compared to PAG and NL (TF-2 14.1 ± 1.4% *vs.* PAG 19.8 ± 3.6% *vs.* 20.0 ± 1.5%, $p<0.05$). No differences were found in peri-vascular fibronectin percentages. Peri-vascular fibronectin, corrected for vascular lumen area, did not differ in TF (TF-1 ratio 5.7 ± 0.6 *vs.* TF-2 ratio 7.1 ± 1.2, $p<0.05$), but showed higher values compared to PAG and NL (TF-2 ratio 7.1 ± 1.2 *vs.* PAG ratio 4.9 ± 0.9 *vs.* NL ratio 3.7 ± 0.5, $p<0.05$) (table 3.1 and Fig. 3.3).

Discussion

Our results indicate an increased amount of myocardial extracellular matrix deposition in RV myocardium in TF-2 patients as compared to TF-1. Collagen content increased to

above values for normal myocardium, in contrast to the fibronectin values. This indicates a larger contribution in TF-2 of collagen in the remodeling process than fibronectin.

The apparent development of cardiac hypertrophy in TF is induced by changes in cardiac gene expression that provide means of compensation for increased haemodynamic load. In this regard, our data are in agreement with the histopathologic findings from the RV myocardium in preoperative TF that show interstitial fibrosis, myofibrillar disorganization, disarray and degenerative changes in addition to myocardial cell hypertrophy[21,22].

The changes as found in our study for collagen and fibronectin expression may be induced by an altered structure or function of the myocardium and should be regarded as the result of a multifactorial process. The observed changes may therefore be concomitant phenomena. We assume that the changes in the RV collagen expression in TF patients could be a result of increased haemodynamic load with a parallel increase in ventricular mass[23,24]. We have as yet no adequate explanation for the finding of limited increase of fibronectin expression, where the values for TF-2 were even below the normal control values. It might be necessary to correct the TF-2 values for the increased myocyte diameter which will result in a lower percentage of staining per total tissue area per image.

Our findings in the TF groups show a prominent increase in the amount of collagen in TF-2 as compared to TF-1. It is important to recognize that corrective surgery limits the myocardial overload and may therefore limit the amount of damage to the myocardial collagen matrix[9].

An additional striking finding of our studies was the increased amount of collagen in PAG patients as compared to normal controls. In the PAG patients values for fibronectin were comparable to normal values. However, our findings preclude the use of biopsies of PAG patients as a control group in the study of fibrosis in tetralogy of Fallot.

Our study provides further evidence that myocardial architecture in patients with TF depicts increased fibrosis at the expression level of extracellular matrix component. Video image analysis proved to be a useful tool in this regard. An important aspect is the

constant and consequent approach to the tissue handling and staining techniques on one hand and the settings of the software and hardware on the other hand. In this way more specific and objective measurements can be done. Computerized image analysis allows to objectivate the small differences in the peri-vascular accumulation of collagen and fibronectin (panels C and D in Fig. 3.1 and 3.2). In addition, further research at the mRNA level would add to the notion that the gene expression in fibrosis was altered.

Nevertheless, studies of this kind provide information that leaves room for improvement of contemporary clinical treatment of patients with tetralogy of Fallot by allowing an assessment of the adequacy of timing for surgery and consequently provide data that may be useful with regard to long-term postoperative prognosis.

Acknowledgements

Financial support from the Netherlands Heart Foundation (NHS 96.082) is gratefully acknowledged. We thank Mrs Yilmaz for technical support advice and the Heart Valve Bank Rotterdam for providing the control biopts.

References

1. Starnes VA, Luciani GB, Latter DA, et al. Current surgical management of tetralogy of Fallot. *Ann Thorac Surg*. 1994;58:211-215.
2. Warner KG, Anderson JE, Fulton DR, et al. Restoration of the pulmonary valve reduces right ventricular volume overload after previous repair of tetralogy of Fallot. *Circulation*. 1993;88:II189-197.
3. Murphy JG, Gersh BJ, Mair DD, et al. Long-term outcome in patients undergoing surgical repair of tetralogy of Fallot. *N Engl J Med*. 1993;329:593-599.
4. Schwartz K, Carrier L, Mercadier JJ, et al. Molecular phenotype of the hypertrophied and failing myocardium. *Circulation*. 1993;87:VII 5-10.
5. van Bilsen M, Chien KR. Growth and hypertrophy of the heart: towards an understanding of cardiac specific and inducible gene expression. *Cardiovasc Res*. 1993;27:1140-1149.
6. Boluyt MO, L. O, Meredith AL, et al. Alterations in cardiac gene expression during the transition from stable hypertrophy to heart failure. Marked upregulation of genes encoding extracellular matrix components. *Circ Res*. 1994;75:23-32.

7. Bishop JE, Rhodes S, Laurent GJ, et al. Increased collagen synthesis and decreased collagen degradation in right ventricular hypertrophy induced by pressure overload. *Cardiovasc Res*. 1994;28:1581-1585.
8. Weber KT, Sun Y, Tyagi SC, et al. Collagen network of the myocardium: function, structural remodelling and regulatory mechanisms. *J Mol Cell Cardiol*. 1994;26:279-292.
9. Whittaker P. Collagen and ventricular remodelling after acute myocardial infarction: concepts and hypotheses. *Basic Res Cardiol*. 1997;92:79-81.
10. Jalil JE, Doering CW, Janicki JS, et al. Fibrillar collagen and myocardial stiffness in the intact hypertrophied rat left ventricle. *Circ. Res*. 1989;64:1041-1050.
11. McLenachan JM, Dargie HJ. Ventricular arrhythmias in hypertensive left ventricular hypertrophy. Relationship to coronary artery disease, left ventricular dysfunction, and myocardial fibrosis. *Am J Hypertens*. 1990;3:735-740.
12. Kawai S, Okada R, Kitamura K, et al. A morphometrical study of myocardial disarray associated with right ventricular outflow tract obstruction. *Jpn Circ J*. 1984;48:445-456.
13. Farhadian F, Contard F, Corbier A, et al. Fibronectin expression during physiological and pathological cardiac growth. *J Mol Cell Cardiol*. 1995;27:981-990.
14. Seliem MA, Wu YT, Glenwright K. Relation between age at surgery and regression of right ventricular hypertrophy in tetralogy of Fallot. *Pediatr Cardiol*. 1995;16:53-55.
15. Hokken RB, Bogers AJJC, Spitaels SEC, et al. Pulmonary homograft insertion after repair of pulmonary stenosis. *J Heart Valve Dis*. 1995;4:182-186.
16. Bogers AJJC, Roofthooft M, Pisters H, et al. Longterm follow-up of gamma irradiated transannular homograft patch in surgical treatment of tetralogy of Fallot. *Thorac Cardiovasc Surgeon*. 1994;42:337-339.
17. Schoof PH, Cromme-Dijkhuis AH, Bogers AJJC, et al. Aortic root replacement with pulmonary autograft in children. *J Thorac Cardiovasc Surg*. 1994;107:367-73.
18. Hokken RB, Bogers AJJC, Taams MA, et al. Aortic root replacement with a pulmonary autograft. *Eur J Cardiothor Surg*. 1995;9:378-383.
19. Takahashi T, Schunkert H, Isoyama S, et al. Age-related differences in the expression of proto-oncogene and contractile protein genes in response to pressure overload in the rat myocardium. *J Clin Invest*. 1992;89:939-946.
20. Brilla CG, Janicki JS, Weber KT. Impaired diastolic function and coronary reserve in genetic hypertension. Role of interstitial fibrosis and medial thickening of intramyocardial coronary arteries. *Circ Res*. 1991;69:107-115.
21. Brand T, Sharma HS, Fleischmann KE, et al. Proto-oncogene expression in porcine myocardium subjected to ischemia and reperfusion. *Circ Res*. 1992;71:1351-1360.
22. Brand T, Sharma HS, Schaper W. Expression of nuclear proto-oncogenes in isoproterenol-induced cardiac hypertrophy. *J Mol Cell Cardiol*. 1993;25:1325-1337.
23. Schwartz SM, Gordon D, Mosca RS, et al. Collagen content in normal, pressure, and pressure-volume overloaded developing human hearts. *Am J Cardiol*. 1996;77:734-738.
24. Vikstrom KL, Bohlmeyer T, Factor SM, et al. Hypertrophy, pathology, and molecular markers of cardiac pathogenesis. *Circ Res*. 1998;82:773-778.

Chapter 4

DNA micro-array and myocardial fibrosis in patients with tetralogy of Fallot

Based on:
Peters THF, Bogers AJJC, Staal FJT, Poelmann RE, Saxena PR and Hari S Sharma. DNA micro-array and quantitative analysis reveal up-regulation of myocardial genes encoding extracellular matrix proteins in patients with tetralogy of Fallot. (submitted).

Abstract

Background: Tetralogy of Fallot (TF) is a congenital heart disease with adaptive right ventricular hypertrophy where cardiac surgery is performed at a young age to prevent cardiac failure on the long term. To unravel molecular phenotype, we investigated the myocardial differential gene expression profile and quantitatively analyzed the expression of extracellular matrix (ECM) markers in TF patients.

Methods and Results: Differential gene expression profile was assessed using high density Affymetrix® GeneChip analysis on right ventricular biopsies from TF patients who underwent primary correction (TF-1, n=12, mean age 0.8 year). Employing quantitative immunohistochemistry, ECM proteins (collagens and fibronectin) and myocyte cross sectional area were evaluated in TF-1 and adult patients (TF-2, n=8, mean age 30 years) who underwent surgery for pulmonary regurgitation and were compared with data of age matched controls (n=8/11). Among 236 differentially expressed genes in TF-1 patients, ECM markers were clearly up-regulated (fibronectin, 2.4; collagen Iα, 7.5 and collagen III, 4.4 fold). Most MMPs remained either unchanged or declined (MMP-13 and 17) whereas, TIMPs were down regulated. TF-1 patients showed myocyte hypertrophy (261±21 *vs.* 81±7μm^2, $p<0.01$) with linear correlation with age ($r=0.92$, $p<0.01$). Interstitial as well as peri-vascular fibronectin and total collagen contents were increased ($p<0.01$) in TF patients as compared to age matched controls.

Conclusions: Myocardial phenotype in TF patients depicts a complex gene expression profile with elevated tissue distribution of ECM markers, that eventually contribute to the cardiac fibrosis and failure.

Introduction

Tetralogy of Fallot (TF) is a cyanotic congenital heart malformation where primary cardiac surgery is inevitable during the first year of life by closing the ventricular septal defect and removing the right ventricular (RV) outflow tract obstruction[1-4]. However, some patients suffer from pulmonary regurgitation after primary correction causing RV failure due to volume overload and they undergo a second corrective surgery later in life by implanting a pulmonary allograft heart valve between the RV and the pulmonary artery[5]. Information on myocardial phenotype, specially at gene level may help in developing innovative treatment strategies and perhaps halt the ongoing debate for the optimal timing of corrective surgery in patients with TF.

Right ventricular hypertrophy (RVH) develops in TF patients as an adaptive response to the increased pressure overload caused by (sub) pulmonary stenosis in combination with a ventricular septal defect[2,6-8]. Experimental animal studies have shown that this adaptive response leads to myocardial remodeling accompanied with interstitial fibrosis that give rise to cardiac stiffness and abnormal function[9-16]. The developing human heart predominantly contains collagen type I that provides cardiac stiffness, whereas tissue elasticity is provided by the less abundant collagen III[14,16]. Expression levels of extracellular matrix (ECM) protein fibronectin, that serves as a bridge between cells and interstitial collagen mesh network, has been shown to be up-regulated during cardiac hypertrophy[17]. Studies demonstrated that only the RV collagen levels in TF patients during pressure and volume overload were affected[7]. Normally, the collagen turnover rate is high where mature cross-linked collagens fibers are degraded extracellularly by a family of matrix metalloproteinases (MMPs) that play an important role in tissue remodeling[9,18,19]. The activity of MMPs can be regulated by different cytokines and tissue inhibitors of MMPs (TIMPs)[18-20]. Increased expression or activation of the MMPs and/or decreased levels of TIMPs lead to enhanced proteolytic activity and ECM remodeling with myofibril disarray and progressive myocyte loss[21,22].

Most attention in research on human TF so far has been focused on clinical treatment and surgical procedures. Reduction in myocardial cell diameter in TF patients after corrective surgery has been observed[6,23] indicating for the diminished degree of RVH.

But to what extent the RVH in TF patients after corrective surgery regresses is still uncertain. Additionally, information concerning myocardial architecture in TF at a molecular level is limited. To assess the differential myocardial gene expression in patients with TF at the time of corrective surgery, we performed DNA micro-array followed by quantitative expression analysis of genes encoding ECM proteins in relation to age matched controls.

Material and Methods

Study subjects

The study design was approved by the Medical Ethical Committee of the University Hospital Rotterdam (MEC153.268/119). Studied groups and their clinical parameters are described in table 4.1. 12 patients underwent primary correction (TF-1 group) at a mean age of 0.8 years (range 0.4-1.8 years) whereas, 8 subjects (TF-2 group) with a mean age of 30.0 years (range 19.3-38.8 years) were operated for pulmonary allograft implantation late after primary correction of TF. All operations were done with the use of cardiopulmonary bypass with moderate hypothermia using bicaval cannulation. In selected cases, single right atrial cannulation was used. St.Thomas hospital cardioplegic solution was applied except in some of the TF-2 patients, in whom the pulmonary allograft was implanted in the beating heart[24,25]. In TF-1 patients, pulmonary valve function could be preserved in 5 patients, whereas a transannular patch was necessary in 3 patients. The young controls (C-1 group) comprised of 5 post mortem cases and 3 heart valve donors with a mean age of 0.8 years (range 0.01-1.9 years), whereas the adult controls (C-2 group) were of 11 heart valve donors with a mean age of 26.9 years (range 17.1-44.6 years). All heart valve donors and post mortem cases died due to non-cardiac complications.

Tissue biopsies

Endomyocardial tissue biopsies were removed from the anterior wall of the RV outflow tract in patients with preserved pulmonary valve function whereas, in patients with a transannular patch, the biopsies consisted of a transmural sample from the incision level of anterior RV wall. There was no operative or other early mortality and

Table 4.1. Clinical parameters of the patient-groups.

Clinical data/groups	C-1	TF-1	C-2	TF-2
Diagnosis	Non-cardiac death	Tetralogy of Fallot	Non-cardiac death	Pulmonary insufficiency
Number of patients	8	12	11	8
Sex (m/f)	4/4	9/3	6/5	3/5
Age (years)	0.8±0.3	0.8±0.1	26.9±2.4	30.0±2.2
Oxygen saturation (%)	ND	92±2.2	ND	96.2±0.7
Hb (mmol/L)	ND	8.6±0.34	ND	8.9±0.63
RVP (mm Hg)	ND	75.8±3.4	ND	67.2±12.4
LVP (mm Hg)	ND	74.0±2.9	ND	128.8±6.6

Clinical parameters include oxygen-saturation, hemoglobin content (Hb), right (RVP) and left ventricular pressure (LVP) in patients who underwent primary corrective (TF-1) and redo-surgery (TF-2). Age matched controls were either young donors or young deceased (C-1) and adult donors (C-2). Values are given as mean ± SEM. ND denotes for not determined.

there were no complications that could be attributed to taking the biopsies. Tissue biopsies were divided to snap freeze for RNA analysis and to fix in 4% para-formaldehyde followed by paraffin embedding for (immuno)histochemical analysis.

Total RNA isolation and DNA micro-array analysis

Total RNA was isolated from RV tissue (50-60 mg)[26] and the RNA concentration was spectrophotometrically measured at 260 nm and a RNA/protein ratio of ≥1.8 was accepted. The quality of total RNA was further verified on a denaturing 1% agarose gel. Total RNA samples from TF-1 (n=4) and from age matched controls (C1, n=3) were processed for Affymetrix® GeneChip expression (HG-U95Av2, Santa Clara, CA, USA) analysis following supplier's protocols. In brief, total RNA was subjected to first strand cDNA synthesis using T7-(dT)24 oligonucleotide primers and SuperScript II reverse transcriptase (Life Technologies, Rockville, MD, USA) followed by second strand cDNA synthesis. cDNA was blunted, purified and used for cRNA synthesis using T7-RNA polymerase, biotinylated-11-CTP and 16-UTP. 20 μg of labeled cRNA was hydrolyzed and used to hybridize pre-equilibrated expression GeneChips for 16 hours at 45 °C. The arrays were washed, stained using Streptavidin-phycoerythrin conjugate and biotinylated antibodies to streptavidin. Hybridization signals were scanned using a fluorometric HP ChipScanner (Affymetrix, Santa Clara, CA, USA), analyzed employing GeneChip Micro-array Suite (MPS 4.0) (Affymetrix)

and total gene expression profile was used for normalization[27]. A comparison of the two expression profiles was made and genes changing over 2 fold (up or down regulated) were considered significantly altered in expression[28]. Among the large number of genes screened (www.netaffx.com), a group of genes encoding ECM proteins (e.g. fibronectin and collagens) was further quantitatively analyzed by immunohistochemistry and video image analysis.

Histochemistry

The total collagen in myocardial tissue specimens was stained with Picro-sirius red F3BA[29]. Tissue sections of 5 μm thickness, were treated with aqueous phosphomolybdic acid and incubated in 0.1% Picro-sirius red. For determining the myocyte surface size, the cell (membrane) reticulin fibers were stained by Gomori's reticulin silver staining technique[30]. All sections were mounted and visualized under light microscope.

Immunolocalization of fibronectin, collagen Iα and collagen III

Immunohistochemical staining was performed on 5 μm thick paraffin sections of myocardial tissue, using a multiple step avidin-biotin complex (ABC) method (Biogenex, San Ramon, CA, USA). In brief, after deparaffinization in xylene and rehydration through graded alcohol, the slides were processed for antigen retrieval using citrate boiling method (collagen Iα, fibronectin) or using 0.1 % pronase treatment (collagen III). 10% normal goat serum was used to block non-specific binding. Human specific mouse monoclonal antibodies against fibronectin (Life Technologies, Breda, The Netherlands), collagen Iα (Sigma, St Louis, MO, USA) or collagen III (BioGenex, San Ramon, CA, USA) were applied as primary antiserum. The sections were further incubated with mouse biotinylated anti-rabbit IgG (BioGenex, San Ramon, CA) followed with alkaline phosphate conjugated streptavidin. Color was developed using Naphtol AS-MX phosphate and new fuchsin. For collagen III, streptavidin conjugated to peroxidase (BioGenex, San Ramon, CA) was applied and subsequently sections were colored using 3,3-diaminobenzidine (Sigma, St Louis, MO, USA). The supra optimal dilution was obtained by examining the intensity of staining obtained with a series of dilutions of the antibody and selecting the dilution that gave specific, weak but easily visible signal. Negative

controls were performed by omission of the primary antibody. All sections were counter stained with Mayer's hematoxylin, mounted and visualized under the light microscope.

Video image analysis

Expression of fibronectin, total collagen as well as collagen sub-type Iα and III were quantitatively analyzed using a Leica Qwin video image analysis system (version 3.0, Leica, Rijswijk, The Netherlands). From each section, series of 12 rectangular digital color images (736x574 pixels) were taken using a CCD video camera connected to the light microscope (Leica DM RBE, Leica GmbH, Wetzlar, Germany) and were analyzed with an image analysis software (QWin-V 2.8, Cambridge Biotech, UK). After optimization for hue, saturation and intensity, the staining detection levels for all images were assessed as pixel counts at the constant settings of the microscope-image analysis system. Interstitial expression was represented as staining per total tissue area, excluding vascular areas. For peri-vascular measurements, the entire vessel was drawn manually and analyzed. Peri-vascular localization was depicted as peri-vascular collagen/fibronectin area (PVCA/PVFA) normalized to vessel luminal area (VA)[11]. In the similar set-up, the myocyte cross sectional area was calculated in μm^2 after drawing the reticulin stained cell membrane in 20 transversely cut myocytes with intact nucleus. Influence of RVH was taken into account and interstitial expression of ECM markers was normalized with the increase in cell size of the respective patient.

Statistical analysis

Statistical analysis for micro-array results was performed with comparison ranking within software Data Mining Tool (Affymetrix). Using SPSS software (SPSS Inc. Chicago, USA), statistical probability was assessed by (non-parametric) Kruskal-Wallis one way analysis of variance and linear (Pearson's) regression analysis was performed for assessing RVH. Values are expressed as mean ± SEM and accepted as statistically significant with $p \leq 0.05$.

Results

DNA micro-array analysis

To asses the differential gene-expression profile, RNA samples obtained from TF-1 and age matched controls were processed for Affymetrix® GeneChip analysis. Gene expression was considered to be up or down regulated if the expression levels were 2 fold higher/lower than the controls as presented in a differential scatter graph in the figure 4.1. Comparison ranking analysis revealed that in TF-1 patients, 236 genes showed altered expression pattern. Analysis of a selected group of genes dedicated to ECM homeostasis in the heart, showed that a number of genes encoding ECM proteins were up-regulated in TF-1 patients as compared to the age matched controls (table 4.2). With the same threshold no fibrosis markers were found to be down regulated. Collagen type I and III drastically (up to 7.5 fold) and collagen type IX and XV were moderately up-regulated in TF patients whereas, other subtypes remained unchanged (table 4.2). Expression levels for fibronectin were also enhanced (2-3 fold) in TF patients. The MMP expression profile remained unchanged or declined (MMP-13,17) whereas, their physiological inhibitors (TIMP-1, 4) showed decreased (2-4 fold) expression levels in TF group (table 4.3).

Quantitative analysis of collagen expression

Picro-sirius red staining showed myocardial collagen localization in the interstitium as well as in peri-vascular areas in all patients (Fig. 4.2). TF patients showed altered distribution of collagen fibers, myocyte organization and shape as compared to age matched controls. Controls showed an arrayed pattern of uniform shaped long myocyte bundles surrounded by tight collagen fibers invading between the myocytes, whereas, TF patients showed less uniformity in shape and array of myocytes with small dense collagen bundles. In TF-1, collagen fibers were more randomly localized in the interstitium, whereas in TF-2, collagen layers around the myocytes were thicker as compared to respective controls. Immunoreactive collagen Iα and III were confined to the interstitial and peri-vascular areas (Fig. 4.2). Video image analysis of interstitial as well as peri-vascular total collagen contents revealed significantly increased ($p<0.01$) expression in both TF-1 and TF-2 groups as compared to respective controls (Fig. 4.3). The data presented for interstitial expression was

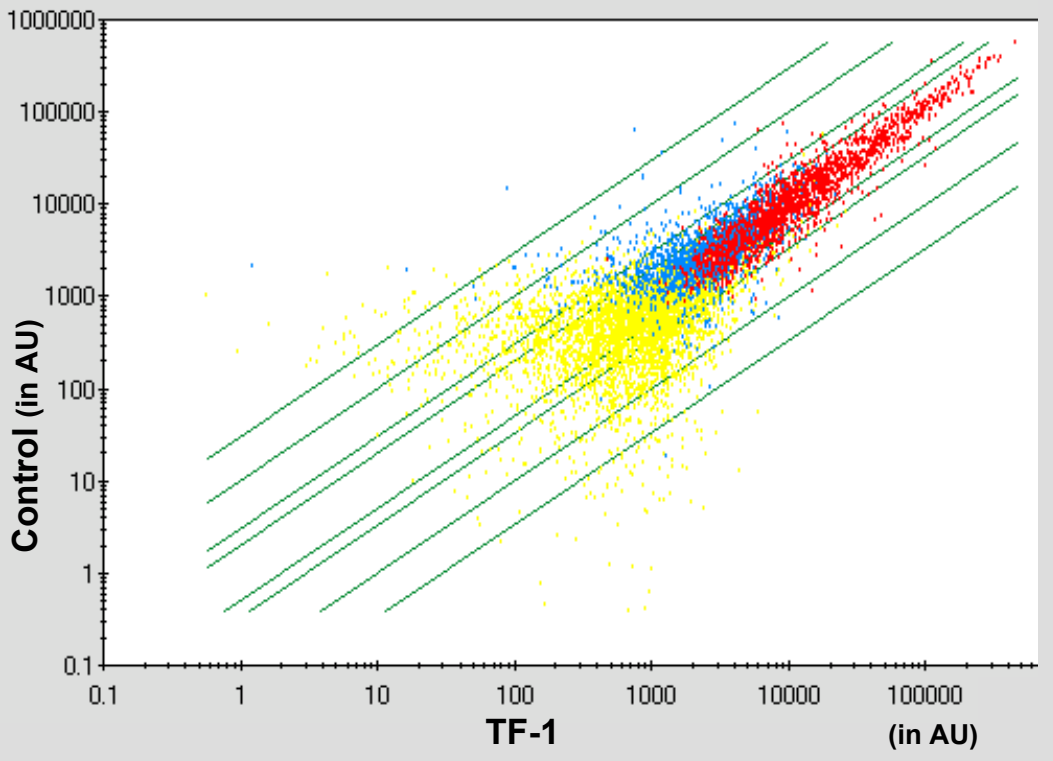

Figure 4.1. Differential scatter graph for DNA micro-array analysis of myocardial genes in patients with tetralogy of Fallot.
Total RNA samples from TF-1 (n=4) and from age matched controls (C-1, n=3) were processed for Affymetrix® GeneChip expression (HG-U95Av2) and subsequently scanned and analyzed as described in Materials and Methods section. A differential graph represents the up and down regulated genes in both control as well as TF-1. (AU; Artificial Units, representing the normalized spot intensities of the analyzed genes)

corrected for the myocyte cross sectional area in order to circumvent the influence of cellular hypertrophy. Likewise, the peri-vascular expression was normalized with vascular lumen area. Interstitial collagen Iα and III were also elevated ($p<0.05$) in TF patients, whereas, peri-vascular levels for both remained unchanged (Fig. 4.3). Furthermore, age dependent deposition of collagens were observed in both TF and controls. However, the magnitude of collagen deposition was much higher in TF patients.

Quantitative analysis of fibronectin

Fibronectin localization was confined to the interstitial and peri-vascular region, as well as to the cytoplasm of some cardiomyocytes (Fig. 4.2). The fibronectin staining pattern was comparable to the total collagen expression pattern, although less intense

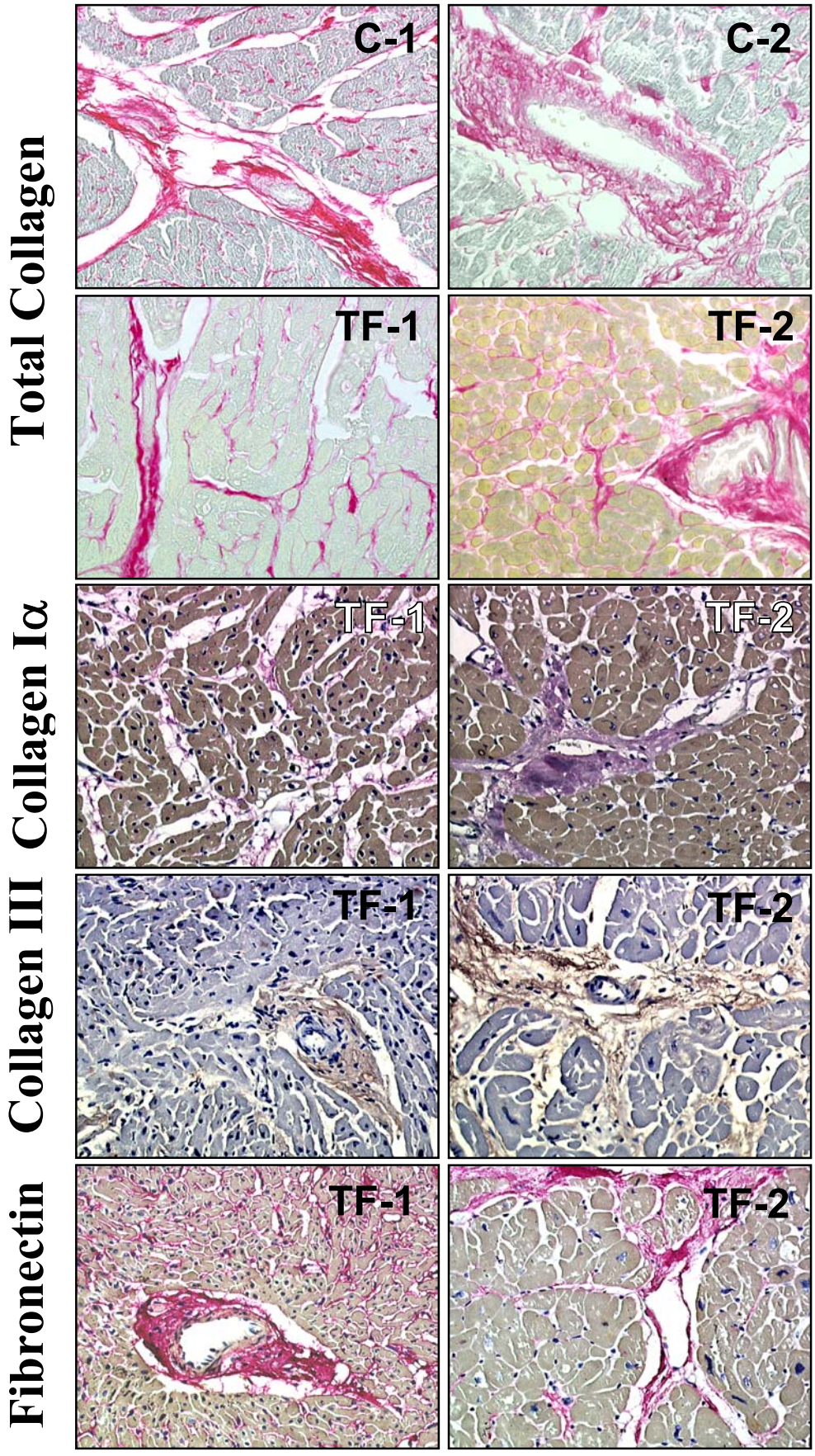
Total Collagen
C-1
C-2
TF-1
TF-2
Collagen Iα
TF-1
TF-2
Collagen III
TF-1
TF-2
Fibronectin
TF-1
TF-2

Figure 4.2. Myocardial staining for total collagens, collagen subtype Iα and III and fibronectin in patients with tetralogy of Fallot.
Micro-photographs showing the tissue localization of ECM proteins in human right ventricular tissue from TF-1, TF-2 and controls. The staining represents the specific fibers localized in peri-vascular as well as in interstitial tissue area. Note the interstitial fibrosis in the case of TF patients. Bar represents 25 μm.

Fibronectin fibers were localized in dots, short bundles and around the myocytes in TF patients but there were no side-bundles connecting to myocytes like in young controls. Furthermore, fibronectin fibers around the myocytes were more abundant and more randomly distributed in TF-1, whereas in TF-2, the fibronectin layer around the myocytes was less prominent (Fig. 4.2). Video image analysis of interstitial fibronectin expression corrected for myocyte cross sectional area showed increased levels in TF-1 ($p<0.01$) and TF-2 ($p<0.01$) as compared to respective controls (Fig. 4.3). Also interstitial fibronectin levels in the adult controls (C-2) were enhanced as compared to the young controls (C-1, $p<0.01$). Peri-vascular fibronectin levels normalized with vascular lumen area (PVFA/VA) showed higher ratio in TF-1 ($p<0.01$) and TF-2 ($p<0.05$) as compared to the age matched controls (Fig. 4.3).

Myocyte surface area

Video image analysis showed a significant increase of myocyte cross sectional area in TF-1 ($262\pm21\mu m^2$ *vs*. $81\pm7\mu m^2$) and TF-2 ($1617\pm177\mu m^2$ *vs*. $463\pm33\mu m^2$) groups as compared to respective age matched controls ($p<0.05$), indicating for cellular hypertrophy (Fig. 4.4). A positive linear correlation between the myocyte-size and age at time of surgery in TF-1 patients ($r= 0.92$; $p= 0.01$) was seen (Fig. 4.4).

Discussion

Our study demonstrate the differential gene expression profile during RVH in the developing heart with congenital anomaly. Using high density DNA micro-array, we show that more than 200 myocardial genes are up or down regulated in patients with TF. Among other genes, the expression of ECM proteins, such as collagens and fibronectin were predominantly elevated whereas, MMPs and TIMPs either remained unchanged or

Table 4.2. Differential expression of genes encoding extracellular matrix proteins in TF-1 patients

Protein	Accession no.	Type	Fold Change	Diff Call	Gene description of human mRNA encoding for
Collagens:					
	Y15915	*col 1α1*	*6.6*	*I*	*chimaeric transcript of collagen type I α1 and PDGF*
	AL034452	*col novel*	*4.7*	*I*	*chromosome 6p11.2-12.3 containing the 3 part of a novel collagen triple helix repeat protein*
	Z74615	*col 1α1*	*2.5*	*I*	*prepro-α1(type I) collagen /cds*
	J03464	*col 1α2*	*7.5*	*I*	*collagen α-2 type I, complete cds*
	V00503	*col 1α2*	*3*	*I*	*Pro-α2 chain of type I procollagen. (major part) /cds*
	M60299	col 2α1	1.6	NC	α-1 collagen type II gene, exons 1, 2 and 3
	X14420	*col 3α1*	*4.4*	*I*	*pro-α-1 type 3 collagen /cds*
	M26576	col 4α1	1.3	NC	α-1 collagen type IV gene /cds
	X05610	col 4α2	1.2	NC	type IV collagen α (2) chain /cds
	U02519	col 4α3	1.3	NC	collagen type IV α 3 alternatively spliced, partial cds
	X81053	col 4α4	1.1	NC	collagen type IV α 4 chain /cds
	M58526	col 4α5	1.1	NC	α-5 collagen type IV, 3 end /cds
	D21337	col 4α6	-1.5	NC	collagen α-6 type IV /cds
	M76729	col 5α1	-1.6	NC	pro-α-1 (V) collagen, complete cds
	Y14690	*col 5α2*	*2.1*	*I*	*procollagen α 2(V) /cds*
	M20776	col 6α1	1.2	NC	α-1 (VI) collagen /cds
	M20777	col 6α2	-1.5	NC	α-2 (VI) collagen /cds
	X52022	col 6α3	-1.1	NC	type VI collagen α3 chain /cds
	L02870	col 7α1	1.1	NC	α-1 type VII collagen, complete cds
	X57527	col 8α1	1.3	NC	α 1(VIII) collagen /cds
	X54412	col 9α1	3.8	NC	α1(IX) collagen (long form) /cds
	M95610	col 9α2	-2.4	NC	α 2 type IX collagen, partial cds
	L41162	col 9α3	1.1	NC	collagen α 3 type IX, complete cds
	X60382	col 10α1	-1.1	NC	collagen (α-1 type X) /cds
	J04177	col 11α1	-1.7	NC	α-1 type XI collagen, complete cds
	U41068	col 11α2	1.4	NC	collagen α2(XI) gene, exons 61 and 62, partial cds
	M59217	col 13α1	1.1	NC	collagen type XIII α-1 mRNA, complete cds
	Y11710	col 14	1.4	NC	extracellular matrix protein collagen type XIV, C-terminus /cds
	L25286	*col 15α1*	*2.4*	*I*	*α-1 type XV collagen mRNA, complete cds*
	M92642	col 16α1	-1.3	NC	α-1 type XVI collagen mRNA, complete cds
	AF018081	col 18α1	1.5	NC	type XVIII collagen mRNA, alternatively spliced, long form, complete cds
	D38163	col 19α1	-1.4	NC	α1(XIX) collagen chain, complete cds
Fibronectin:					
	X02761	*Fibro*	*2.2*	*I*	*fibronectin (FN precursor) /cds*
	M10905	*Fibro*	*2.4*	*I*	*cellular fibronectin /cds*
	Alt. Splice 1	*Fibro*	*2.6*	*I*	*Fibronectin, alt. Splice 1*

Clearly up-regulated genes are shown in italics. I = increased; NC = not changed

Table 4.3. Differential expression of genes encoding matrix metalloproteinase and their inhibitors in TF-1 patients

MMP subgroups	Main name	Accession no.		Fold change	Diff call	Gene description of human mRNA encoding for:
Collagenases						
	Collagenase-2	J05556	MMP-8	1.3	NC	*collagenase, complete cds*
	Collagenase-3	*X75308*	*MMP-13*	*-2.1*	*D*	*collagenase 3 /cds*
Gelatinases						
	Gelatinase A	M55593	MMP-2	-1.4	NC	*collagenase type IV (CLG4)/cds*
	Gelatinase B	J05070	MMP-9	1.8	NC	*type IV collagenase mRNA, cds*
Stromelysins						
	Stromelysin-1	X05232	MMP-3	-1.3	NC	*stromelysin*
	Stromelysin-2	X07820	MMP-10	1.0	NC	*metalloproteinase stromelysin-2*
	Stromelysin-3	X57766	MMP-11	-1.2	NC	*stromelysin-3 /cds*
	Matrilysin	L22524	MMP-7	1.5	NC	*matrilysin gene, exon 6 , cds*
	Metalloelastase	L23808	MMP-12	1.7	NC	*metalloproteinase (HME), cds*
Membrane-type matrix metalloproteinase (MT-MMPs)						
	MT1-MMP	X83535	MMP-14	-1.6	NC	*MT-MMP/cds*
		Z48481	MMP-14	1.1	NC	*MT-MMP 1*
	MT2-MMP	Z48482	MMP15	1.6	NC	*MT-MMP 2*
		D86331	MMP15	1.9	NC	*MT2-MMP gene for MMP, cds*
	MT3-MMP	D83646	MMP-16	-1.2	NC	*metalloproteinase, complete cds*
	MT4-MMP	*AB021225*	*MMP-17*	*-2.1*	*D*	*MT-MMP-4, complete cds*
	MT5-MMP	AB021227	MT5-MMP	1.3	NC	*MT5-MMP, complete cds*
Tissue inhibitors of metalloproteinases (TIMP)						
		D11139	*TIMP-1*	*-3.6*	*D*	*gene for TIMP, partial sequence*
		U44385	TIMP-2	-1.1	NC	*TIMP-2 (TIMP-2) gene /cds*
		U14394	TIMP-3	-1.6	NC	*TIMP-3, complete cds*
		U76456	*TIMP-4*	*-2.9*	*D*	*TIMP-4, complete cds*

Clearly down-regulated genes are shown in italics. D = decreased; NC = not changed

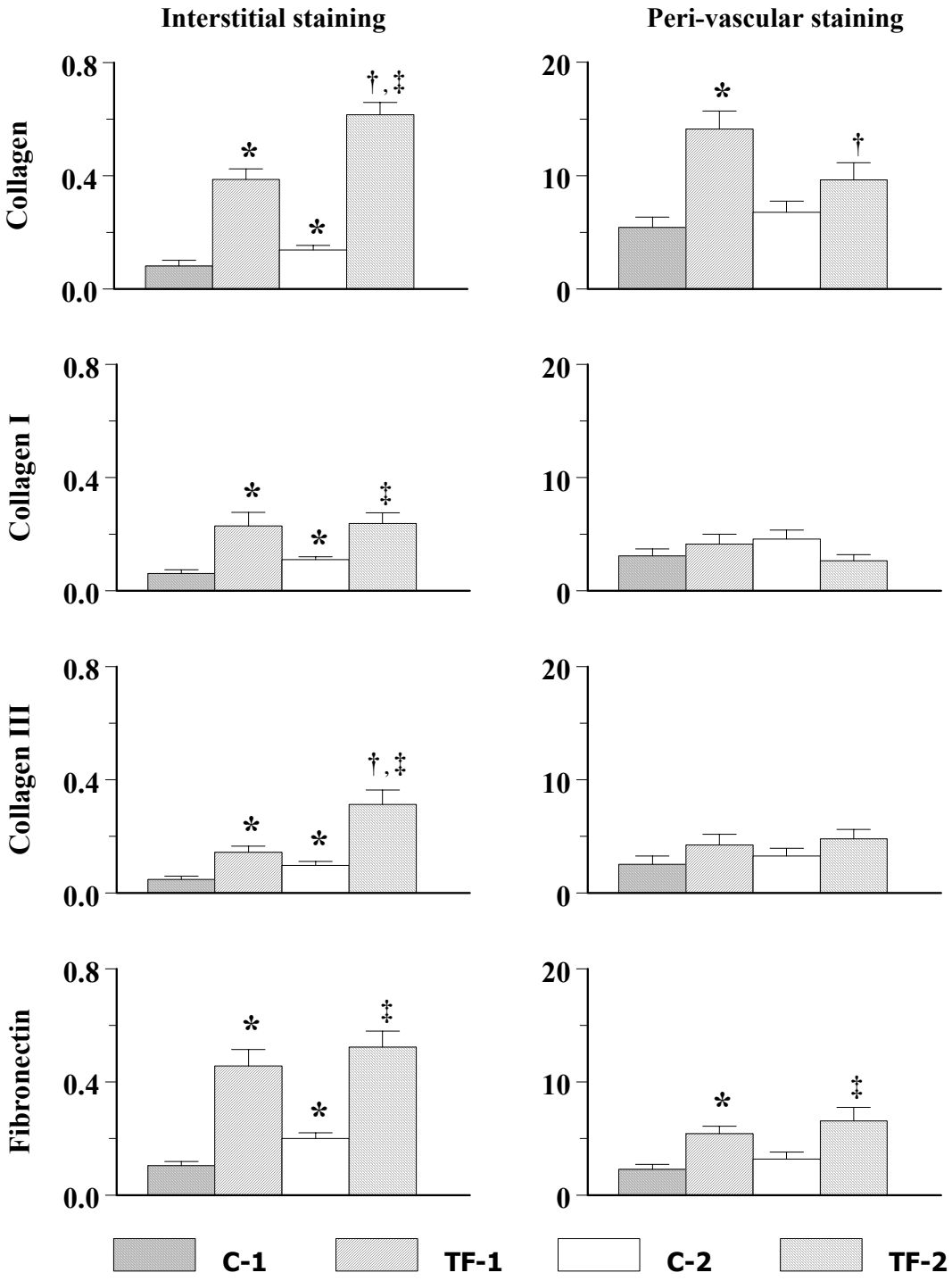

Figure 4.3. Quantitative analysis of total collagen, collagen I and III and fibronectin in patients with tetralogy of Fallot.

Expression levels of ECM proteins in TF patients were quantified using video image analysis for interstitial and peri-vascular expression. The bar diagrams depict the ratio between stained area per total tissue area, corrected for the myocyte size (left column) and vascular lumen (VA) area (right column). Values are shown as mean ± SEM, where * denotes significantly different ($p<0.01$) as compared to C-1, † ($p<0.01$) *vs*. TF-1 and ‡ ($p<0.01$) *vs.* C-2.

decreased in TF patients. The global mRNA expression profile of ECM proteins was further verified by quantitative immunohistochemistry where the distribution of both collagens and fibronectin was clearly enhanced in the myocardium of patients with TF. Our results indicate for the myocardial fibrosis that may account for diminished function in patients with TF.

In the heart fibroblasts, which produces most of the collagen fibers, represent as much as two-third of the cardiac cells[9,15,16,19,31]. Collagens are the major ECM proteins in the heart that surround and interconnect myocytes and muscle fibers to provide mechanical support to the myocardium and govern tissue stiffness[16,19,31]. A balance between synthesis and degradation of ECM has been shown to be important in the process of ventricular hypertrophy and remodeling during heart failure[15,16,18,19]. The apparent development of cardiac hypertrophy in TF could be attributed to the induced gene expression that provide means of compensation for increased haemodynamic load[10,32]. In this regard, our data on histopathological findings in TF patients show interstitial fibrosis, myofibrillar disorganization and disarray in addition to myocardial cell hypertrophy. The degree of myocardial hypertrophy (cell radius of 22 μm) in TF-2 group is in accordance with previously reported myocyte radius of more than 20 μm[23]. Whether or not the myocytes of TF patients were already hypertrophied during pregnancy and at birth is unclear, because no biopsies before the time of primary corrective surgery are available. But it is assumed that the RV haemodynamic overload in TF begins after birth when the ductus arteriosus closes and readily results in RVH.

Hypertrophy of the cardiomyocytes in TF patients will increase the total (tissue) volume. It is likely that the increase in myocyte cross sectional area during hypertrophy would influence the staining levels of ECM markers as measured by video image analysis (expressed as a ratio between stained area and total tissue area). Therefore, the interstitial staining data in this study is corrected for the morphological changes by multiplying the tissue staining data with the increase in myocyte size of the respective patients.

Altered expression levels of ECM proteins found in our study could be attributed to the altered structure or function of the myocardium as an concomitant phenomena. The

alteration in ventricular gene expression as a suggested indicator of cardiac hypertrophy may result from a number of different stimuli. The changes in the RV collagen and fibronectin contents in TF patients could be as a result of increased haemodynamic load with a parallel increase in ventricular mass[7,31]. Nevertheless, from our findings for the peri-vascular collagen and fibronectin expression it is clear that the levels are already high in patients with TF at a very young age (TF-1) and remains elevated later in life (TF-2). This indicates that surgical correction at young age could be an adequate treatment to stop peri-vascular fibrosis. Furthermore, our findings on the developing myocardial hypertrophy in TF patients (Fig. 4.4) support the policy of corrective surgery at a young age. The positive linear correlation between myocyte size and age in the TF-1 group suggest that unless hypertrophic stimuli will be removed by early corrective surgery, the myocyte hypertrophy and accompanied myocardial fibrosis will persist, although it is still not clear if or to what extend myocytes really regress in size after corrective surgery.

The early increase of collagen deposition in the RV as found at primary correction may occur due to the fact that the original myocardial ECM has been expanded and weakened due to the haemodynamic overload. Additionally, pulmonary regurgitation and volume overload as in case of TF-2 may account for even higher myocardial collagen deposition. Adequate corrective surgery limits the myocardial overload and may therefore limit the amount of damage to the myocardial collagen matrix[33].

Higher collagen contents as an adaptive response to hypertrophy is thought to be a result of a decreased collagen destruction rate and/or a higher synthesis rate[9]. DNA micro-array data on MMPs and TIMPs support the notion that in patients with TF, degradation rate of ECM protein either remains unchanged or is slightly stimulated to allow RVH. At the same time collagen synthesis appears to be accelerated, resulting in a net increase in myocardial fibrosis in patients with TF. The increased levels of mRNA for collagens as well as fibronectin found during cardiac hypertrophy by pressure-overload[10,12,17,34] support our findings in patients with TF. Affymetrix® DNA micro-array hybridization verified that mRNA levels for collagen Iα2 (3-4 times), fibronectin (2.4 times), collagen III α1 (4.4 times) and for a novel collagen triple helix repeat containing protein (4.7 times) were up-regulated.

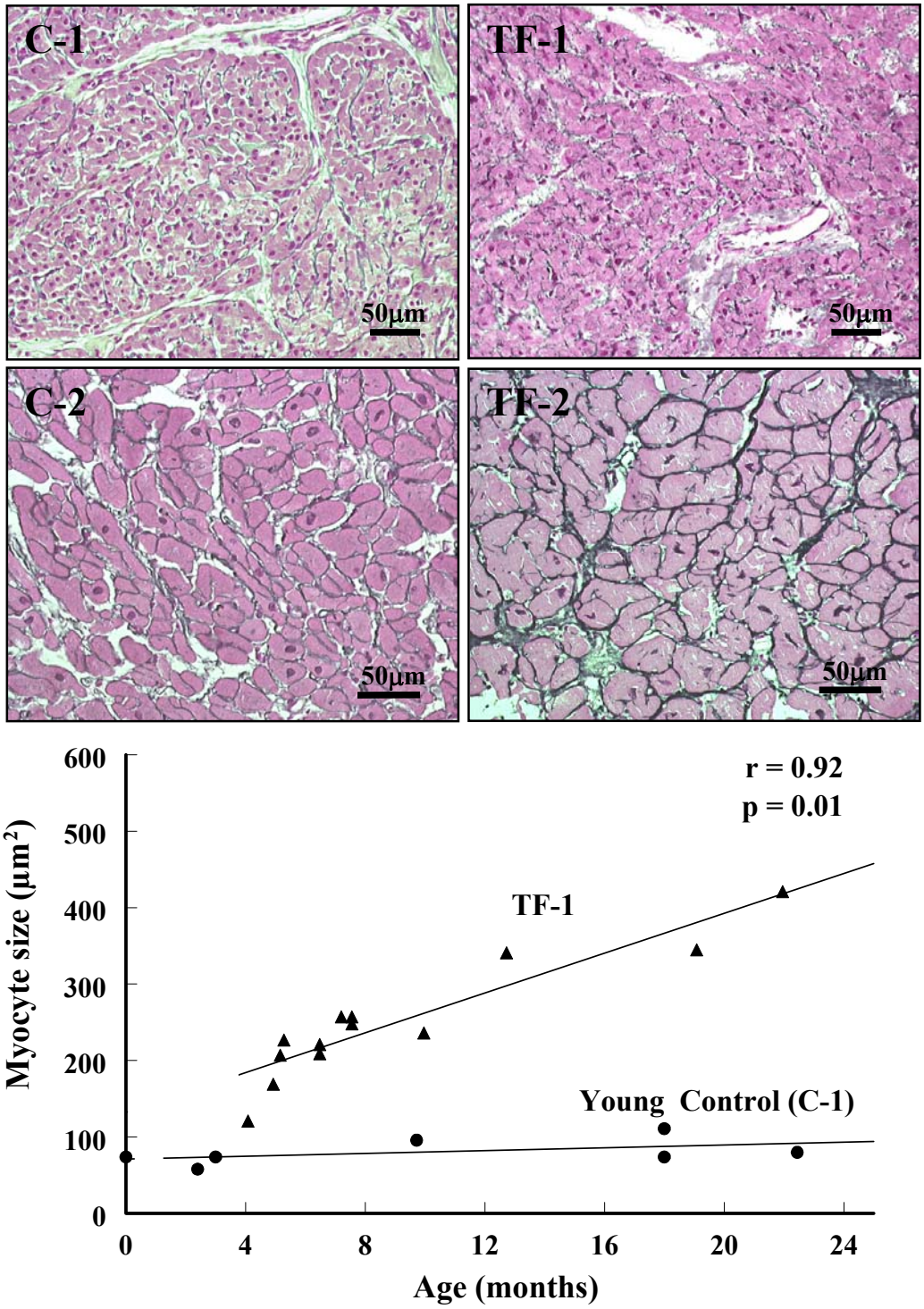

Figure 4.4. Developmental pattern of right ventricular myocytes in patients with tetralogy of Fallot.

Micro-photograph of the human right ventricular myocytes where (membrane) reticulin fibers were stained by routine Gomori's reticulin silver stain. The myocyte cross sectional areas were measured from digital microscopic pictures with an video image analysis set up. TF-1 patients depicted an increased myocyte size with a linear correlation with age at time of primary corrective surgery as compared to normal RV.

Taken together, our study provides further evidence that myocardial architecture in patients with TF depicts a complex and differential gene expression pattern with drastically increased expression level of ECM proteins (collagen Iα and III and fibronectin) at mRNA (DNA micro-array) and protein levels (quantitative immunohistochemistry). We conclude that this up-regulation of genes involved in ECM homeostasis is associated with RVH and diminished cardiac function in TF patients. This information leaves room for improvement of contemporary clinical treatment of patients with tetralogy of Fallot by allowing an assessment of timing for surgery and possibly support long term postoperative prognosis.

Acknowledgements

Financial support from the Netherlands Heart Foundation (NHS 96.082) is gratefully acknowledged. Authors thank Mrs. Emine Yilmaz and Mrs. Caroline van den Burg for their technical assistance.

References

1. Starnes VA, Luciani GB, Latter DA, et al. Current surgical management of tetralogy of Fallot. *Ann Thorac Surg*. 1994;58:211-215.
2. Pigula FA, Khalil PN, Mayer JE, et al. Repair of tetralogy of Fallot in neonates and young infants. *Circulation*. 1999;100:II157-61.
3. Reddy VM, Liddicoat JR, McElhinney DB, et al. Routine primary repair of tetralogy of Fallot in neonates and infants less than three months of age. *Ann Thorac Surg*. 1995;60:S592-6.
4. Van Arsdell GS, Maharaj GS, Tom J, et al. What is the optimal age for repair of tetralogy of Fallot? *Circulation*. 2000;102:III123-9.
5. Warner KG, Anderson JE, Fulton DR, et al. Restoration of the pulmonary valve reduces right ventricular volume overload after previous repair of tetralogy of Fallot. *Circulation*. 1993;88:II189-97.
6. Seliem MA, Wu YT, Glenwright K. Relation between age at surgery and regression of right ventricular hypertrophy in tetralogy of Fallot. *Ped Cardiol*. 1995;16:53-55.
7. Schwartz SM, Gordon D, Mosca RS, et al. Collagen content in normal, pressure, and pressure-volume overloaded developing human hearts. *Am J Cardiol*. 1996;77:734-8.
8. Castaneda AR, Jonas RA, Mayer JE, et al. *Cardiac surgery of neonate and infant*. Philadelphia, USA: Saunders; 1994.

9. Bishop JE, Rhodes S, Laurent GJ, et al. Increased collagen synthesis and decreased collagen degradation in right ventricular hypertrophy induced by pressure overload. *Cardiovasc Res*. 1994;28:1581-1585.
10. Boluyt MO, L. O, Meredith AL, et al. Alterations in cardiac gene expression during the transition from stable hypertrophy to heart failure. Marked upregulation of genes encoding extracellular matrix components. *Circ Res*. 1994;75:23-32.
11. Brilla CG, Janicki JS, Weber KT. Impaired diastolic function and coronary reserve in genetic hypertension. Role of interstitial fibrosis and medial thickening of intramyocardial coronary arteries. *Circ Res*. 1991;69:107-115.
12. Jalil JE, Doering CW, Janicki JS, et al. Fibrillar collagen and myocardial stiffness in the intact hypertrophied rat left ventricle. *Circ Res*. 1989;64:1041-1050.
13. Lamparter S, Sun Y, Weber KT. Angiotensin II receptor blockade during gestation attenuates collagen formation in the developing rat heart. *Cardiovasc Res*. 1999;43:165-72.
14. Marijianowski MM, van der Loos CM, Mohrschladt MF, et al. The neonatal heart has a relatively high content of total collagen and type I collagen, a condition that may explain the less compliant state. *J Am Coll Cardiol*. 1994;23:1204-8.
15. Tyagi SC. Extracellular matrix dynamics in heart failure: a prospect for gene therapy. *J Cell Biochem*. 1998;68:403-10.
16. Weber KT, Sun Y, Tyagi SC, et al. Collagen network of the myocardium: function, structural remodelling and regulatory mechanisms. *J Mol Cell Cardiol*. 1994;26:279-92.
17. Farhadian F, Contard F, Corbier A, et al. Fibronectin expression during physiological and pathological cardiac growth. *J Mol Cell Cardiol*. 1995;27:981-990.
18. Mann DL, Spinale FG. Activation of matrix metalloproteinases in the failing human heart: breaking the tie that binds. *Circulation*. 1998;98:1699-702.
19. D'Armiento J. Matrix metalloproteinase disruption of the extracellular matrix and cardiac dysfunction. *Trends Cardiovasc Med*. 2002;12:97-101.
20. Galis ZS, Muszynski M, Sukhova GK, et al. Cytokine-stimulated human vascular smooth muscle cells synthesize a complement of enzymes required for extracellular matrix digestion. *Circ Res*. 1994;75:181-9.
21. Li YY, Feldman AM, Sun Y, et al. Differential expression of tissue inhibitors of metalloproteinases in the failing human heart. *Circulation*. 1998;98:1728-34.
22. Spinale FG. Matrix metalloproteinases: regulation and dysregulation in the failing heart. *Circ Res*. 2002;90:520-30.
23. Mitsuno M, Nakano S, Shimazaki Y, et al. Fate of right ventricular hypertrophy in tetralogy of Fallot after corrective surgery. *Am J Cardiol*. 1993;72:694-8.
24. Hokken RB, Bogers AJJC, Spitaels SEC, et al. Pulmonary homograft insertion after repair of pulmonary stenosis. *J Heart Valve Dis*. 1995;4:182-186.
25. Bogers AJJC, Roofthooft M, Pisters H, et al. Longterm follow-up of gamma irradiated transannular homograft patch in surgical treatment of tetralogy of Fallot. *Thorac Cardiovasc Surgeon*. 1994;42:337-339.
26. Sharma HS, van Heugten HA, Goedbloed MA, et al. Angiotensin II induced expression of transcription factors precedes increase in Transforming Growth

Factor-b1 mRNA in neonatal cardiac fibroblasts. *Biochem Biophys Res Comm*. 1994;205:105-112.
27. Tan FL, Moravec CS, Li J, et al. The gene expression fingerprint of human heart failure. *Proc Nat Acad Sci U S A*. 2002;99:11387-92.
28. Yajima N, Masuda M, Miyazaki M, et al. Oxidative stress is involved in the development of experimental abdominal aortic aneurysm: a study of the transcription profile with complementary DNA microarray. *J Vasc Surg*. 2002;36:379-85.
29. Takahashi T, Schunkert H, Isoyama S, et al. Age-related differences in the expression of proto-oncogene and contractile protein genes in response to pressure overload in the rat myocardium. *J Clin Invest*. 1992;89:939-946.
30. Bancroff JD, Cook HC. *Manual of Histological Techniques and Their Diagnostic Aplication*. London: Churchill Livingstone; 1994.
31. Vikstrom KL, Bohlmeyer T, Factor SM, et al. Hypertrophy, pathology, and molecular markers of cardiac pathogenesis. *Circ Res*. 1998;82:773-778.
32. Brand T, Sharma HS, Fleischmann KE, et al. Proto-oncogene expression in porcine myocardium subjected to ischemia and reperfusion. *Circ Res*. 1992;71:1351-1360.
33. Whittaker P. Collagen and ventricular remodelling after acute myocardial infarction: concepts and hypotheses. *Basic Res Cardiol*. 1997;92:79-81.
34. Heling A, Zimmermann R, Kostin S, et al. Increased expression of cytoskeletal, linkage, and extracellular proteins in failing human myocardium. *Circ Res*. 2000;86:846-53.

Chapter 5

Right ventricular fibrosis levels in patients with pulmonary atresia and ventricular septal defect

Based on:
Peters THF, de Jong PL, Klompe L, Saxena PR, Sharma HS and Bogers AJJC. Right ventricular collagen and fibronectin levels in patients with pulmonary atresia and ventricular septum defect. Mol Cell Biochem 2003; 251:27-32.

Abstract

Pulmonary atresia (PA) with ventricular septal defect (VSD) is an extreme form of tetralogy of Fallot with characteristic right ventricular hypertrophy. To reduce the right ventricular overload, these children get a staged corrective surgery to restore physiological pulmonary perfusion.

We studied the degree of fibrosis by analyzing the myocardial expression pattern (at mRNA and protein level) of the extracellular matrix proteins, fibronectin and collagen subtype Iα and III in right ventricular biopsies of PA-VSD patients (n=14; mean age 2.5 years) obtained at corrective surgery and compared them with age matched controls (n=6; mean age 2.5 years). Furthermore the myocyte surface size was measured, after Gomori's reticulin staining by video image analysis, to asses the degree of hypertrophy.

Expression analysis by RT-PCR showed significantly higher levels for collagen III ($p=0.03$), whereas collagen Iα ($p=0.31$) and fibronectin ($p=0.47$) mRNA levels remained unaltered in PA-VSD patients as compared to age matched controls. The myocyte surface area showed enhanced myocyte hypertrophy in PA-VSD as compared to the control ($285 \pm 27 \mu m^2$ *vs.* $145 \pm 50 \mu m^2$; $p<0.02$). Video image analysis of immunohistochemical sections, corrected for hypertrophy, showed unchanged interstitial levels for total collagen, collagen subtype Iα and III as well as for fibronectin in the patients with PA-VSD. Peri-vascular staining, represented as the peri-vascular stained area corrected for the vessel lumen area, showed significantly decreased total collagen ($p<0.01$) levels in the PA-VSD group as compared to controls, whereas fibronectin levels ($p=0.51$) remained unchanged.

Our results indicate that the patients with PA-VSD have inadequate extracellular matrix support for their coronary blood vessels, perhaps due to an altered biosynthesis of collagen and fibronectin network.

Introduction

Pulmonary atresia with ventricular septal defect (PA-VSD) is an extreme form of tetralogy of Fallot where antegrade blood flow to the pulmonary artery is completely obstructed[1,2]. Some PA-VSD patients have a normal central pulmonary arterial system with a duct-dependent pulmonary circulation, whereas others have either partial or complete absence of the native pulmonary arteries. Their pulmonary circulation depends on systemic-pulmonary collateral arteries (SPCAs)[1,2]. SPCAs are highly variable in number and usually arise from the aortic arch, descending aorta or from the side branches.

At the Erasmus Medical Centre Rotterdam, the correction for PA-VSD with or without SPCAs, is performed in stages. The patients with a duct-dependent pulmonary circulation are initially palliated with a modified Blalock-Taussig shunt. The patients with SPCA-dependent pulmonary circulation are initially palliated by unifocalization of the pulmonary vasculature in either lung, combined with a modified Blalock-Taussig shunt. In both groups corrective surgery consists of closure of the modified Blalock-Taussig shunts, closure of the VSD and installing a pulmonary homograft between the right ventricle and the (unifocalized) pulmonary arterial system. At correction, the right ventricle in patients with PA-VSD shows without exception hypertrophy as an adaptive response to the increased pressure overload. This response could lead to remodeling of the myocardium and to the development of interstitial fibrosis[3-5].

In experimental models cardiac hypertrophy by pressure overload has been shown to accompany myocardial collagen deposition contributing to the increased stiffness of the cardiac muscle[6,7]. Most collagen subtypes in the heart are exclusively produced by cardiac fibroblasts, with the exception of type IV, which also is produced by other cell types including cardiac myocytes[8]. The collagen Iα and III subtypes are the most abundant forms in the heart. Collagen type Iα represents 80% of the total cardiac collagen content and is important for the cardiac stiffness[8,9]. Collagen type III represents about 12% of the total cardiac collagen content and is important for tissue elasticity[8,9]. Collagen type Iα and III are widely distributed between myocytes and

among muscle fibers and morphologic studies have defined the spatial distribution of these collagen types in normal and hypertrophic hearts[7,9-11].

Myocardial fibronectin is homogeneously localized throughout the extracellular space and is closely associated with collagen fibers[12]. It is a glycoprotein and serves as a bridge between cardiac myocytes to the interstitial collagen network[5]. Fibronectin binds collagen and modulates the collagen fibrillogenesis, consequently resulting in higher contents of collagen type Iα and a lower collagen type III concentration[13]. Furthermore, fibronectin influences several processes, including cell growth, adhesion, migration and wound repair[14].

The present study was undertaken to describe the degree of myocardial fibrosis in patients with PA-VSD by investigating the expression of collagens and fibronectin (both at mRNA and protein level) in right ventricular biopsies obtained from patients undergoing surgery for PA-VSD. Secondly, we attempted to correlate the expression data with clinical data.

Materials and Methods

Patients

Present study was approved by the Medical Ethical Committee of the University Hospital Rotterdam (MEC153. 268/1996/119). Biopsies from the right ventricular outflow tract were taken at corrective surgery for PA-VSD in 14 patients. Mean age of the patients at the time of surgery was 2.54 ± 0.32 years (range 0.76-5.51 years). Age-matched controls (C-1) consists of 2 post mortem biopsies and biopsies from 4 heart valve donors, who died due to non-cardiac cause (mean age 2.52 ± 0.75 years (range 0.01-5.70 years)). Part of the myocardial biopsy was immediately frozen in liquid nitrogen for mRNA expression studies, and the other part was fixed in 4% paraformaldehyde in phosphate buffered saline (PBS) for at least 24 hours and further processed for histological and immunohistochemical studies.

Total RNA isolation and RT-PCR

Right ventricular tissue biopsies (50-60 mg) were homogenized in 500 µl guanidinium thiocyanate (GTC) buffer and processed for the extraction of total cellular RNA[15]. The RNA concentration was estimated by optical density measurements at 260 nm and a RNA/protein ratio of ≥ 1.8 was accepted. The quality of total RNA was further verified on a 1% agarose gel.

Reverse transcriptase polymerase chain reaction (RT-PCR) analysis was used to asses the mRNA expression levels of collagen Iα, collagen III and fibronectin. For RT-PCR, first strand of cDNA was synthesized from total cellular RNA using Promega's Universal RiboClone cDNA Synthesis System (Promega, BNL, Leiden, The Netherlands). Appropriate oligonucleotide primers for the PCR were designed from the respective published human sequences for collagen Iα[16], collagen III[17] and fibronectin[18] and β-actin[19] cDNAs. Following oligonucleotide primers were procured commercially (Life Technologies BV, Breda, The Netherlands):

Primer	Bases	Sequence	Size of PCR product
Collagen Iα-F	20	GATGCCAATGTGGTTCGTGA	569bp
Collagen Iα-R	20	GCTGTAGGTGAAGCGGCTGT	
Collagen III-F	20	CAGTGGACCTCCTGGCAAAG	519bp
Collagen III-R	20	TGTCCACCAGTGTTTCCGTG	
Fibronectin-F	20	CACCATCCAACCTGCGTTTC	531+456bp
Fibronectin-R	19	TGTCCTACATTCGGCGGGT	(splice variants)
β -actin-F	30	TGACGGGGTCACCCACACTGTGCCCATCTA	625bp
β -actin-R	28	ACTCGTCATACTCCTGCTTGCTGATCCA	

The PCR amplified products were analyzed on the same 1.5% agarose gel, digitally photographed. Quantification was done by measuring the intensity of the bands with a Molecular Annalist (V 1.5) image analysis program (Biorad Laboratories, Hercules, CA, USA) running under Windows 98. The measurements of the intensity of the bands were corrected for background. The intensity of the β-actin band of each patient was set to the value of one as the internal standard and the values of the collagen Iα,

collagen III and fibronectin bands were divided by the β-Actin band values of the respective patient.

Gomori reticulin staining

For determining the myocyte surface size, the cell (membrane) reticulin fibers were stained by routine Gomori's reticulin silver staining technique[20] on 5 μm thick sections. After the silverstaining was developed, slides were mounted and visualized under light microscope.

Collagen staining

The total collagen in myocardial tissue specimens was stained with Picro-sirius red F3BA[11]. Tissue sections of 5 μm thickness, were treated with 0.2% aqueous phosphomolybdic acid and incubated in 0.1% Picro-sirius red. Before dehydration, the slides were treated with 0.01N HCl and mounted. Slides were visualized under light microscope and eventually collagen contents were quantified.

Immunolocalization of fibronectin, collagen Iα and collagen III

Paraffin sections (5 μm thickness) of the myocardial tissues were cut and mounted on 3-amino-propyl-trioxysilane (Sigma, St Louis, MO, USA) coated glass slides. Immunohistochemical staining was performed using the avidin-biotin complex (ABC) method following supplier's instructions (BioGenex, San Ramon, CA, USA). Optimal dilutions for all antibodies were identified by examining the intensity of staining obtained with a series of dilutions, which gave specific signal on paraffin sections derived from the same control tissue prior to perform the staining protocol on all section.

In brief, after deparaffinization in xylene and rehydration through graded alcohol the slides were rinsed with water. Slides to be stained for collagen Iα were pretreated in a boiling citrate solution in a microwave for 20 min. and slides to be stained for collagen III were pretreated with 0.1 % pronase for 10 min. After rinsing in PBS, slides were pre-incubated with 10% normal goat serum diluted in 5% bovine serum albumin in phosphate buffered saline (5% BSA/PBS, pH=7.4) for 15 minutes to block non-specific binding. Specific anti-human antibodies were added in different

solutions for the specific positive staining whereas negative controls were performed by omission of the primary antibody. For fibronectin staining specific antibodies against human fibronectin (Clone Ab-3, Neomarkers, Fremont, CA, USA) in 1:150 dilution were applied as primary antiserum, whereas for collagen Iα, specific human antibodies against collagen Iα (mouse monoclonal anti-collagen type 1 (Sigma, St Louis, MO, USA)) and for collagen III mouse monoclonal antibodies to collagen III (BioGenex, San Ramon, CA, USA), were used in a optimal dilutions of 1: 100. Anti-human mouse monoclonal antibodies against smooth muscle actin (α-SMA, Clone 1A4, NeoMarkers Fremont, CA, USA) in a 1: 1000 dilution were used as a positive control.

After incubation over night at 4°C sections were washed in 0.5% tween-20 in PBS solution. Sections stained for fibronectin and collagen Iα, were incubated with mouse biotinylated anti-rabbit IgG (BioGenex, San Ramon, CA, USA) for 30 min. and subsequently, with streptavidin conjugated alkaline phosphatase (label 1:50 dilution, Biogenex, San Ramon, CA, USA) for 30 min. Color was developed using a substrate of 18 mg Naphtol AS-MX phosphate (N5000), 200 μl new fuchsin, 200 μl sodium nitrite, 60 ml Tris HCl (pH 8,0)), while endogenous alkaline phosphatase activity was inhibited by 15 mg of levamisol. Sections stained for collagen III and α-SMA were incubated with multilink for 30 min., rinsed followed by 30 min. incubation with peroxidase conjugated streptavidin at a dilution of 1:50 (Biogenex, San Ramon, MO, USA). Subsequently, sections were colored, for 7 min. using, 0.025% of 3,3-diaminobenzidine (DAB) (Sigma, St Louis, MO, USA) in 0.01 mol/L PBS, containing 0.03% H_2O_2, as a substrate. All sections were counter stained with hematoxylin, mounted and visualized under the light microscope and photographed.

Video image analysis

Video image analysis was used to quantify the expression levels of collagen and fibronectin. After staining, the sections were mounted and visualized under light microscope (Leica DM RBE, Leica GmbH, Wetzlar, Germany) using 20x lens and grey-filters. From each section, series of 12 consecutive digital color images (736x574 pixels) for staining analysis were taken form a representative area. All sections from one staining were photographed at the same time using same microscopic and computer settings. A mm-scale was photographed which was used as a reference to control the

measured values. The digital images were analyzed using a specialized computer program for the Leica Qwin standard (Y2.2b) image analysis software package (Leica Imaging Systems Ltd., Cambrige, England).

Distribution of the stained fibers in the interstitial space as well as in the peri-vascular region was measured as a positive area. To analyze the positive staining areas of the extra cellular matrix the staining detection levels for hue, saturation and intensity in the computer program were optimized and set. Those settings were used for analysis of the all images derived from one staining. Interstitial expression was represented as ratio staining per total tissue area, excluding vascular areas, whereas peri-vascular localization was depicted as staining per peri-vascular area. Since the Peri-Vascular Collagen Area (PVCA) and vessel Luminal Area (LA) are positively correlated, the stained PVCA was normalized to the LA and represented as PVCA/LA ratio[21]. The Peri-Vascular Fibronectin Area (PVFA) was normalized in the same way for the LA and represented as PVFA/LA ratio.

To asses the degree of myocardial hypertrophy myocyte cell sizes were measured. From each section 3-4 digital images were photographed with a 20x (adult) or 40x (young) lens and stored in the computer. With the image analysis software the myocyte outline of at least 20 transfers cut myocytes, containing a nucleolus, per section were drawn manually where after the program calculated the myocyte surface in μm^2. Interstitial staining values were corrected for the increase in myocyte size by multiplying the interstitial staining with the increase in cell surface divided by the average control cell surface.

Statistical analysis

Results were expressed as mean ± standard error of mean (SEM). Statistical probability was assessed by (non-parametric) Kruskal-Wallis one way analysis of variance. Results were considered statistically significant with $p<0.05$. Regression analysis of clinical data with collagen and fibronectin expression data was performed using SPSS software. The correlation coefficient and significance level were calculated using linear (Pearson's) regression.

Results

mRNA expression analysis

Employing RT-PCR, the myocardial expression of collagen Iα, collagen III and fibronectin mRNAs were assessed in 9 patients who underwent surgery for PA-VSD and the mRNA levels were compared with 3 age matched controls. The data obtained are reported in figure 5.1 and 5.2. Quantitative analysis using optical density of bands obtained for Collagen III gene in relation to β–actin band showed significantly higher (p=0.03) mRNA levels in patients with PA-VSD (0.96 ± 0.11) as compared to the controls (0.61 ± 0.07). No significant differences in collagen Iα (0.65 ± 0.10 *vs.* 0.85 ± 0.13, p=0.31) and fibronectin (0.11 ± 0.02 *vs.* 0.15 ± 0.04, p=0.47) mRNA levels between PA-VSD patient and control groups were observed (Fig. 5.2).

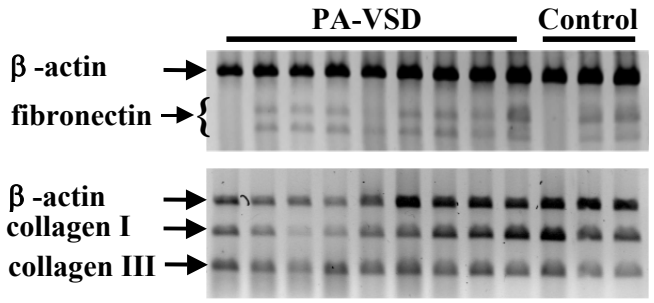

Figure 5.1. RT-PCR products of fibronectin, collagen Iα, collagen III and β-actin in human right ventricular tissue, using specific primers.

Myocyte surface size

The assessment of the myocyte surface area showed an increased surface for PA-VSD as compared to age matched controls (284 ± 27 μm^2 *vs.* 145 ± 50 μm^2; p<0.02), indicating hypertrophy. Pearson's linear correlation analysis did not result resulted in a linear correlation between the myocyte-size and age.

Myocyte surface size

The assessment of the myocyte surface area showed an increased surface for PA-VSD as compared to age matched controls (284 ± 27 μm^2 *vs.* 145 ± 50 μm^2; p<0.02), indicating hypertrophy. Pearson's linear correlation analysis did not result resulted in a linear correlation between the myocyte-size and age.

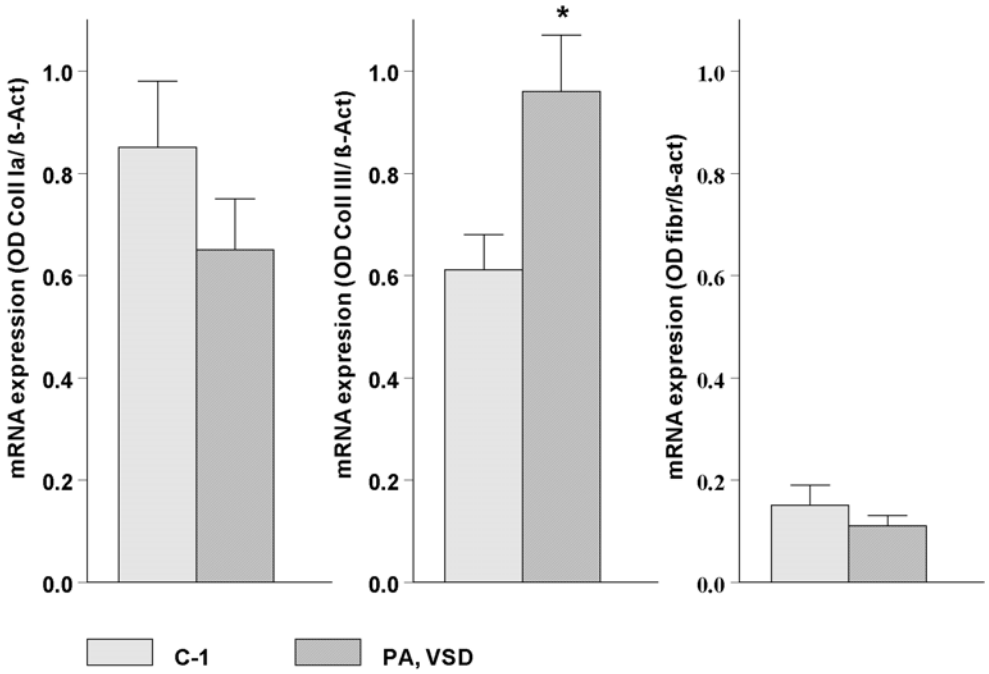

Figure 5.2. Quantitative analysis of mRNA expression for fibronectin, collagen Iα and collagen III in patients with PA-VSD in relation to age matched control.

RT-PCR products for fibronectin, collagen Iα and collagen III in PA-VSD patients and controls were separated on agarose gels and visualized by ethidium bromide staining and photographed. The optical density values of the bands were corrected for background and the intensity of the myocardial β-actin band of each patient was used as an internal standard to normalise the collagen Iα, collagen III and fibronectin bands as described in the "materials and methods". Values are shown as mean ± SEM and * represents significant increased ($p<0.05$) as compared to control.

Collagen expression

Total collagen staining using Picro-sirius red depicts that collagen bundles are localized in the interstitium as well as in the peri-vascular areas in the right ventricular tissue obtained from both groups. However, the expression pattern in patients with PA-VSD was different than in control as the collagen bundles were disarrayed and irregular in shape and size (Fig. 5.3). Video image analysis of interstitial total collagen, collagen type Iα and collagen type III showed no significant differences in staining ratios in patients with PA-VSD as compared to control (7.61 ± 0.71 *vs*. 10.68 ± 1.45; 4.77 ± 0.51 *vs*. 7.16 ± 1.19; 5.72 ± 0.80 *vs*. 5.92 ± 1.18 respectively). The interstitial collagen staining values corrected for the increase in myocyte size remained statistically unaltered (total collagen: 14.28 ± 1.88 *vs*. 10.81 ± 4.06, p=0.07;

collagen Iα: 9.23 ± 1.49 *vs*. 6.77 ± 2.07, p=0.11; collagen III: 5.72 ± 0.80 *vs*. 5.92 ± 1.18, p=0.08) in the PA-VSD group as compared to control (Fig. 5.4). However, for the normalized peri-vascular collagen area, the PVCA/LA ratio was significantly lower in the PA-VSD group as compared to control (3.22 ± 0.34 *vs.* 7.23 ± 1.13, p<0.01) (Fig. 5.4).

Fibronectin expression

The pattern of fibronectin localization was similar to that of collagens as it was localized in the interstitial spaces and around the blood vessels (Fig. 5.3). Video image analysis of interstitial fibronectin showed that the expression levels in the PA-VSD group were not significantly changed as compared to control (11.03 ± 1.49 *vs.* 12.22 ± 1.43). The expression pattern remained unaltered when the interstitial fibronectin ratios were corrected for the increase in myocyte size (7.11 ± 1.08 *vs*. 14. 18 ± 4.10, p=0.10) when patients with PA-VSD were compared to respective controls (Fig. 5.4). Also the normalized peri-vascular fibronectin area the PVFA/LA ratio showed no significantly changed levels in the PA-VSD group as compared to control (2.65 ± 0.48 *vs.* 2.62 ± 0.47, p=0.52) (Fig. 5.4).

Correlation analysis

Pearson's correlation and regression analysis was performed on several clinical parameters, obtained from medical records of the Thoraxcentre, Dijkzigt Hospital and Sophia Childrens Hospital Rotterdam (Table 5.1), such as, right ventricular pressure and transcutaneous O_2-saturation with the expression levels of collagens and fibronectin in both interstitium and peri-vascular area. The data on correlation with right ventricular pressure as well as with O_2-saturation showed no significant regression values. Correlation coefficient (r) and significance level (p value) using linear regression (Pearson's) analysis is shown in table 5.2. The data on correlation with right ventricular pressure as well as with aortic O_2 saturation showed no significant regression values (Table 5.2).

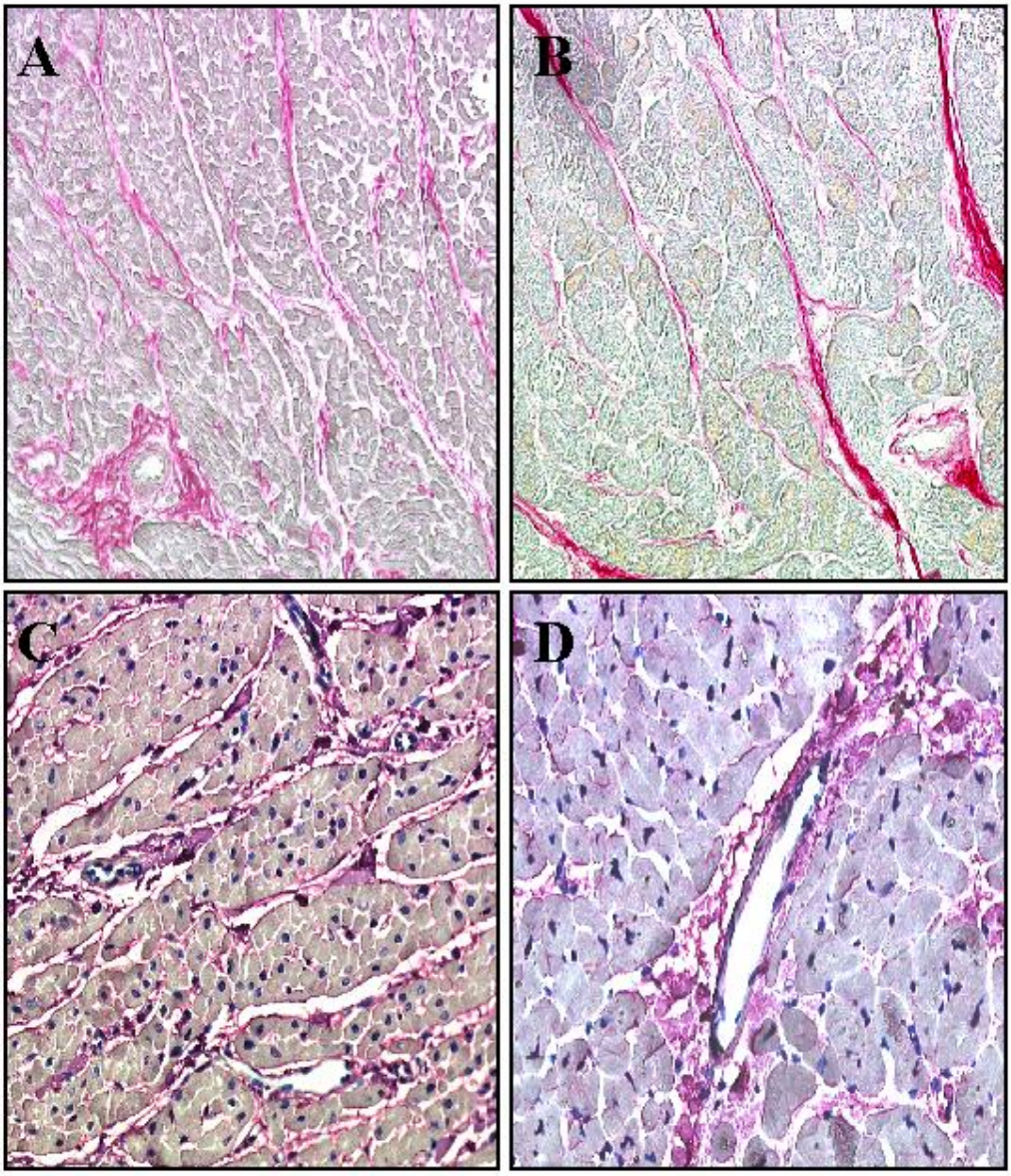

Figure 5.3. (Immuno)histochemical localization of collagen and fibronectin in the right ventricular tissue of patients with PA-VSD and controls.
Micro-photographs showing human right ventricular tissue stained with Picro-sirius red for collagen (**A** and **B**) and with antibodies against fibronectin (**C** and **D**) (as described in materials and methods). Panel **A** and **C:** control donors, panel **B** and **D:** patients corrected for PA-VSD. The staining represents collagen and fibronectin fibers localized in the peri-vascular as well as in the interstitial area.

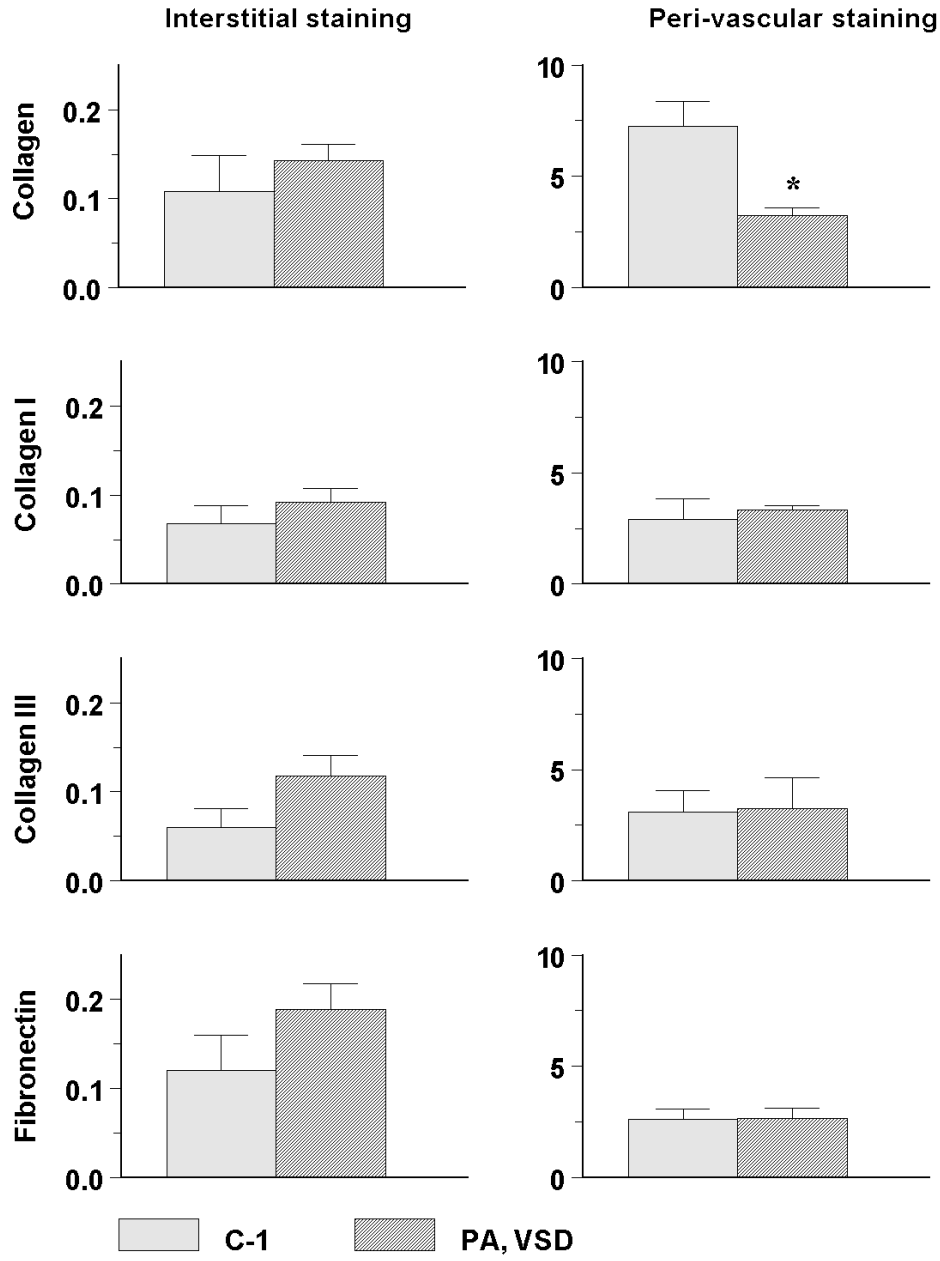

Figure 5.4. ***Quantitative video image analysis of interstitial and peri-vascular collagens and fibronectin in patients with PA-VSD.***
Total collagen and collagen subtype Iα and III as well as fibronectin levels in the different myocardial tissue specimens were quantified using a video image analysis system. Bar diagrams depict, ratio of interstitial stained area with total tissue area corrected for the increase in myocyte surface size, whereas the peri-vascular stained area was normalised to the vascular lumen area (PVSA/LA). Values are shown as mean ± SEM and * means significantly decreased ($p<0.05$) as compared to respective control.

Table 5.1. Clinical data of patients underwent surgery for PA-VSD.

Biopt nr.	Age (Yrs)	Ht	Right ventricular pressure			Syst. RVP/ Syst. LVP	O_2-sat. aorta (%)	Qp/Qs	Right atrial pressure	
			Syst.	Diast.	End.				A	M
1	0.76	0.49	65	0	5	0.96	79.0	0.86	7	4
2	3.49	0.44	78	5	9	0.96	90.0	2.53	9	5
3	2.75	0.48	90	6	13	0.99	81.0	1.19	12	7
4	2.13	0.47	79	5	9	0.90	80.0	0.66	7	4
5	2.62	0.62	81	0	10	0.99	72.6	0.65	7	5
6	2.74	0.53	79	3	7	1.07	93.8	1.32	5	2
7	2.15	0.41	76	2	9	1.00	93.0	4.32	8	6
8	2.34	0.49	75	6	14	0.96	80.8	0.75	16	10
9	5.51	0.50	84	-3	9	0.95	87.5	1.95	6	5
10	1.80	0.53	75	-1	11	1.00	78.7	0.65	9	7
11	1.89	0.45	76	-3	11	0.93	89.5	2.20	5	3
12	1.37	0.45	89	7	13	1.07	76.5	0.48	ND	ND
13	1.95	0.45	83	3	8	1.01	89.8	2.51	9	6
14	4.04	0.46	82	-1	13	1.09	83.0	0.72	8	6
mean	**2.54**	**0.48**	**79**	**2**	**10**	**0.99**	**83.9**	**1.48**	**8.3**	**5.4**
SEM	**0.32**	**0.01**	**2**	**1**	**1**	**0.01**	**1.8**	**0.29**	**0.8**	**0.6**

ND, not determined; Syst., Systolic pressure in mmHg; Diast., Diastolic pressure in mmHg; End., End diastolic pressure in mmHg; Syst. RVP / Syst. LVP represents the ratio between systolic Right Ventricular Pressure and systolic Left Ventricular Pressure; O_2-sat. aorta (%), O_2-saturation in aorta; Qp/Qs represents the ratio between pulmonary blood flow and systemic blood flow; A, Atrial pressure; M, Mean pressure; Ht, Haematocrite.

Table 5.2. Regression analysis of clinical data with collagen and fibronectin expression data. Correlation coefficient (r) and p values are given.

Clinical data		Interstitial collagen	Peri-vascular collagen	Interstitial fibronectin	Peri-vascular fibronectin
RVP (syst.)	r	-0.17	0.33	0.26	-0.27
	p	0.55	0.24	0.57	0.96
O_2 sat. aorta	r	0.05	0.35	0.49	-0.10
	p	0.87	0.22	0.26	0.83

RVP, Right Ventricular Pressure; Syst., Systolic pressure; O_2-sat. aorta, O_2-saturation in aorta.

Discussion

The present study investigated the degree of hypertrophy and the expression of fibrosis markers in the right ventricular biopsies obtained from patients with PA-VSD and the altered patterns were compared with that of right ventricular tissue obtained

from age matched control individuals. The presence of myocyte hypertrophy in patients with PA-VSD, as a response to the right ventricular pressure overload, is obvious. This is thought to be accompanied by myocardial fibrosis to increase the myocardial stiffness and prevent further dilatation[6,7]. Analyzing the expression pattern of two fibrosis markers in the myocardium, we found a tendency for limited increase collagen and fibronectin contents without statistically significant differences when the study group of PA-VSD patients was compared to the control group. However, in the peri-vascular stained area, corrected for lumen area, total collagen levels were significantly lower in the patient group, suggesting a lower amount of collagen accumulation around the vessels. Additionally, it can be emphasized that the collagen and fibronectin deposition in the interstitial areas showed an altered pattern, depicting irregularities in the network of collagen and fibronectin fibers. Our results indicate that the patients with PA-VSD may have an impaired extracellular matrix support for their coronary blood vessels.

The expression of collagen and fibronectin was also evaluated at mRNA level by RT-PCR analysis, where we found significantly increased levels for collagen type III and unchanged levels for collagen Iα and fibronectin in patients with PA-VSD. Enhanced levels for collagen III could be attributed to the altered, more compliant, myocardial architecture due to hypoxemia as well as hypertrophy. Furthermore, the enhanced levels of collagen III mRNA in the patients with PA-VSD may be attributed to the decreased degradation of this mRNA. Interestingly, decreased levels of collagen Iα mRNA did not result in a decreased biosynthesis and accumulation. Perhaps an altered biosynthesis and an inadequate collagen fibers network around the coronary blood vessels could contribute to the existing cardiac pathology.

Limited research has been done so far on PA-VSD patients. This study contributes in the understanding of myocardial architecture in patients with PA-VSD. In a study on collagen and fibronectin content in patients with tetralogy of Fallot, also no significant changes in the interstitial collagen or fibronectin expression were found[22], whereas only the peri-vascular collagen area corrected for lumen area was significantly altered, resulting in a lower expression of total collagen in the peri-vascular area in adult patients with tetralogy of Fallot. In the present study we found

an increased expression of collagen type III in the myocardium, whereas the collagen type Iα expression was not changed. Other studies also show that cardiac collagen expression in normal and hypertrophied myocardium differs qualitatively[23].

The PCR amplification with specific primers for fibronectin resulted in two splice variant products of fibronectin (531 bp and a 456 bp) as shown in figure 5.1. Those two products are the result of alternative splicing of a common precursor[24]. When the semi-quantitative PCR analysis was done, the bands of both splice variants were taken into account for optical density measurement.

We realize the limitations posed in our human study based on myocardial biopsies obtained during surgical correction of the congenital anomaly. As the myocytes are hypertrophied the ratio of cells per digital image will decrease, with consequently decreasing staining ratios. This will influence the staining data. Therefore the staining data was corrected for the increase in myocyte size. Hence the interpretation of the obtained results should be cautiously taken. Yet not much is known about patients with PA-VSD at a cellular level, so any available new data for this group is taken along in the understanding of this disease. As mentioned earlier, we studied limited numbers of patients and controls. Therefore the conclusions can only be drawn with caution. It may be added here that the limited clinical data on normal myocardium in young healthy children is a limitation of our study as well. We are currently accumulating appropriate tissue biopsies to increase the number of controls.

In conclusion, our data suggest that in patients with PA-VSD have an inappropriate state of the extracellular matrix support for their coronary blood vessels. Speculations can be made whether or not this is due to an altered biosynthesis of collagen and fibronectin in the extracellular network. As yet, no correlation with clinical parameters or outcome could be established.

Acknowledgement

This study was financially supported by the Netherlands Heart Foundation, grant number NHS 96.082.

References

1. Kirklin JW, Barrat-Boyes BG. *Ventricular septal defect and pulmonary stenosis or atresia*. 2nd ed. ed. New York: Churchill-Livingstone: Churchill-Livingstone; 1993.
2. Tchervenkov CI, Roy N. Congenital Heart Surgery Nomenclature and Database Project: pulmonary atresia-ventricular septal defect. *Ann Thorac Surg*. 2000;69:S97-105.
3. van Bilsen M, Chien KR. Growth and hypertrophy of the heart: towards an understanding of cardiac specific and inducible gene expression. *Cardiovasc Res*. 1993;27:1140-1149.
4. Schwartz K, Carrier L, Mercadier JJ, et al. Molecular phenotype of hypertrophied and failing myocardium. *Circulation*. 1993;87:VII 5-10.
5. Pelouch V, Dixon IM, Golfman L, et al. Role of extracellular matrix proteins in heart function. *Mol Cell Biochem*. 1994;129:101-120.
6. Samuel JL, Barrieux A, Dufour S, et al. Accumulation of fetal fibronectin mRNAs during the development of rat cardiac hypertrophy induced by pressure overload. *J Clin Invest*. 1991;88:1737-1746.
7. Bishop JE, Rhodes S, Laurent GJ, et al. Increased collagen synthesis and decreased collagen degradation in right ventricular hypertrophy induced by pressure overload. *Cardiovasc Res*. 1994;28:1581-1585.
8. Chapman D, Weber KT, Eghbali M. Regulation of fibrillar collagen types I and III and basement membrane type IV collagen gene expression in pressure overloaded rat myocardium. *Circ Res*. 1990;67:787-794.
9. Bashey RI, Martinez-Hernandez A, Jiminez SA. Isolation, characterization, and localization of cardiac collagen type VI. Associations with other extracellular matrix components. *Circ Res 70*. 1992;70:1006-1017.
10. Factor SM, Robinson TF, Dominitz R, et al. Alterations of the myocardial skeletal framework in acute myocardial infarction with and without ventricular rupture. *Am J Cardiovasc Pathol*. 1986;1:91-97.
11. Takahashi T, Schunkert H, Isoyama S, et al. Age-related differences in the expression of proto-oncogene and contractile protein genes in response to pressure overload in the rat myocardium. *J Clin Invest*. 1992;89:939-946.
12. Speiser B, Weihrauch D, Reiss CF, et al. The extracellular matrix in human cardiac tissue part II: Vimentin, laminin, and fibronectin. *Cardioscience*. 1992;3:41-49.
13. Speranza ML, Valentini G, Calligaro A. Influence of fibronectin on the fibrillogenesis of type I and type III collagen. *Coll Relat Res*. 1987;7:115-123.
14. Farhadian F, Contard F, Corbier A, et al. Fibronectin expression during physiological and pathological cardiac growth. *J Mol Cell Cardiol*. 1995;27:981-990.
15. Chomczynski P, Sacchi N. Single-step method of RNA isolation by acid guanidinium thiocyanate-phenol-chloroform extraction. *Anal Biochem*. 1987;162:156-159.
16. Bernard MP, Chu ML, Myers JC, et al. Nucleotide sequence of complementary deoxyribonucleic acids for the pro alpha 1 chain of human type 1 procollagen. Statistical evaluation of structures that are conserved during evolution. *Biochem*. 1983;22:5213-5223.
17. Ala-Kokko L, Kontusaari S, Baldwin CT, et al. Structure of cDNA clones coding for the entire prepro alpha 1 chain of human type III procollagen. Differences in protein structure from type I procollagen and conservation of codon preferences. *Biochem J*. 1989;260:509-516.
18. Kornblihtt AR, Vibe-Petersen K, Baralle FE. Isolation and characterization of cDNA clones for human and bovine fibronectins. *Proc Nat Acad Sci USA*. 1983;80(11):3218-3222.

19. Yamaguchi T, Iwano M, Kubo A, et al. IL-6 mRNA synthesis by peripheral blood mononuclear cells (PBMC) in patients with chronic renal failure. *Clin Exp Immunol*. 1996;103:279-328.
20. Bancroff JD, Cook HC. *Manual of Histological Techniques and Their Diagnostic Aplication*. London: Churchill Livingstone; 1994.
21. Brilla CG, Janicki JS, Weber KT. Impaired diastolic function and coronary reserve in genetic hypertension. Role of interstitial fibrosis and medial thickening of intramyocardial coronary arteries. *Circ Res*. 1991;69:107-115.
22. Peters THF, Sharma HS, Yilmaz E, et al. Quantitative analysis of collagens and fibronectin expression in human right ventricular hypertrophy. *Ann N Y Acad Sci*. 1999;874:278-285.
23. Iimoto DS, Covell JW, Harper E. Increase in crosslinking of type I and type III collagens associated with volume-overloaded hypertrophy. *Circ Res*. 1988;63:399-408.
24. Kornblihtt AR, Umezawa K, Vibe-Pedersen K, et al. Primary structure of human fibronectin: differential splicing may generate at least 10 polypeptides from a single gene. *EMBO J*. 1985;4(7):1755-1759.

Chapter 6

Myocardial angiogenesis and fibrosis in human tetralogy of Fallot

Based on:
Sharma HS, Peters THF and Bogers AJJC. Angiogenesis and fibrosis during right ventricular hypertrophy in human tetralogy of Fallot. In: N. Takeda, M. Nagano and NS. Dhalla (eds). The Hypertrophied Heart. Kluwer Academic Publishers, Boston 2000; 227-241.

Abstract

Right ventricular hypertrophy (RVH) due to pressure as well as volume overload, caused by (sub) pulmonary stenosis and ventricular septal defect, is one of the main features in human tetralogy of Fallot (TF). Currently, primary correction at a very young age is the treatment of choice. However, it is not yet known to what extent RVH in TF patients regresses after corrective surgery. The aim of our study was to evaluate the changes in magnitude of the myocardial fibrosis and angiogenesis during RVH in patients undergoing corrective surgery For this purpose, we examined endomyocardial biopsies for the expression of extracellular matrix proteins such as collagens, fibronectin, and an angiogenic growth factor, vascular endothelial growth factor (VEGF), in TF patients with RVH and compared the expression with patients without RVH. Myocardial tissue biopsies were obtained from patients undergoing primary correction (TF-1 group, mean age 0.4 ± 0.1 years, n=8), from those undergoing secondary surgery (TF-2 group, mean age 38.1 ± 3.7 years, n=6), and from control patients with normal right ventricle (control group, mean age 36.4 ± 1.8 years, n=12). Picro-sirius red staining, depicting total collagens, and fibronectin staining were semi-quantitatively analyzed. Interstitial levels for total collagens were significantly increased in the TF-2 group as compared to the TF-1 group ($p<0.04$) and control ($p<0.05$) groups. Immunolocalization of fibronectin showed the expression in the interstitium and peri-vascular areas. Semi-quantitative analysis of fibronectin staining revealed that the expression levels were not significantly different in the TF-2 group as compared to the TF-1 and control groups. Angiogenesis, assessed by the increased number of small ($p<0.05$) vessels, was observed in both TF groups as compared to the control group. Densitometric analysis of mRNAs encoding VEGF showed significant enhanced expression in TF-1 ($p<0.02$) and TF-2 ($p<0.05$) groups as compared to control. Immunoreactive VEGF was localized mainly in the myocytes and smooth muscle cells and not in fibrotic areas in the case of TF groups. Our results show an increased degree of myocardial fibrosis and angiogenesis during RVH in TF patients. This information leaves room for the improvement in contemporary clinical treatment of patients with TF by allowing an assessment of timing for surgery and possibly supports long-term postoperative prognosis.

Introduction

With an incidence of 5 per 10,000 live births, tetralogy of Fallot (TF) is a fairly common congenital cardiac anomaly[1]. TF is characterized by overriding of the aorta, a ventricular septal defect (VSD), (sub)valvular pulmonary stenosis, and right ventricular hypertrophy (RVH) resulting in hypoxemia due to diminished pulmonary flow[1,2]. Without appropriate treatment, TF ultimately results in cyanotic complications and cardiac failure. For this reason, nearly 70% of patients with TF require an operation during the first year of life. Due to improved peri-operative care, the results of primary repair have increased dramatically in the past decade, and such repair is now the surgical treatment of choice[3,4]. Nowadays, most TF patients usually are operated during their first year of life by primary repair. The aim of early primary repair, by closing the VSD and removing the right ventricular outflow tract obstruction, is to relieve the hypoxemia and to eliminate the stimulus for the adaptive RVH as well as to preserve right ventricular function[2-4]. However, some patients suffer from pulmonary regurgitation after primary correction, causing right ventricular failure due to volume overload. For these patients, further secondary corrective surgery later in life is performed by implanting a pulmonary allograft heart valve between the right ventricle and the pulmonary artery[5,6].

Most attention in research on human TF so far has been focused on clinical treatment and surgical methods. In addition, histopathological data on TF myocardial tissue showed a reduction of the myocardial cell diameter in patients after corrective surgery[7]. This would indicate a diminishing degree of RVH. But to what extent the RVH in TF patients finally regresses is still uncertain. Only very limited information is available concerning the complex molecular phenotype of (right ventricular) myocardium in the different stages of TF. In this regard, we have developed strategies to evaluate whether different forms and stages of disease could be correlated with histopathological and molecular biological data. To elucidate the myocardial phenotype and fate of RVH after corrective surgery in patients with TF, we examined the degree of fibrosis and angiogenesis in endomyocardial biopsies obtained during corrective surgery. We investigated the total collagens and fibronectin contents and the expression pattern of an angiogenic glycopeptide, vascular endothelial growth

factor (VEGF), and compared the data with those of age matched patients with a normal right ventricle.

Myocardial hypertrophy

Cellular hypertrophy is an adaptive mechanism in response to chronic haemodynamic overload, leading to remodeling of the myocardium with an increased risk of ultimately developing cardiac failure[8,9]. Histopathological alterations in TF myocardium in patients under 3 years of age have been reported, but data on regression of RVH in the later postoperative period are scarce[10,11]. Recently, a histopathological study on TF myocardial tissue biopsies reported that the myocardial cell diameter was reduced in postoperative patients as compared to preoperative patients with TF, but postoperative cellular diameter was still larger than that in the age-matched normal subjects [7,12]. These findings suggest that RVH after corrective surgery of TF can regress to some extent, provided that residual pulmonary stenosis can be avoided. Until now, no data on molecular markers or their dynamics in RVH in human TF have been available. Several animal models of ventricular hypertrophy[8,13,14] have been described, but none can approximate the TF situation in humans. Experimental animal studies have mainly focused on the morphological and cellular changes in the hypertrophic myocardium in response to volume or pressure overload. A battery of genes, including immediate early genes (such as proto-oncogenes, c-fos, c-jun and c-myc) and genes from the foetal period (such as ANF, β-MHC, α-skeletal actin) have been implicated in the cellular alterations leading to ventricular hypertrophy[8,13-15]. It is believed that alterations in gene expression play an important role in myocardial adaptation in response to increased work load[13]. Employing molecular biological methods, we have shown in experimental animal work that a number of genes get induced and reprogrammed during the adaptive phase of myocardium after an ischemic or a hypertrophic stimulus[14,16-18]. Exploring molecular mechanisms contributing to cardiac hypertrophy, we have recently shown that angiotensin II, a potent vasoconstricting octapeptide, induces expression of transcription factors that precedes an increase in TGF-β_1, in cultured rat cardiac fibroblasts[19]. The information on the complex cascade of molecular mechanisms contributing to RVH in humans is very limited and warrants further investigation.

Myocardial fibrosis in TF

Progressive myocardial fibrosis due to cardiac hypertrophy is an important cause of myocardial dysfunction, clinical deterioration, and cardiac death. One of the major contributing factors to myocardial fibrosis is a disproportionate accumulation of, either reactive or reparative, collagens[20-23]. Collagen fibers are organized in the collagen network found in the extracellular space of the myocardium[21,23]. In a morphometrical study, increased fibrosis in TF was associated with an increased diameter of myocytes and an increase in myocardial disarray[11]. In rats, type Iα and III collagen mRNA were associated with fibroblasts and type IV collagen mRNA with interstitium as well as myocytes[23]. The levels of mRNA encoding for collagen and fibronectin were found to be increased in experimental models of pressure-overloaded cardiac hypertrophy[24]. Studying the expression and localization of genes encoding for fibronectin, collagens, and collagenases at all stages of RVH in TF may further elucidate the dynamics of the collagen network and myocardial fibrosis. RVH with expansion of cardiomyocytes in human TF is an adaptive response to the increased pressure overload caused by (sub) pulmonary stenosis in combination with the ventricular septal defect. This response requires a proportionate increase of coronary flow or growth of the coronary vasculature and leads to remodeling of the myocardium and to development of fibrosis[8,9,25]. Collagens and fibronectin play an important role in myocardial fibrosis. The collagen network, in the extracellular space of the myocardium, consists of collagen fibers, which support the myocardial strength and stiffness[21,22]. When this network is damaged, the myocyte support is compromised and allows tissue expansion[26]. Disproportionate accumulation of collagen, either reactive or reparative, has been observed during myocardial fibrosis. Experimental[27] and clinical data[28] show that a rise in the collagen content increases the myocardial stiffness and promotes abnormalities of cardiac function during hypertrophy.

Fibronectin located in the extracellular matrix of most tissue serves as a bridge between cells and the interstitial collagen mesh network. If further influences diverse processes, including cell growth, adhesion, migration, and wound repair[29]. During the development of cardiac hypertrophy due to pressure overload, fetal fibronectin has been shown to accumulate in rats[24]. In a hypertrophied heart, a significant change in

the expression pattern, qualitative as well as quantitative, for several genes has been observed. Focused on fibronectin and collagen, animal studies show an increased level of mRNA during cardiac hypertrophy.

Myocardial angiogenesis

Cardiac hypertrophy, being an adaptive response of cardiomyocytes to increased work load, requires proportionate increase of coronary flow or growth of the coronary vasculature (angiogenesis)[15,30]. It has been suggested that mechanical factors such as stretch, shear stress, and wall tension may provide an initial stimulus for capillary angiogenesis during cardiac hypertrophy[15]. A number of peptide growth factors, which are widely attributed to angiogenesis in vivo and in vitro, could play a role in modulating the angiogenesis during cardiac hypertrophy. An increase in mRNA for TGF-β_1, has been reported in cardiac hypertrophy[15]. Virtually nothing is known regarding the molecular mechanisms and role of specific endothelial cell mitogens in cardiac angiogenesis particularly during right ventricular hypertrophy in TF.

Material and Methods

Patient selection and biopsies

The present study was approved by the Medical Ethical Committee of the University Hospital, Erasmus University, Rotterdam (MEC153. 268/1996/119). The group operated upon for primary correction of TF (TF-1) consisted of eight patients. The mean age of the TF-1 group at the time of operation was 0.4 ± 0.1 years. The group of patients operated upon for pulmonary allograft implantation late after correction of TF (TF2) consisted of six patients, with a mean age of 38.1 ± 3.7 years. Their age-matched control group (Control) consisted of 12 patients who were operated upon for a pulmonary autograft replacement and who had a mean age of 36.4 ± 1.8 years. All patients operated upon for a pulmonary autograft procedure showed clinically normal right ventricular function.

All operations were done with the use of cardiopulmonary bypass with moderate hypothermia using bicaval cannulation. In selected cases of both Control and TF-2, single right atrial cannulation was used. The St. Thomas hospital cardioplegic solution

was applied except in some of the TF-2 patients, in whom the pulmonary allograft was implanted in the beating heart. In primary correction of TF (TF-1), the aim of preserving pulmonary valve function was met in five patients; a transannular patch was necessary in the remaining three patients. In those with preserved pulmonary valve function, the biopsies consisted of removed endomyocardial tissue from the right ventricular outflow tract. In those patients with a transannular patch, the biopsies consisted of a transmural sample from the incision level of anterior right ventricular wall. In late secondary surgery after correction of TF (TF-2), pulmonary allografts were implanted as previously described[31,32]. Biopsies consisted of tissue from the anterior free wall of the right ventriculotomy. All autograft procedures were done as previously described[33,34]. In harvesting the pulmonary autograft, the main pulmonary artery was transacted just proximal to its bifurcation and through the right ventricular outflow tract, leaving a ridge of supporting myocardial cuff. From the area of the free right ventricular wall of this cuff, the control biopsies were taken as a transmural sample. There was no operative or other early mortality. There were no complications that could be attributed to taking the biopsies.

Part of the myocardial tissue biopsy was immediately frozen in liquid nitrogen for mRNA expression studies, and the other part was fixed in 4% paraformaldehyde in PBS for at least 24 hours and further processed for dehydration and embedding in paraffin for histological and immunohistochemical studies.

Total RNA isolation and Northern blot analysis

Right ventricular tissue biopsies (50-100 mg) were homogenized in guanidinium isothiocyanate buffer and processed for the extraction of total cellular RNA according to the methods described elsewhere[16,17]. The RNA concentration was measured by spectrophotometry, and the quality of RNA was tested on a denatured formaldehyde agarose gel. For Northern hybridization, 15 μg of total RNA was electrophoresed on 1% agarose gel containing 2.2 M formaldehyde, and subsequently, RNA was transferred to hybond-N membrane (Amersham Nederland, Den Bosch, The Netherlands). Thereafter, filters were air dried and UV cross-linked in a gene linker (Bio-Rad Laboratories, Veenendaal, The Netherlands), and ribosomal RNA bands were marked under UV light. Blots were hybridized with a radioactively labeled cDNA probe encoding human VEGF[35] at 42°C in a buffer containing 50% deionized

formamide, 1.0 M sodium chloride, 1% sodium dodecylsulfate (SDS), 0.2% polyvinyl pyrrolidone, 0.2% ficoll, 0.2% bovine serum albumin, 50 mM TrisHCl (pH 7.5), 0.1% sodium pyrophosphate, 10% dextran sulfate and denatured salmon sperm DNA (100 μg/ml). Filters were washed at room temperature for 5 min. in 2xSSC (1xSSC; 150 mM NaCl, 15 mM trisodium citrate) containing 0.1% SDS and at 55°C in 0.1xSSC containing 0.1% SDS for 20 min. Subsequently, filters were wrapped in household plastic wrap and exposed to Kodak X-OMAT AR films (Kodak Nederland, Odijk, The Netherlands) at -80°C for 1-3 days. A glyceraldehyde-3-phosphate dehydrogenase (GAPDH) cDNA probe encoding human enzyme (ATCC, Rockville, MD, USA) was used to rehybridize membranes for references purposes. Hybridization signals on autoradiographs were quantified by video scanning in optical density mode using a densitometer (LKB-Pharmacia Biotech, Roosendaal, The Netherlands). For normalization, the optical density (OD) of the hybridization signal for VEGF was divided by the OD of the corresponding GAPDH signal, and relative percentages of mRNA levels were calculated in each group relative to control.

Picro-sirius red staining

The total collagen in myocardial tissue specimens was stained with Picro-sirius red F3BA[21,36]. Tissue sections of 6 μm thickness were treated with 0.2% aqueous phosphomolybdic acid and incubated in 0.1% Picro-sirius red. Before dehydration, the slides were treated with 0.01 N HCl and mounted. Slides were visualized under a light microscope using a polarized filter, and eventually collagen contents were quantified.

Immunohistochemistry

Expression of fibronectin

Paraffin sections (6 μm thickness) of the myocardial tissues were cut and mounted on 3-amino-propyl-trioxysilane (Sigma, St. Louis, MO, USA) coated glass slides. Immunohistochemistry using a multiple-step avidin-biotin complex (ABC) method was performed, essentially following the supplier's instructions. In brief, after deparaffinization in xylene and rehydration through graded alcohol, the slides were rinsed with water and phosphate buffered saline and were quenched for endogenous peroxidase by 2% hydrogen peroxide in methanol. The slides were placed in Sequeza

Immunostaining Workstation (Shandon Scientific Ltd, Astmoor, Runcorn). Slides were preincubated for 15 min. with 10% normal goat serum to block non-specific binding. Specific human-preabsorbed polyclonal antibodies, against human fibronectin in 1: 1000 dilution (Life Technologies, Breda, The Netherlands), were applied as primary antiserum, and the sections were incubated at room temperature for 30 min. The supraoptimal dilution was obtained by examining the intensity of staining obtained with a series of dilutions of the antisera from 1:100 to 1:2500 and selecting the dilution that gave specific, weak, but easily visible signals[36]. Negative controls were performed by omission of the primary antibody. After washing in 0.5% tween-20 in PBS solution, the sections were incubated with mouse biotinylated anti-rabbit IgG (BioGenex, San Ramon, CA, USA) for 30 min. and, subsequently, with peroxidase conjugated streptavidin. Color was developed using DAB (3,3-diaminobenzidine tetrahydrochloride dehydrate), and sections were counterstained with Mayer's hematoxylin. Sections were mounted and visualized under the light microscope and photographed.

Expression of VEGF

Immunohistochemistry was performed using a standard avidin-biotin complex (ABC) method, as described earlier[37,38]. In brief, after deparaffinization in xylene and rehydration through graded alcohol, the slides were rinsed with water and phosphate buffered saline (PBS) and placed in a Sequeza Immunostaining Workstation (Shandon Scientific Ltd, Astmoor, Runcorn). Slides were pre-incubated for 15 min. with normal goat serum to block non-specific binding, then incubated for 30 min. at room temperature with affinity-purified rabbit polyclonal antibodies in a dilution of 1:200. The anti-VEGF antiserum used was raised against a 20-amino-acid synthetic peptide corresponding to residues 1-20 of the amino terminus of human VEGF[39] (Santa Cruz Biotechnology, Inc., Santa Cruz, CA, USA). The optimal dilution was identified by examining the intensity of staining obtained with a series of dilutions of the antiserum from 1:50 to 1:500. The dilution (1:200) resulted in specific and easily visible signals in paraffin sections of a capillary hemangioma. The hemangioma sections served as a positive control in the study. After washing with PBS, the test and control slides were incubated for 30 min. with biotinylated secondary antibody (Multilink, 1:75 dilution, Biogenex, San Ramon, MO, USA). After two washes in PBS, slides were incubated for 30 min. with alkaline phosphatase-conjugated streptavidin (Biogenex) in a dilution

of 1:50. Finally, the slides were rinsed with 0.2 M TRIS-HCl pH 8.0, Levamizole (Sigma) was used to block the endogenous alkaline phosphatase activity, and then the slides were stained for 30 min. with 0.3% New Fuchsin/TRIS-HCl (Sigma) as a color enhancement system. Negative controls were prepared by omission of the primary antiserum. Slides were lightly counterstained with Mayer's hematoxylin for 10 seconds.

Expression of CD31 and α-SMA

Immunolocalization of VEGF in endothelial cells as well as in vascular smooth muscle cells was verified by staining these cells with specific markers. Endothelial cells were identified by CD31 immunostaining[37,38]. Staining was done by the ABC method, but using 0.025% 3,3-diaminobenzidine (DAB) as chromogen. Slides were incubated for 20 min. in methanol with 0.3% H_2O_2 to block the endogenous peroxidase activity. Slides were incubated with the primary anti-human CD31 monoclonal antibody in dilution of 1:80 (Dako Corporation, Glostrup, Denmark) at room temperature for 30 min. and subsequently visualized after developing the color using 0.025% DAB. Employing the DAB-based color development method, consecutive tissue sections were stained with anti-human mouse monoclonal alpha-smooth muscle actin (α-SMA) antibody (clone 1A4: Biogenex) in a dilution of 1:1000.

Semi-quantitative analysis

Prior to screening, sections were coded, so the observers were unaware of the clinical details of the case under study. The expression VEGF, fibronectin, and collagens was analyzed semi-quantitatively, using a visual scale that ranged from 0-4: grade 0=no staining, grade 1; focal staining, grade 2; diffuse faint staining, grade 3; diffuse moderate staining, and grade 4; diffuse strong staining[37]. The entire surface area of the tissue section on the slides was visualized and scored at the same magnification by three independent observers. The interstitial staining for collagens and fibronectin was quantified. The average of the three scores was used for subsequent analysis. This scoring method has previously been shown to allow the detection of differences in expression level as small as 1.5 times[37,40].

Statistical analysis

The expression of collagens and the fibronectin staining score were calculated for the three different groups, and the results are expressed as mean ± standard error of mean (SEM). Statistical analysis was performed after ranking using a non-parametric test- either the Mann-Whitney test or Fisher's exact test, according to what was appropriate to the compared groups. Interobserver variability was analyzed by linear regression and analysis of agreement. Densitometric values for VEGF mRNA expression were statistically tested. Results were accepted as statistically significant with $p<0.05$.

Results and discussion

Collagens and fibronectin expression

Myocardial Picro-sirius red staining patterns from both the TF groups showed extensive staining for collagens in the interstitium as well as around the blood vessels in all patients. Semi-quantitative analysis revealed an increased interstitial staining for total collagens in the TF-2 group as compared to the TF-1 group (scoring: 3.1 ± 0.2 *vs.* 2.4 ± 0.2, $p<0.04$; Fig. 6.1). Furthermore, collagen contents in the TF-2 group were also significantly higher than those in the age-matched controls (scoring: 3.1 ± 0.2 *vs.* 2.6 ± 0. 1, $p<0.05$; Fig. 6.1). Statistically, interobserver agreement was high ($r=0.9$, $p<0.05$).

Myocardial localization of fibronectin showed that the expression is confined to the interstitial peri-vascular region, as well as to the cytoplasm of some cardiomyocytes in all groups. Semi-quantitative analysis revealed that fibronectin expression was not increased in the TF-1 group (Fig. 6.2) as compared to controls (3.2 ± 0.4 *vs.* 3.2 ± 0.6, p=ns). There were no significant differences in fibronectin expression in patients from the TF-2 group when compared either with the TF-1 group (3.1 ± 0.4 *vs.* 3.2 ± 0.4, p=ns) or with age-matched controls (3.1 ± 0.4 *vs*. 3.2 ± 0.6, p=ns). Interobserver agreement was high ($r=0.9$, $p<0.05$).

Despite the fact that data are lacking on normal myocardium regarding the amount of collagens and fibronectin in children, our results indicate an increased amount of

myocardial extracellular matrix deposition in RVH in patients with TF, with an apparent increase of total collagen at a young age. The extracellular matrix deposition is a sign of fibrosis during RVH in patients with TF. The apparent development of cardiac hypertrophy is induced by changes in cardiac gene expression that provide a means of compensation for increased haemodynamic load. In this regard, our data are in agreement with the histopathologic findings from the right ventricular myocardium in preoperative TF that show interstitial fibrosis, myofibrillar disorganization, disarray, and degenerative changes in addition to myocardial cell hypertrophy[14,21].

The changes as found in our study for collagen, along with an altered structure or function of the myocardium, may induce the findings of fibronectin expression. It is believed that changes in gene expression accompanying cardiac hypertrophy are the result of a multifactorial process. The observed changes may therefore be concomitant phenomena. The alteration in right ventricular gene expression might be an indicator of cardiac hypertrophy and may result from a number of different stimuli. We assume that the changes in the right ventricular collagen expression in TF patients could be a result of increased haemodynamic load, with a parallel increase in right ventricular mass[41,42]. We have as yet no adequate explanation for the finding of fibronectin expression, the need for young control biopsies being obvious. Nevertheless, it is clear from our results that fibronectin levels are already high in patients with TF at a very young age (TF-1) and remain elevated later in life (TF-2).

The early increase of collagen deposition in the right ventricle as found at primary correction may occur because the original myocardial extracellular matrix has been expanded and weakened due to the haemodynamic overload. The myocardium will compensate until enough new collagen has been produced to restore tensile strength and to resist the distending forces. Our findings in the TF-1 and TF-2 groups fit into this concept, since the TF-2 group shows a more prominent increase in the amount of collagen as compared to the TF-1 group. Corrective surgery limits myocardial overload and may therefore limit the amount of damage to the myocardial collagen matrix[26].

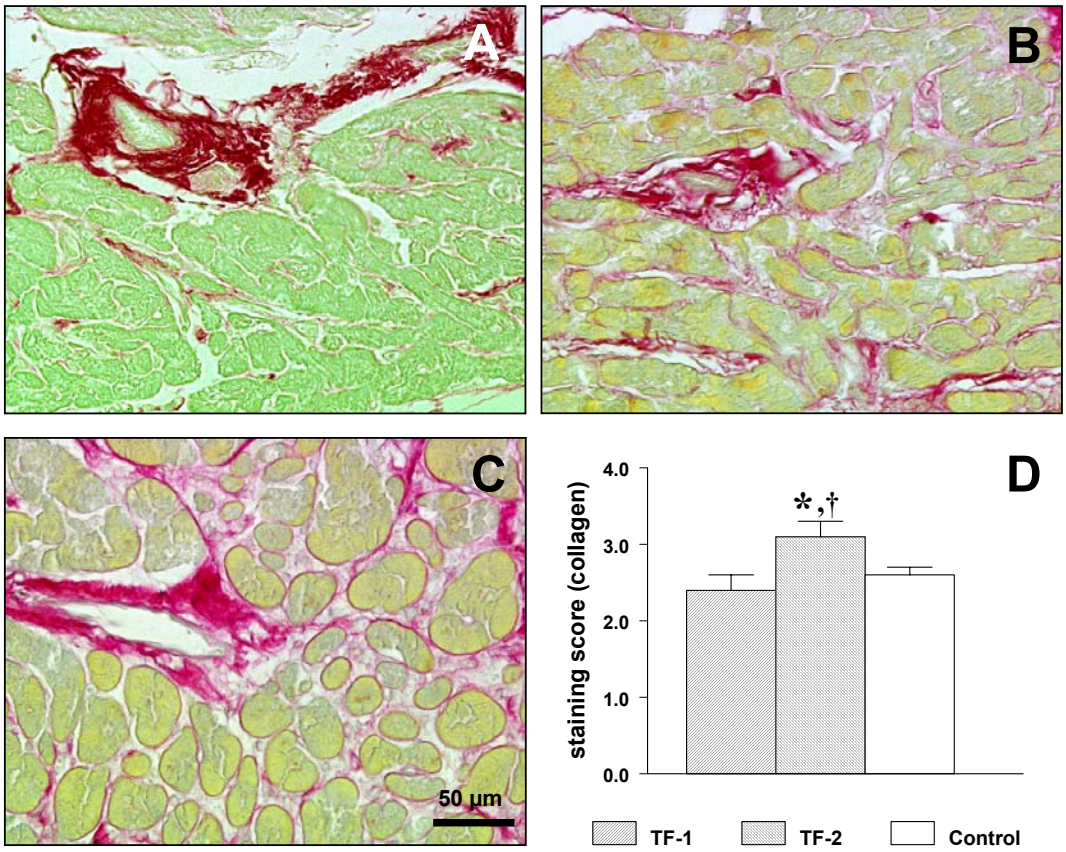

Figure 6.1. Right ventricular total collagen content in patients with tetralogy of Fallot. Microphotographs of the human right ventricular tissue obtained from patients undergoing surgery (**A**) for autograft aortic root replacement (Control), (**B**) for primary repair of tetralogy of Fallot (TF-1), and (**C**) for secondary surgery (TF-2). Tissue sections were prepared and stained with the collagen-specific stain Picro-sirius red. Collagen fibers appear red and are localized in interstitial and peri-vascular areas. Note the interstitial fibrosis in the case of TF patients. (**D**) Bar diagram depicting significantly enhanced interstitial collagen content in the TF-2 group as compared to the Control group and TF-1. Distribution of collagen fibers in tissue was visualized under normal light microscopy. Red positive interstitial collagen in the tissue area was analyzed semi-quantitatively by three independent observers using a staining score ranging from 0 (no staining) to 4 (strong red staining) to assess the levels of staining. Values are shown as mean ± SEM.

VEGF expression and angiogenesis

At clinical analysis, all patients from the TF-1 group showed RVH, and all TF-2 patients showed RVH as well as right ventricular dilatation. All control patients had a normal right ventricle at clinical analysis. VEGF expression was evaluated employing Northern blot analysis. Using a human-specific cDNA insert probe encoding VEGF, we detected two mRNA species of 3.9 and 1.7 kb, respectively, expressed in the

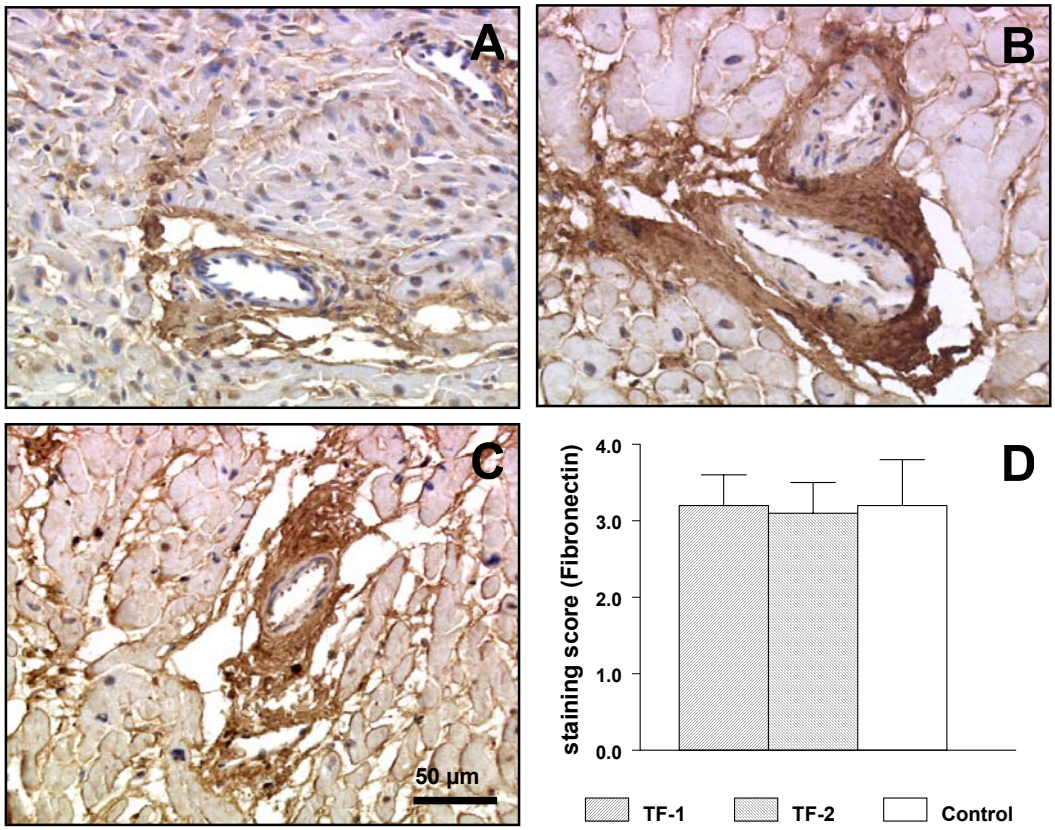

Figure 6.2. Immunahistochemical localization of fibronectin in right ventricular tissue of patients with tetralogy of Fallot.
Microphotographs showing human right ventricular tissue immunostained with fibronectin as described in Materials and Methods from patients who underwent surgery (**A**) for antograft aortic root replacement (Control), (**B**) for primary repair of tetralogy of Fallot (TF-1), and (**C**) for secondary surgery (TF-2). (**D**) Bar diagram depicting semi-quantitative analysis of interstitial fibronectin staining in the three groups. Values are shown as mean ± SEM.

human right ventricular tissue. Densitometric analysis of the mRNAs bands encoding VEGF on the autoradiographs showed significantly enhanced (1.8 ± 0.3-fold) expression in the TF-1 group as compared to the control group (Fig. 6.3D). VEGF expression was not significantly altered in the TF-2 group when compared to the control group. To immunolocalize VEGF, we incubated tissue sections with affinity-purified anti-human rabbit polyclonal antibody and processed the tissue specimens for color development. A clear cytoplasmic staining pattern was observed in myocytes and in smooth muscle cells around the blood vessels but not in the fibrotic area in the case of the TF groups (Fig. 6.3B and C). In order to assess angiogenesis in the myocardial tissue from patients with TF and controls, tissue section were immuno-

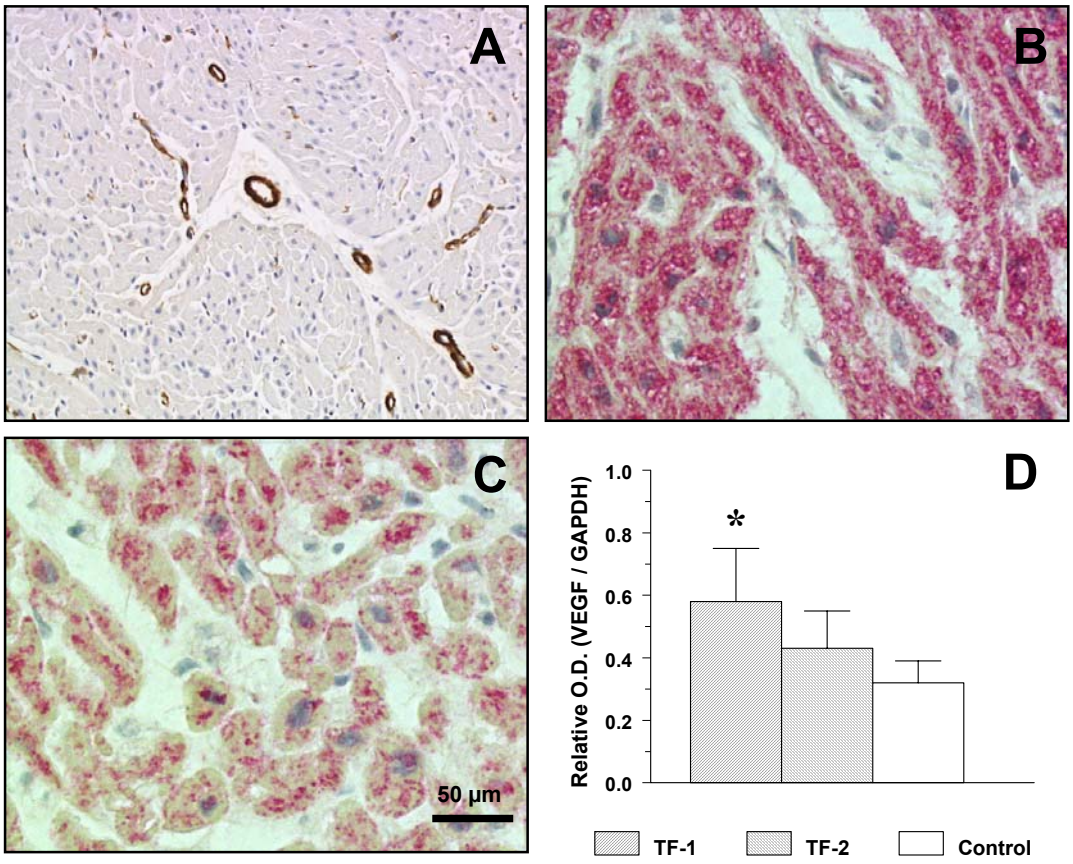

Figure 6.3. Myocardial expression of vascular endothelial growth factor and angiogenesis during RVH in TF patients. (**A**) Myocardial tissue sections (6 µm thick) obtained from TF patients were immunostained using human-specific monoclonal antibody raised against (α-smooth muscle actin, and all the blood vessels in the range of more than 200 µm were counted. The blood vessel counts were also assessed using CD31 immunostaining and compared with the above staining values. Note several small and large blood vessels stained for smooth muscle-specific actin. (**B, C**) Immunohistochemical localization of VEGF was performed on 6 µm-thick paraffin sections of myocardial tissue from a control patient (**B**) and from a patient derived from group TF-1 (**C**). Sections were incubated with a monospecific polyclonal anti-VEGF antibody followed by immunoalkaline phosphatase color reaction and visualization under light microscope as described in Materials and Methods. Immunoreactive VEGF is seen in the smooth muscle cells and in the cardiomyocytes. (**D**) Line diagram showing densitometric analysis of VEGF mRNA expression. Total RNA (10 µg) from right ventricular biopsies obtained from the control as well as from the TF- 1 and TF-2 groups of patients were subjected to Northern hybridization with ^{32}P-labeled cDNA probes encoding VEGF and GAPDH as described in Materials and Methods. Scanning densitometric values for VEGF were normalized with respective GAPDH values and expressed as relative optical density (O.D.). Results represent the mean values from three different blots ± SEM. *, $p<0.05$ *vs.* control group.

stained with anti-a-smooth muscle actin (Fig. 6.3A) and CD31 antibodies. CD31 antibody stained all endothelial cells in both small (<200 µm) and large vessels (>200 µm), whereas vascular smooth muscle cells intensely with α-smooth muscle actin

antibodies. Qualitatively, the tissue obtained from TF patients showed an enhanced number of vessels as compared to the controls[35].

In order to assess myocardial angiogenesis in the tissue specimens obtained from TF patients, the VEGF expression, was examined at the mRNA and protein levels. At the mRNA level, VEGF showed significantly enhanced expression in the TF-1 group as compared to the control group. Immunohistochemical localization of VEGF indicates that cardiac myocytes and vascular smooth muscle cells produce this mitogen, which could be secreted from these cells to act on endothelial cells in a paracrine manner, resulting in cardiac angiogenesis. Experimental animal studies from our research group as well as from others have shown that myocardial ischemia is a strong inducer of VEGF gene expression[17,35,43]. It is very likely in the TF situation that right ventricular tissue experiences hypoxia, which in term could be responsible for inducing the expression of VEGF. At this juncture, we think that the enhanced expression of VEGF mRNA could contribute to the angiogenesis in the right ventricle of TF patients. The increased number of blood vessels as observed by light microscopy could explain this finding of enhanced VEGF expression in the RV myocardium from patients with TF. Furthermore, a detailed morphometric analysis of existing blood vessels would allow us to validate this point.

Conclusion

In conclusion, we have shown that RVH in patients with TF was accompanied with enhanced myocardial collagen deposition in the interstitium and around the blood vessels, giving rise to abnormal myocardial architecture. Though we did not measure the cell size, our data correspond with the finding that after early primary corrective surgery, RVH appears to regress and eventually leads to less collagen contents, as observed in the TF-2 group. Our study provides further evidence that myocardial architecture in patients with TF depicts increased fibrosis at the expression level of extracellular matrix components such as collagens. However, the lack of data on normal myocardium in young patients limits the interpretation of data. Additionally, the hypertrophic state of the myocardium seems to be correlated with increased angiogenesis. This is evident by enhanced levels of VEGF mRNAs in the children

with TF at the time of primary surgery. Furthermore, histochemical examination of tissue biopsies showed increased number of blood vessels in patients with TF as compared to the control group. Thus, our results as presented here clearly indicate an increased degree of fibrosis and ongoing angiogenesis during RVH in patients with TF. This information leaves room for the improvement of contemporary clinical treatment of patients with TF by allowing an assessment of timing for surgery and possibly supports long-term postoperative prognosis.

Acknowledgements

Financial support from the Netherlands Heart Foundation (NHS 96.082) is gratefully acknowledged. The authors thank Mrs. E. Yilmaz for her technical assistance.

References

1. Jordan SC, Scott O. *Heart disease in pediatrics*. Oxford: Butterworth Heinneman; 1989.
2. Bogers AJ, van der Laarse A, Vliegen HW, et al. Assessment of hypertrophy in myocardial biopsies taken during correction of congenital heart disease. *Thorac Cardiovasc Surg*. 1988;36:137-40.
3. Castaneda AR, Jonas RA, Mayer JE, et al. *Cardiac surgery of neonate and infant*. Philadelphia, USA: Saunders; 1994.
4. Starnes VA, Luciani GB, Latter DA, et al. Current surgical management of tetralogy of Fallot. *Ann Thorac Surg*. 1994;58:211-215.
5. Murphy JG, Gersh BJ, Mair DD, et al. Long-term outcome in patients undergoing surgical repair of tetralogy of Fallot. *N Engl J Med*. 1993;329:593-599.
6. Warner KG, Anderson JE, Fulton DR, et al. Restoration of the pulmonary valve reduces right ventricular volume overload after previous repair of tetralogy of Fallot. *Circulation*. 1993;88:II189-197.
7. Seliem MA, Wu YT, Glenwright K. Relation between age at surgery and regression of right ventricular hypertrophy in tetralogy of Fallot. *Pediatr Cardiol*. 1995;16:53-55.
8. Schwartz K, Carrier L, Mercadier JJ, et al. Molecular phenotype of hypertrophied and failing myocardium. *Circulation*. 1993;87:VII 5-10.
9. van Bilsen M, Chien KR. Growth and hypertrophy of the heart: towards an understanding of cardiac specific and inducible gene expression. *Cardiovasc Res*. 1993;27:1140-1149.
10. Kato M. Right ventricular hypertrophy in tetralogy of Fallot, a pathohistologic study. *Jpn Ass Thorac Surg*. 1976;24:1436-1445.
11. Kawai S, Okada R, Kitamura K, et al. A morphometrical study of myocardial disarray associated with right ventricular outflow tract obstruction. *Jpn Circ J*. 1984;48:445-456.

12. Mitsuno M, Nakano S, Shimazaki Y, et al. Fate of right ventricular hypertrophy in tetralogy of Fallot after corrective surgery. *Am J Cardiol*. 1993;72:694-698.
13. Boheler KR, Chassagne C, Martin X, et al. Cardiac expressions of alpha- and beta-myosin heavy chains and sarcomeric alpha-actins are regulated through transcriptional mechanisms. Results from nuclear run-on assays in isolated rat cardiac nuclei. *J Biol Chem*. 1992;267:12979-85.
14. Brand T, Sharma HS, Schaper W. Expression of nuclear proto-oncogenes in isoproterenol-induced cardiac hypertrophy. *J Mol Cell Cardiol*. 1993;25:1325-1337.
15. Tomanek RJ, Torry RJ. Growth of the coronary vasculature in hypertrophy: mechanisms and model dependence. *Cell Mol Biol Res*. 1994;40:129-136.
16. Brand T, Sharma HS, Fleischmann KE, et al. Proto-oncogene expression in porcine myocardium subjected to ischemia and reperfusion. *Circ Res*. 1992;71:1351-1360.
17. Sharma HS, Wunsch M, Brand T, et al. Molecular biology of the coronary vascular and myocardial responses to ischemia. *J Cardiovasc Pharmacol*. 1992;20:S23-31.
18. Sharma HS, Verdouw PD, Lamers JMJ. Involvement of sarcoplasmic reticulum calcium pump in myocardial contractile dysfunction: Comparison between chronic pressure-overload and stunning. *Cardiovasc Drug Ther*. 1994;8:468-468.
19. Sharma HS, van Heugten HA, Goedbloed MA, et al. Angiotensin II induced expression of transcription factors precedes increase in Transforming Growth Factor-b1 mRNA in neonatal cardiac fibroblasts. *Biochem Biophys Res Comm*. 1994;205:105-112.
20. Volders PG, Willems IE, Cleutjens JP, et al. Interstitial collagen is increased in the non-infarcted human myocardium after myocardial infarction. *J Mol Cell Cardiol*. 1993;25:1317-1323.
21. Weber KT, Sun Y, Tyagi SC, et al. Collagen network of the myocardium: function, structural remodelling and regulatory mechanisms. *J Mol Cell Cardiol*. 1994;26:279-292.
22. Bishop JE, Rhodes S, Laurent GJ, et al. Increased collagen synthesis and decreased collagen degradation in right ventricular hypertrophy induced by pressure overload. *Cardiovasc Res*. 1994;28:1581-1585.
23. Chapman D, Weber KT, Eghbali M. Regulation of fibrillar collagen types I and III and basement membrane type IV collagen gene expression in pressure overloaded rat myocardium. *Circ Res*. 1990;67:787-794.
24. Samuel JL, Barrieux A, Dufour S, et al. Accumulation of fetal fibronectin mRNAs during the development of rat cardiac hypertrophy induced by pressure overload. *J Clin Invest*. 1991;88:1737-1746.
25. Boluyt MO, L. O, Meredith AL, et al. Alterations in cardiac gene expression during the transition from stable hypertrophy to heart failure. Marked upregulation of genes encoding extracellular matrix components. *Circ Res*. 1994;75:23-32.
26. Whittaker P. Collagen and ventricular remodelling after acute myocardial infarction: concepts and hypotheses. *Basic Res Cardiol*. 1997;92:79-81.
27. Jalil JE, Doering CW, Janicki JS, et al. Fibrillar collagen and myocardial stiffness in the intact hypertrophied rat left ventricle. *Circ. Res*. 1989;64:1041-1050.
28. McLenachan JM, Dargie HJ. Ventricular arrhythmias in hypertensive left ventricular hypertrophy. Relationship to coronary artery disease, left ventricular dysfunction, and myocardial fibrosis. *Am J Hypertens*. 1990;3:735-740.
29. Farhadian F, Contard F, Corbier A, et al. Fibronectin expression during physiological and pathological cardiac growth. *J Mol Cell Cardiol*. 1995;27:981-990.
30. Villarreal FJ, Dillmann WH. Cardiac hypertrophy-induced changes in mRNA levels for TGF-ß1, fibronectin and collagen. *Am J Physiol*. 1992;262:H1861-H1866.
31. Bogers AJJC, Roofthooft M, Pisters H, et al. Long-term follow-up of gamma irradiated transannular homograft patch in surgical treatment of tetralogy of Fallot. *Thorac Cardiovasc Surgeon*. 1994;42:337-339.
32. Hokken RB, Bogers AJJC, Spitaels SEC, et al. Pulmonary homograft insertion after repair of pulmonary stenosis. *J Heart Valve Dis*. 1995;4:182-186.

33. Schoof PH, Cromme-Dijkhuis AH, Bogers AJJC, et al. Aortic root replacement with pulmonary autograft in children. *J Thorac Cardiovasc Surg*. 1994;107:367-73.
34. Hokken RB, Bogers AJJC, Taams MA, et al. Aortic root replacement with a pulmonary autograft. *Eur J Cardiothor Surg*. 1995;9:378-383.
35. Sharma HS, Tang ZH, Gho BC, et al. Nucleotide sequence and expression of the porcine vascular endothelial growth factor. *Biochem Biophys Acta*. 1995;1260:235-238.
36. Peters THF, Sharma HS, Yilmaz E, et al. Quantitative analysis of collagens and fibronectin expression in human right ventricular hypertrophy. *Ann N Y Acad Sci*. 1999;874:278-285.
37. Shehata SM, Mooi WJ, Okazaki T, et al. Enhanced expression of vascular endothelial growth factor in lungs of newborn infants with congenital diaphragmatic hernia and pulmonary hypertension. *Thorax*. 1999;54:427-31.
38. Sharma HS, Hokken RB, Bosman FT, et al. Myocardial expression and immunohistochemical localization of Vascular Endothelial Growth Factor in human tetralogy of Fallot. *Eur Heart J*. 1995;16:353.
39. Ferrara N, Houck KA, Jakeman LB, et al. The vascular endothelial growth factor family of polypeptides. *J Cell Biochem*. 1991;47:211-8.
40. Giaid A, Michel RP, Stewart DJ, et al. Expression of endothelin-1 in lungs of patients with cryptogenic fibrosing alveolitis. *Lancet*. 1993;341:1550-1554.
41. Vikstrom KL, Bohlmeyer T, Factor SM, et al. Hypertrophy, pathology, and molecular markers of cardiac pathogenesis. *Circ Res*. 1998;82:773-778.
42. Schwartz SM, Gordon D, Mosca RS, et al. Collagen content in normal, pressure, and pressure-volume overloaded developing human hearts. *Am J Cardiol*. 1996;77:734-738.
43. Sharma HS, Peters THF, Yilmaz E, et al. Right ventricular hypertrophy in human tetralogy of Fallot is associated with increased myocardial fibrosis and vascularization. *circulation*. 1997;96:I 17-18.

Chapter 7

Right ventricular hypertrophy in human tetralogy of Fallot is associated with enhanced vascularization and expression of vascular endothelial growth factor

Based on:
Peters THF, Bogers AJJC, Saxena PR and Sharma HS. Right ventricular hypertrophy in human tetralogy of Fallot is associated with enhanced vascularization and expression of vascular endothelial growth factor. (Submitted).

Abstract

Aims: Tetralogy of Fallot (TF) is a cyanotic congenital heart disease with prominent right ventricular (RV) hypertrophy where the impaired oxygen and nutrient supply may lead to an altered myocardial phenotype. The aim of the present study was to investigate the myocardial differential gene expression profile and to assess myocardial vascularization in patients with TF.

Methods and Results: DNA micro-array analysis on right ventricular biopsies from TF patients operated for primary corrective surgery (TF-1, n=7, mean age 0.5 year) and age matched controls was validated by Northern hybridization and RT-PCR. Employing immunohistochemistry and video image analysis of vascular endothelial growth factor (VEGF) expression, vascular density (by α-SMA and CD31 staining) and myocyte cross sectional area (Gomori's reticulin staining) were assessed in TF-1 and adult patients (TF-2, n=5, mean age 30 years) who underwent surgery for pulmonary regurgitation and compared the data with age matched controls (n=8/11). DNA micro-array analysis revealed altered expression pattern for 236 genes including 1.5-2.2 fold increased expression of angiogenic factors, VEGF, flt-1, flk-1 angiopoietin-2, FGF-2, FGF-R1, PDGF-A, whereas, flt-4, Tie, TGF-β, TGF-β3R showed decreased (1.6-3.4 fold) expression in TF patients. Northern blot analysis verified VEGF expression whereas, flk-1 expression remained unaltered in both TF-1 and TF-2 patients. VEGF staining in cardiomyocytes was increased in TF-1 (1.5 fold, $p<0.05$) as compared to TF-2. Video image analysis revealed enhanced vascular density ($p<0.01$) with unchanged wall thickness and enlarged myocyte cross sectional area ($p<0.01$) in both TF-1 and TF-2 as compared to respective age matched controls.

Conclusions: Right ventricular hypertrophy in TF is associated with an altered gene profile for a number of genes where the VEGF/VEGF-R system plays an important role in enhanced myocardial angiogenesis with limited vascular remodeling.

Introduction

In tetralogy of Fallot (TF) the (sub)valvular pulmonary stenosis in combination with the ventricular septal defect (VSD) causes hypoxemia, diminished pulmonary flow, right ventricular pressure overload and adaptive right ventricular hypertrophy (RVH) with expansion of cardiomyocytes. The treatment strategy consists of primary surgical repair during the first year of life by closing the VSD and removing the RV outflow tract (RVOT) obstruction in order to relieve the hypoxemia and to eliminate the hypertrophic stimulus as well as preserving RV function. Some patients however, suffer from pulmonary regurgitation later in life, causing RV failure due to volume-overload. Those patients get further secondary corrective surgery by implanting a pulmonary allograft heart valve between the RV and the pulmonary artery[1].

The adaptive RVH will go along with remodeling of the myocardium accompanied with fibrosis[2] and will require a proportionate increase of coronary flow or growth of the coronary vasculature (angiogenesis) to reduce the increased capillary-myocyte diffusion distance, to prevent hypoxia and increase nutrient delivery[3-5]. Angiogenesis, the formation of new blood vessels from pre-existing vessels, not only concerns the formation of capillary, but also includes the formation of small and large blood vessels. In adults, angiogenesis is the only way by which new blood vessels are formed[6]. It is a multi-step process involving endothelial cell activation, migration, proliferation, and tube formation and maturation. Beside endothelial cells several other cell types like vascular smooth muscle cells, pericytes and fibroblasts and non-cellular structures, such as the basal lamina and the extracellular matrix are involved[6,7].

Under pathological conditions, autocrine induction or upregulation of angiopoietin 2, can reinitiate (angiogenic) vascular remodeling and angiogenic sprouting. In the presence of vascular endothelial growth factor (VEGF) new vessels will be formed, however without VEGF destabilized vessels will go into regression[7]. VEGF-A is the most potent and crucial regulatory factor during myocardial angiogenesis,[7] induced in a wide range of cells under conditions of hypoxia[8] and hypo-glycemia[9] and in the presence of some (growth) factors[10] like phorbol ester, adenosine, TGF-β, PDGF and TNF-α[7]. It binds to the endothelial cell surface receptors, flt-1 and flk-1[11], where

VEGF-flk-1 binding activates a cascade which promotes angiogenesis, hyperpermeability and enhances glucose transport[12].

Not much is known about the degree of angiogenesis in human RVH. Especially information about angiogenesis in TF patients, is rare. Most research on human TF is focussed on clinical treatment. In the present study, we studied the degree of angiogenesis in the RV of human TF by determining the expression pattern of VEGF and its receptor flk-1. Furthermore we examined the vessel distribution and assessed the degree of hypertrophy to elucidate the myocardial phenotype and fate of RVH at time of corrective surgery.

Material and Methods

Patients

The present study was approved by the Medical Ethical Committee of the University Hospital Rotterdam (MEC153.268/1996/119). The group of patients operated upon for primary correction of TF (TF-1), consisted of 7 patients with a mean age of 0.5±0.1 years. The group of patients operated upon for pulmonary allograft implantation late after primary correction of TF[13](TF-2), consisted of 5 patients with a mean age of 33.6±3.5 years. The young control group (C-1) consisted of 4 post mortem biopsies and 3 heart donors with a mean age of 0.7±0.3 years. The adult control group (C-2) consisted of 6 donors with a mean age of 23.8±2.3 years. All controls died on non-cardiac causes.

Tissue biopsies

Endomyocardial tissue biopsies were taken from the anterior free wall of the RVOT. Part of the myocardial tissue biopsy was immediately frozen in liquid nitrogen for mRNA expression studies, and the other part was fixed in 4% paraformaldehyde in PBS for at least 24 hours and further processed for dehydration and embedding in paraffin for (immuno)histochemical studies.

Total RNA isolation

Tissue biopsies (50-60 mg) were homogenized in guanidinium thiocyanate and processed for the total cellular RNA extraction as described previously[14]. The RNA

concentration was spectrophotometrically measured at 260 nm and a RNA/protein ratio of ≥1.8 was accepted. The quality of total RNA was further verified on a 1% agarose gel and considered of sufficient quality when ribosomal RNA bands were intact.

DNA micro-array hybridization

Total RNA samples from TF-1 (n=4; mean age 0.66±0.12) and controls (n=3; mean age 3.76±1.11) of respective groups, were pooled and processed for Affymetrix® HG-U95Av2 GeneChips expression analysis according to suppliers protocols (Santa Clara, CA, USA). For practical purposes only micro-arrays of TF-1 patients were analyzed. In brief, 5 μg total RNA was subjected to first strand cDNA synthesis using T7-(dT)24 primers and SuperScript II reverse transcriptase (Life Technologies, Rockville, MD, USA) followed by second strand cDNA synthesis. cDNA was blunted, purified and used for cRNA synthesis using T7-RNA polymerase and biotinylated-11-CTP and 16-UTP. After spectrophotometrical analysis, 11 μg of labeled and hydrolyzed cRNA (0.05μg/μl) was hybridized with a pre-equilibrated GeneChip U95Av2 for 16 hours at 45 °C. The arrays were washed, stained with streptavidin-phycoerythrin and biotinylated antibodies to streptavidin and hybridization signals were scanned using a fluormetric HP ChipScanner (Affymetrix, Santa Clara, CA, USA). Hybridization signals were analyzed employing GeneChip Micro-array Suite (MPS 4.0) (Affymetrix) and total gene expression profile was used for normalisation[15]. A comparison of the two expression profiles was made and genes changing over 1.5 fold (up or down regulated) were considered significantly changed in expression[16]. Among the large number of genes screened (www.netaffx.com), a group of genes involved in angiogenesis was further analyzed.

Northern blot analysis

From each patients 10 μg of total RNA was used for Northern-blot analysis as described previously[14]. Blots were hybridized with ^{32}P-labeled cDNA probes against human VEGF (3.9 and 1.7kb) and GAPDH (1.2 kb) mRNA. Hybridization signals quantified with Molecular Annalist (V 1.5) software (Biorad Laboratories, Hercules, CA, USA) were corrected for background and normalized with respect to GAPDH values.

Reverse transcriptase polymerase chain reaction (RT-PCR) analysis

Flk-1 mRNA expression levels were semi-quantitatively assessed by RT-PCR analysis. First strand cDNA was synthesized from total RNA using Universal RiboClone cDNA Synthesis System (Promega, Leiden, The Netherlands). Appropriate oligonucleotide primers for PCR were designed for human flk-1 (accession number: AF035121; Forward TCCCTGTGGATCTGAAACGG, Reverse CAGCAGTCCAGCATGGTCTG, product size 560bp), and β-actin (accession number: BC001301; Forward TGACGGGGTCACCCACACTG TGCCCATCTA, Reverse ACTCGTCATACTCCTGCTTGCTGATCCA, product size 625bp). After PCR amplification (30 cycles) the ethidium-bromide stained products were analyzed on the same 1.5% agarose gel, digitally photographed and quantified using Molecular Annalist (V 1.5) software. Measured flk-1 intensity were corrected for background and normalized with β-actin values of the respective patients.

Gomori reticulin staining

Myocyte cross sectional area was determined after cell (membrane) reticulin fiber staining by routine Gomori's reticulin silver staining technique[17] in 5 μm thick sections. After the silver staining was developed, slides were mounted and visualized under light microscope.

Immunolocalization of VEGF, CD31 and α-smooth muscle actin (α-SMA)

Immunohistochemical detection was performed on 5 μm thick paraffin-embedded myocardial tissue sections, using a multiple step avidin-biotin complex (ABC) method (Biogenex, San Ramon, CA, USA). Affinity purified rabbit anti-human-VEGF antibodies (Santa Cruz Biothechnology, Santa Cruz, USA) were applied as primary antibody followed by biotinylated anti-immunoglobulins and tertiary streptavidin conjugated alkaline phosphatase. Color was developed using Naphtol AS-MX phosphate and new fuchsin. Mouse monoclonal antibodies against human vascular α-SMA (Clone 1A4, NeoMarkers Fremont, CA, USA) and mAb against endothelial specific CD31 marker (Ab-3; NeoMarker), to immunulocalize capillaries, were applied as primary antibodies. Streptavidin conjugated to peroxidase (BioGenex, San Ramon, CA) was applied and subsequently sections were colored using 3,3-diaminobenzidine

(Sigma, St Louis, MO, USA). All sections were counter stained with Mayer's hematoxylin, mounted and visualized under the light microscope.

Visual-scoring

VEGF staining, in the myocyte and vascular area, was semi-quantitative analyzed by visually scoring, in a blinded fashion in random order, by two independent observers, using arbitrary visual grading scores of 0, 1, 2, 3 and 4 representing no, weak, moderate and intense staining, respectively.

Video image analysis

α-SMA stained vessels were analyzed morphometrically using a Leica Qwin video image analysis system (version 3.0, Leica, Rijswijk, The Netherlands). In 20 rectangular digital photographed images of each section, vessels with an external diameter (ED) larger then 5μm, in a set tissue area of 12.6 million μm^2 were analyzed using the Leica Qwin standard (Y2.2b) image analysis software package (Leica Imaging Systems, Cambrige, UK). The myocardial vascular density was assessed by the number of vessels per unit area. Internal vessel diameters (ID) were calculated from the average of the largest and smallest ID of a vessel. To exclude measurements on longitudinal cut vessels, only ratios largest to smallest ID ≤ 3 were accepted. External vessel diameters (ED) were assessed similarly. The vessel wall thickness was assessed from the smallest ED and ID. Vascular wall thickness was also indexed as ratio of vessel wall area to lumen area and plotted to the ID of the individual vessel to investigated the possibility of vessel wall remodeling[18]. Based on the ID the myocardial vessels were also analyzed in ID-interval (see Fig. 7.4). Myocyte cell size was measured with the same set-up. In series of 3-4 digital photographs from reticulin stained sections, the myocyte outline was drawn of at least 20 transversally cut myocytes showing a nucleolus, where after the program calculated the myocyte cross sectional area in μm^2.

Statistical analysis

Statistical analysis for micro-array results was performed with comparison ranking with software Data Mining Tool (Affymetrix). Using SPSS software (SPSS, Chicago, USA), statistical probability was assessed by (non-parametric) Kruskal-Wallis one

way analysis of variance and linear (Pearson's) regression analysis was performed for developing cell size. Values are expressed as mean±SEM and accepted as statistically significant with $p \leq 0.05$.

Results

DNA micro-array analysis

To assess the differential gene-expression profile from TF patients, RNA samples obtained from TF-1 and age matched controls were processed for Affymetrix® GeneChip expression hybridization followed by scanning and computer analysis. Hybridization analysis data is presented as a differential scatter graph in figure 7.1. Comparison ranking analysis revealed that 236 genes showed altered expression pattern. We analyzed a group of genes involved in myocardial angiogenesis (VEGF-A, VEGF-B, VEGF-C, VEGF-D, PlGF, flk-1, flt-1, angiopoietin 1 and 2, TNF-α, TGF-β, PDGF and it's receptors) (Table 7.1).

VEGF and flk-1 mRNA expression analysis by Northern-blot and RT-PCR

Densitometric analysis of representative Northern-blots, normalized with respect to GAPDH values, revealed elevated VEGF ratios in TF-1 (0.68±0.13; $p<0.05$) and TF-2 (0.85±0.18) as compared to C-1 (0.50±0.05) and C-2 (0.76±0.05) (Fig. 7.2).

Flk-1 expression, semi-quantitatively assessed by RT-PCR, revealed unchanged levels in TF-1 (0.67±0.06) and TF-2 (0.59±0.04) as compared to controls (C-1: 0.60±0.06; C-2: 0.53±0.03)(Fig. 7.2)

VEGF localization and visual scoring

Immunoreactive VEGF was localized mainly in the cytoplasm of cardiomyocytes and vascular smooth muscle cells and not in fibrotic areas (Fig. 7.3). The VEGF staining score in cardiomyocytes, showed unchanged levels in TF patients compared to respective controls (TF-1: 2.5±0.2 *vs.* C-1: 2.2±0.4 and TF-2: 1.7±0.2 *vs.* C-2: 1.5±0.2) whereas the staining score was increased ($p<0.05$) in young patients and controls as compared to adult subjects. Although the VEGF staining in the vascular smooth muscle cells in the young groups was more intense, the staining score

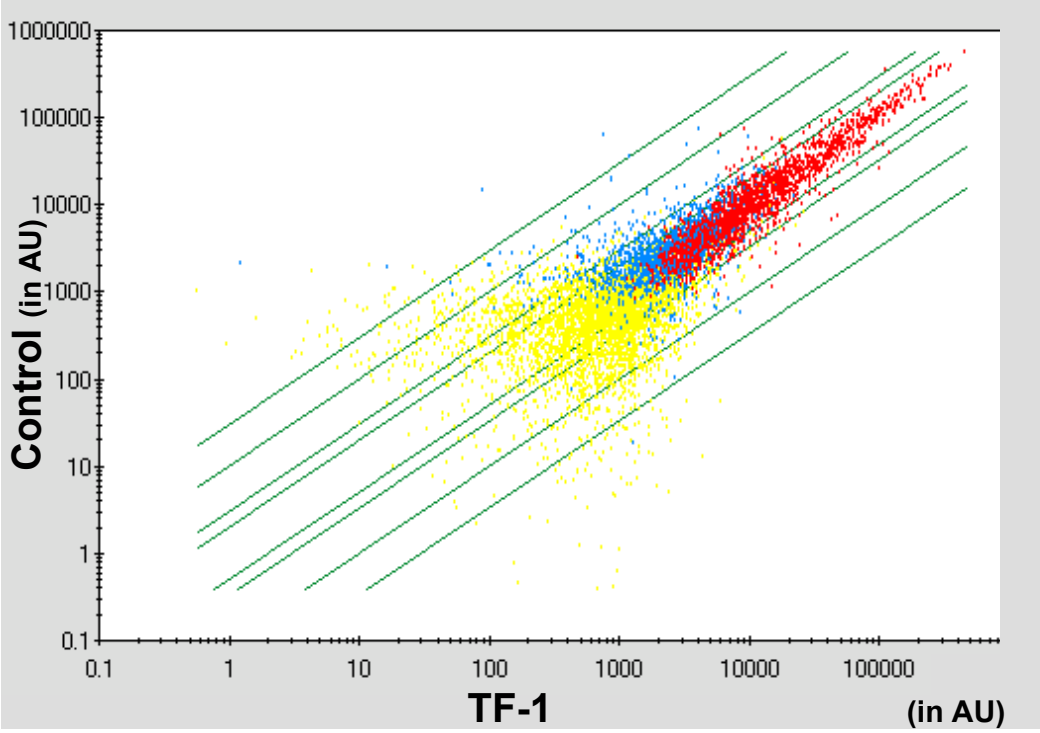

Figure 7.1. Differential scatter graph for DNA micro-array analysis of myocardial genes in patients with TF

Total RNA samples from TF-1 (n=4) and from age matched controls (C-1, n=3) were processed for Affymetrix® GeneChip expression (HG-U95Av2) and subsequently scanned and analyzed as described in Materials and Methods section. A differential graph represents the up and down regulated genes in both control as well as TF-1. (AU; artificial Units, representing the normalized spot intensities of the analyzed genes).

remained unchanged (TF-1: 1.3±0.2 *vs.* C-1: 1.6±0.2 and TF-2: 1.0±0.2 *vs.* C-2: 1.0±0.2). The inter-observer agreement was high (r=0.85, p=0.01 and r=0.71, p=0.01 for cardiomyocyte and vascular scoring respectively).

Myocyte cross sectional area assessment

Video image analysis of myocyte cross sectional area showed enlarged surfaces for TF-1 and TF-2 as compared to age matched controls (TF-1: 262±21μm^2 *vs.* C-1: 81±7μm^2 and TF-2: 1617±177μm^2 *vs.* C-2: 463 ±33μm^2, $p<0.01$). A positive linear Pearson's correlation was found between the myocyte-size and age for the TF-1 group (r= 0.92; p= 0.01).

Table 7.1. Differential expression of genes encoding angiogenic factors in patients with tetralogy of Fallot at time of primary surgical correction

Protein	accession no.	Type	Fold Change	Diff. Call.	Gene description of human mRNA encoding for
Vascular endothelial growth factor: VEGF					
	AF022375	VEGF-A	1.5	I	VEGF, complete cds
	U48801	VEGF-B	1	NC	VEGF B precursor, complete cds
	X94216	VEGF-C	1.4	NC	VEGF-C protein
	AJ000185	VEGF-D	-1.8	D	VEGF-D
VEGF receptors:					
VEGFR-1	X51602	flt	1.6	I	flt ; receptor-related tyrosine kinase,cds
VEGFR-2	AF035121	flk-1	1.4	NC	KDR/flk-1, complete cds
VEGFR-3	X69878	flt-4	-2.2	D	Flt4 for transmembrane tyrosine kinase
Angiopoietin					
	U83508	ang1	1.4	NC	Angiopoietin-1, complete cds
	AA903299	ang1	1.5	NC	cDNA clone similar to angiopoietin-1
	AF004327	ang2	1.6	I	Angiopoietin-2, complete cds
Tie					
	X60957	Tie	-1.6	D	tie for putative receptor tyrosine kinase,
Tumor necrosis factor: TNF					
TNF	X02910	TNF	1.2	NC	TNF-alpha
TNF-rec	*M58286*	TNF-rec	-4.4	D	TNF receptor, complete cds
Transforming growth factor-beta: TGF-β					
	M38449	TGF-β	-3.4	D	TGF-β, complete cds
	M19154	TGF-β 2	-1.4	NC	TGF-β -2, complete cds
	D50683	TGF-β 2R	-1.3	NC	TGF-β IIR alpha, complete cds
	X14885	TGF-β 3	2.4	I	gene for TGF-β 3 exon 1
	L07594	TGF-β 3 R	-2.4	D	TGF-beta type III receptor, complete cds
Platelet-derived growth factor: PDGF					
	M19989	PDGF-A	1.5	I	PDGF-A chain gene, exon 7
Ephrin					
	AJ007292	Ephrin-A	3.3	I	Ephrin-A2

Continuation Table 7.1.

Protein	accession no.	Type	Fold Change	Diff. Call.	Gene description of human mRNA encoding for
Fibroblast growth factor: FGF					
	L22967	a-FGF	1.1	NC	Acidic FGF (aFGF) gene sequence
	J04513	b-FGF	1.3	NC	Basic FGF (bFGF), complete cds
	M27968	b-FGF	1.6	I	Basic FGF (bFGF), complete cds
	M37825	FGF-5	-1.0	NC	FGF -5, complete cds
	U47011	FGF-8	-1.8	D	FGF 8 gene, exon 3, complete cds
	U47011	FGF-8	-1.3	NC	FGF 8 gene, exon 3, complete cds
	Z70276	FGF-12	2.2	I	FGF 12 (partial)
	AF075292	FGF-18	1.3	NC	FGF 18, complete cds
	AF075292	FGF-18	3.9	I	FGF 18, complete cds
Fibroblast growth factor receptor: FGF-rec					
	M34641	FGF-rec1	1.4	NC	FGF receptor-1, complete cds
	M34641	FGF-rec1	1.4	NC	FGF receptor-1, complete cds
	L03840	FGF-rec4	-1.6	D	FGF receptor 4, complete cds
	U28811	FGF-rec	-1	NC	Cysteine-rich FGF-rec, complete cds

Vessel distribution

The endothelial specific markers CD31 was found to be localized in the endothelial cells of arteries and capillaries in between the cardiomyocytes (Fig. 7.4). Examination of α-SMA stained sections revealed an increased number of small vessels with an ID<10 μm in TF as compared to the controls (Fig. 7.4A). The increased vessel density as found in TF-1 (65±9 *vs.* C-1; 33±3 vessels/mm^2; $p<0.01$) and TF-2 (74±15 *vs.* C-2; 34±6 vessels/mm^2; $p<0.05$ was mainly due to the increased number of small vessels (Fig. 7.4C). To compare the vessel size distribution within the different groups, the contribution of each ID-interval is represented as a percentage of the total number of vessels (Fig. 7.4B). Linear (Pearson's) regression analysis between the vessel density and the myocyte size did not result in a significant linear correlation.

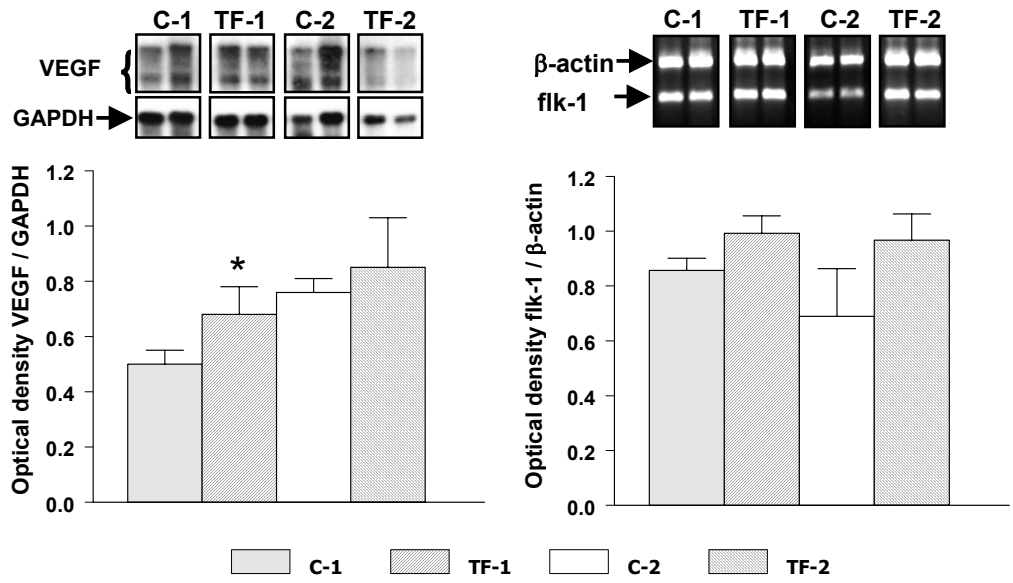

Figure 7.2. VEGF and flk-1 expression analysis in patients with tetralogy of Fallot in relation to age matched controls.
Northern blot analysis revealed two mRNA species of 1.7 and 3.9 kb in RV biopsies from TF patients. The specific hybridization signals and etidium-bromide stained bands were densiometrically quantified. Diagrams are showing the quantification of VEGF and flk-1 mRNA expression, normalized for GAPDH and β-actin values respectively. Expression of VEGF was elevated in the TF-1 group as compared to age matched controls whereas mRNA levels for flk-1 did not reveal a significant increase in TF patients as compared to the respective controls. Values are shown as mean ± SEM, where *$p<0.05$ is considered significant increased as compared to respective control.

Vessel wall remodeling

To examine possible vascular wall remodeling, vessel wall thickness and vessel wall-to-lumen ratios were analyzed. Average vessel wall thickness (C-1: 3.95±0.22 μm *vs*. TF-1: 3.17±0.17 μm and C-2: 4.26±0.0.62 μm *vs*. TF-2: 3.02±0.11 μm) or vessel wall thickness within the ID intervals (Fig. 7.4D) of TF patients remained unchanged. Vessel wall-to-lumen ratios only showed different ratios ($p=0.05$) between the TF-1 and C-1 in vessels with an ID<10 μm. When the vessel wall-to-lumen ratios were plotted to the actual individual ID the distribution pattern was similar in the TF-groups as compared to their respective control.

Discussion

Our results show a significant increase in vascularization of the RV myocardium of patients with TF, which is in accordance with the increased demand for oxygen and energy supply, both at young and adult age. Due to hypertrophy the myocyte cross

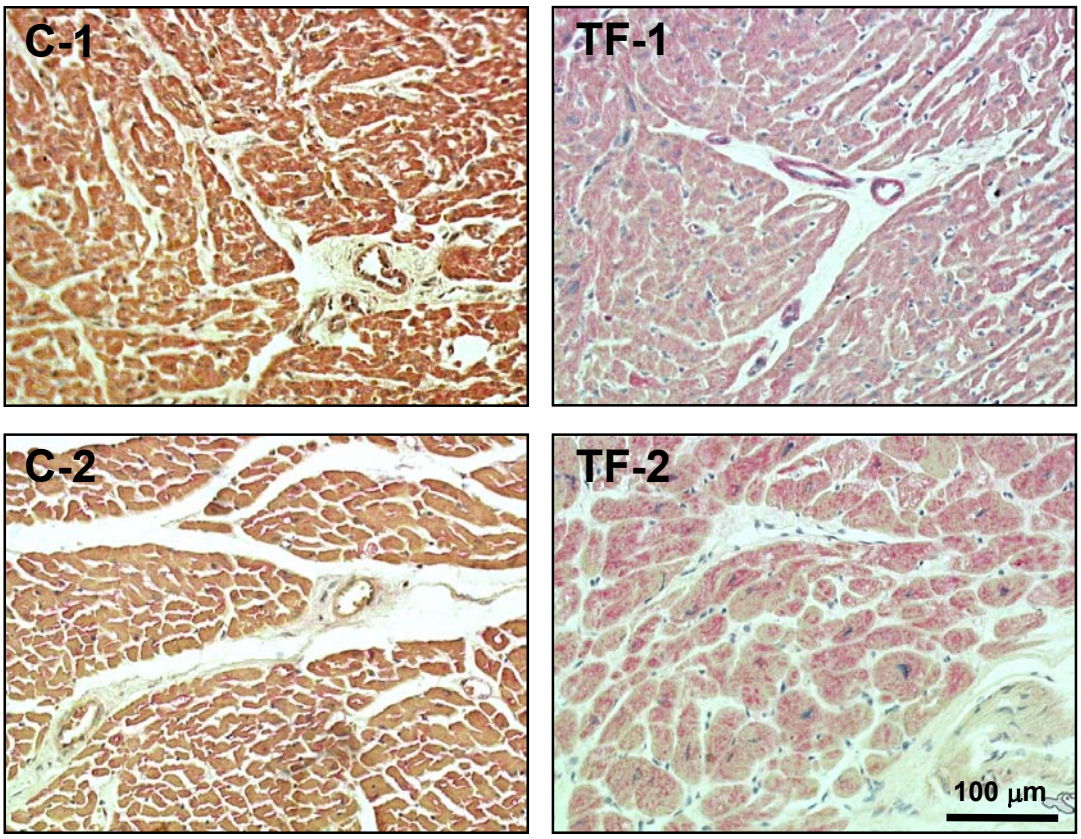

Figure 7.3. Immunohistochemical localization of VEGF in TF patients.
Paraffin sections of myocardial tissue of control and TF patients were incubated with antibodies against VEGF followed by immunoperoxidase color reaction and visualization under light microscope. Immunoreactive VEGF is localized in the smooth muscle cells and in the cardiomyocytes.

sectional area has increased and along with it the nutrient artery-cellular diffusion distance. To overcome hypoxic and hypo-glycemic conditions, myocytes express angiogenic factors like VEGF and angiopoietin 2, as found in our study, to induce angiogenic sprouting, resulting in increased vascular density, to cope with morphologic changes to preserve the RV function.

Not much is known about the vascularization of human RVH myocardium. From animal studies it is known that RVH due to pressure overload, results in increased blood flow per unit myocardial mass at rest, without an increase in minimum coronary resistance[19]. During volume overload RVH however, normal flow values per unit myocardial mass at rest are measured, with normal or mildly increased minimum coronary resistance and normal or mildly decreased coronary reserve[20]. Surgical

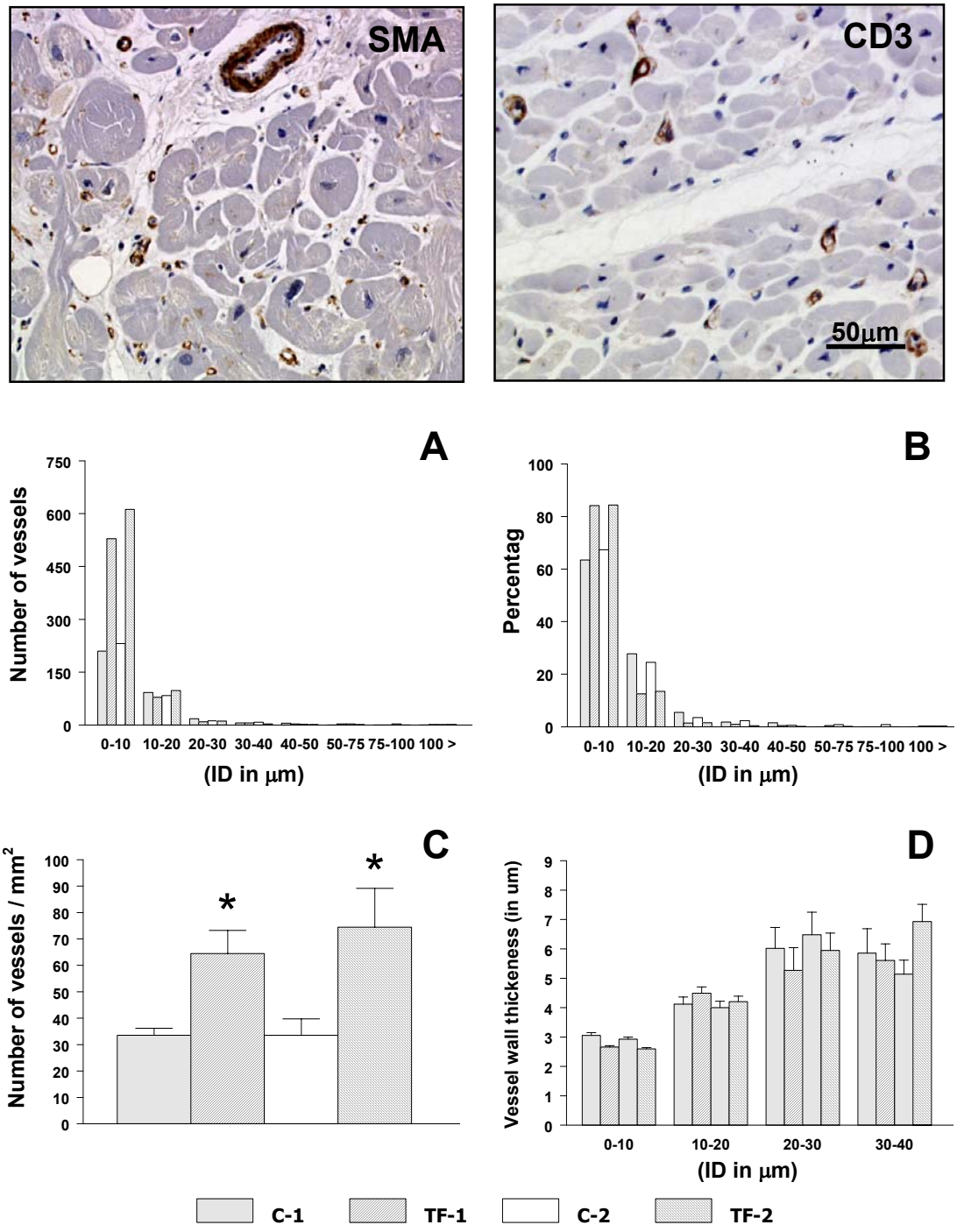

Figure 7.4. Right ventricular vascular analysis.
Images show light microscopic photographs of capillaries and vessels localized with antibodies against CD31and α-smooth muscle actin. In a set area, the number of vessels were counted and analyzed by video image analysis. Histogram **A** and **B** show that the increased number of vessels in TF patients is mainly due to the increase in number of small vessels, resulting in an increased vascular density in the RV of those patients as represented in histogram **C**. The RVH with upregulated angiogenesis in TF patients does not result in vascular remodeling as the vessel wall thickness remained unchanged for all vessel sizes (diagram **D**) (*$p<0.05$ compared to respective control group).

interference can partly take away the hypertropic stimuli in TF patients and might decrease hypertrophy and reverse associated coronary vascular abnormalities[21]

In addition to normal growth, RVH stimuli will initiate enhanced coronary vascular growth by angiogenic sprouting triggered by VEGF-A in the presence of angiopoietin 2. The binding of the VEGF-ligand to flk-1 will activate a cascade of angiogenic factors. This is in accordance with our GeneChip, Northern-blot and semi-quantitative RT-PCR data where the slightly elevated VEGF levels and equal flk-1 levels in TF-1 and TF-2 reflect enhanced angiogenesis via the activated cascade of angiogenic factors. The small difference in VEGF expression, as observed by visual scoring, in TF-1 compared to the age matched control group can be explained by the lower sensitivity of this analysis method. Both control- and TF-biopsies are from hearts from young children were the need of new vessels is obvious, resulting in VEGF upregulation. The young heart has to meet with the increased oxygen and energy demand due to growth of the heart and myocytes and the increased pulmonary flow which has to be effectuated by the RV for a sufficient cardiac output[7]. In addition TF patients continuously are exposed to stimuli of pressure overload, shear stress and, in some, hypoxic spells until corrective surgery. This might result in higher expression levels or slower turnover of angiogenic factors, subsequently resulting in enhanced RV angiogenesis. Moreover the initiated angiogenesis in TF patients is a long lasting process compared to the induction of angiogenic factors in acute pathological processes. Small differences in the expression pattern as detected at time of surgery might therefore have a bigger impact in the long term than other pathological conditions.

Morphological studies in experimental animals and in patients with pressure overload hypertrophy demonstrated that the capillaries-to-myocyte ratio remains unchanged[22]. Studies on patients with pressure overload left ventricular hypertrophy with normal capillary density, showed an increased capillary supply per myocyte, proportional to the increased myocyte size, keeping the capillary–to-myocyte ratio similar[23]. One study on TF patients (age 1-7 years) reported that the overall myocardial capillary density, in the RVOT, was similar to normal myocardial capillary density (1648±123 *vs.* 1782±203 capillaries/mm^2)[24] when the increase in cross sectional myocyte area was not taken into account. Furthermore the capillary domain (cross-sectional tissue area

nearest to that capillary) and the capillary tissue supply volume were found to be the same in TF- as well as in control-group[24]. However the capillary segment length (distance between two branching points) was found to be increased[24]. The capillaries and vessels as detected in this study, localized respectively with specific antibodies against CD31 and vascular SMA, had similar distribution patterns (Fig. 7.4).

Although the overall myocardial capillary density in TF patients was reported to be unchanged[24] the capillary radius was found to be decreased from 2.8 to 2.4 μm, in the sub-endocardial region of hypertrophied rat hearts[25]. Based on those criteria we analyzed vessels with an ED≥5 μm and found enhanced vascular density in TF patients, mainly due to increased numbers of small vessels (Fig. 7.4). This might indicate an ongoing process of angiogenic sprouting in order to preserve the aerobic metabolism in those patients. The enhanced myocyte cross sectional area, indicating myocyte hypertrophy, consequently results in a decrease of the number of cardiomyocytes per area and an increase in the number of vessels per myocyte, compensating the increased diffusion distance. In this respect, our data on the vascular density of larger blood vessels has to be interpreted with some caution as the biopsies were taken from locations of the free wall of the RVOT, deliberately excluding areas with epicardial coronary arteries, thereby decreasing the number of large vessels in our study.

Vascular wall remodeling has been reported by several studies on ischemic hypertrophied hearts. The arterial morphometry, vessel wall thickness and vessel wall-to-lumen ratios in RVH myocardium of TF patients however, appeared to be similar to the arteries in healthy RV. This is supported by the unchanged vessel wall thickness between the different ID-intervals and the unchanged vessel wall-to-lumen ratios, between the respective groups, were the decreased vessel wall-to-lumen ratio as found for the smallest TF-1 vessels (ID: 0-10μm) would rather indicate an ongoing angiogenic sprouting and development of immature vessels than vascular wall remodeling. The interpretation of the average wall thickness should be taken with some caution as the contribution of small vessels in TF patients is much higher than in the control (Fig. 7.4).

To prevent vessel analysis on longitudinally cut vessels, only vessels with ratio largest to smallest ID≤3 were accepted. To check if this arbitrary value would influence the result also vessel with ID-ratios≤2 were analyzed. Although less vessels met with this criterium, the distribution pattern between the ID intervals remained the same (data not shown).

Our study provides further evidence that RVH in TF patients depicts increased RV vascularization besides the earlier reported increased (peri-vascular) fibrosis[2]. However, the lack of data on normal myocardium in young patients limits the interpretation of data. Due to obvious reasons, it is difficult to obtain any age matched young control myocardial tissue biopsies or biopsies after the corrective surgery to control whether pathological stimuli have stopped or the RVH has regressed. In addition, further research at the mRNA level of other angiogenic factors would provide a better understanding of the altered gene expression during those pathological conditions.

In conclusion, our data suggest that RVH in TF is associated with an altered gene expression profile for a number of genes, where the VEGF/VEGF-R system plays an important role in the enhanced myocardial angiogenesis that could be stunted due to limited vascular wall remodeling. This information leaves room for improvement of contemporary clinical treatment of TF patients by allowing an assessment of myocardial condition at the time of surgery and providing information to be correlated with long term postoperative prognosis.

Acknowledgements

We thank Frank Staal, PhD, for his help in with the GeneChip experiments. Financial support from the Netherlands Heart Foundation (NHS 96.082) is gratefully acknowledged.

References

1. Warner KG, Anderson JE, Fulton DR, et al. Restoration of the pulmonary valve reduces right ventricular volume overload after previous repair of tetralogy of Fallot. Circulation. 1993;88:II189-197.

2. Peters THF, Sharma HS, Yilmaz E, et al. Quantitative analysis of collagens and fibronectin expression in human right ventricular hypertrophy. Ann N Y Acad Sci. 1999;874:278-285.
3. van Bilsen M, Chien KR. Growth and hypertrophy of the heart: towards an understanding of cardiac specific and inducible gene expression. Cardiovasc Res. 1993;27:1140-1149.
4. Boluyt MO, L. O, Meredith AL, et al. Alterations in cardiac gene expression during the transition from stable hypertrophy to heart failure. Marked upregulation of genes encoding extracellular matrix components. Circ Res. 1994;75:23-32.
5. Schwartz K, Carrier L, Mercadier JJ, et al. Molecular phenotype of the hypertrofied and failing myocardium. Circulation. 1993;87:VII 5-10.
6. Huminiecki LB, R. Angiogenesis. In: Bikfalvi A, ed. Encyclopedic reference of vascular biology & pathology. Berlin Heidelberg: Springer Verlag; 2000:2-8.
7. Yancopoulos GD, Davis S, Gale NW, et al. Vascular-specific growth factors and blood vessel formation. Nature. 2000;407:242-8.
8. Shweiki D, Itin A, Soffer D, et al. Vascular endothelial growth factor induced by hypoxia may mediate hypoxia-initiated angiogenesis. Nature. 1992;359:843-845.
9. Shweiki D, Neeman M, Itin A, et al. Induction of vascular endothelial growth factor expression by hypoxia and by glucose deficiency in multicell spheroids: implications for tumor angiogenesis. Proc Nat Acad Sci U S A. 1995;92:768-772.
10. Horiuchi T, Weller PF. Expression of vascular endothelial growth factor by human eosinophils: upregulation by granulocyte macrophage colony-stimulating factor and interleukin-5. Am J Respir Cell Mol Biol. 1997;17:70-77.
11. Detmar M, Brown LF, Berse B, et al. Hypoxia regulates the expression of vascular permeability factor/vascular endothelial growth factor (VPF/VEGF) and its receptors in human skin. J Invest Dermatol. 1997;108:263-268.
12. Waltenberger J, Mayr U, Pentz S, et al. Functional upregulation of the vascular endothelial growth factor receptor KDR by hypoxia. Circulation. 1996;94:1647-1654.
13. Hokken RB, Bogers AJJC, Spitaels SEC, et al. Pulmonary homograft insertion after repair of pulmonary stenosis. J Heart Valve Dis. 1995;4:182-186.
14. McKay S, de Jongste JC, Saxena PR, et al. Angiotensin II induces hypertrophy of human airway smooth muscle cells: expression of transcription factors and transforming growth factor-beta1. Am J Respir Cell Mol Biol. 1998;18:823-833.
15. Tan FL, Moravec CS, Li J, et al. The gene expression fingerprint of human heart failure. Proc Nat Acad Sci U S A. 2002;99:11387-92.
16. Yajima N, Masuda M, Miyazaki M, et al. Oxidative stress is involved in the development of experimental abdominal aortic aneurysm: a study of the transcription profile with complementary DNA microarray. J Vasc Surg. 2002;36:379-85.
17. Bancroff JD, Cook HC. Manual of Histological Techniques and Their Diagnostic Aplication. London: Churchill Livingstone; 1994.
18. Simionescu N, Simionescu M. The cardiovascular system. In: Weis L, ed. Cell and Tissue Biology. A Tekstbook of Histology. Baltimore: Urban and Schwarzenberg; 1988:353-400.
19. Murray PA, Vatner SF. Reduction of maximal coronary vasodilator capacity in conscious dogs with severe right ventricular hypertrophy. Circ Res. 1981;48:25-33.
20. Hultgren PB, Bove AA. Myocardial blood flow and mechanics in volume overload-induced left ventricular hypertrophy in dogs. Cardiovasc Res. 1981;15:522-528.
21. Isoyama S, Ito N, Kuroha M, et al. Complete reversibility of physiological coronary vascular abnormalities in hypertrophied hearts produced by pressure overload in the rat. J Clin Invest. 1989;84:288-294.
22. Bache RJ. Effects of hypertrophy on the coronary circulation. Prog Cardiovasc Dis. 1988;30:403-440.
23. Rakusan K, Flanagan MF, Geva T, et al. Morphometry of human coronary capillaries during normal growth and the effect of age in left ventricular pressure-overload hypertrophy. Circulation. 1992;86:38-46.

24. Rakusan K, Cicutti N, Spatenka J, et al. Geometry of the capillary net in human hearts. Int J Microcirc Clin Exp. 1997;17:29-32.
25. Turek Z, Rakusan K. Lognormal distribution of intercapillary distance in normal and hypertrophic rat heart as estimated by the method of concentric circles: its effect on tissue oxygenation. Pflugers Arch. 1981;391:17-21.

Chapter 8

General discussion and conclusions

8.1 Introduction

Tetralogy of Fallot (TF) is a frequent congenital cyanotic heart malformation. The cyanosis is a consequence of the reduced pulmonary flow due to the right ventricular (RV) outflow tract obstruction and intracardiac shunting through the ventricular septal defect (VSD). This results in right ventricular hypertrophy (RVH). Compensatory myocardial remodeling, triggered by the haemodynamic overload, shear stress and myocyte stretch, is necessary to sustain the cardiac performance. Data presented in this thesis support the observation that the RV phenotypic changes stimulated by the forementioned stress-factors initiate the up- or down- regulation and release of a cascade of molecules that co-ordinate the compensatory response. An altered gene expression pattern will finally result in increased synthesis or reduced degradation of structural proteins, changing the structural phenotype of the RV in TF patients.

Three mechanisms known to be involved in myocardial remodeling, are myocyte hypertrophy, myocardial fibrosis and myocardial vascularization. They are assumed to be active in all stages of TF. We were able to sample tissue biopsies at the time of primary corrective surgery for TF at a young age (TF-1) and from TF patients who were operated at an adult age because of pulmonary regurgitation (TF-2). We also collected biopsies at correction of pulmonary atresia with VSD (PA-VSD). The biopsies were studied and compared to normal age matched RV tissue (C-1; young, C-2; adult age) for changes in the RV phenotype (at mRNA and protein level) with regard to myocardial cellular organisation and degree of hypertrophy, with further analysis of the degree of fibrosis (e.g. collagens and fibronectin) and myocardial angiogenesis (e.g. VEGF expression and vascular density) in different stages of human TF.

8.2 Changes in the right ventricular myocardial phenotype

Right ventricular myocardial hypertrophy

During normal cardiac development the increase in myocardial mass is a result of myocyte hyperplasia and hypertrophy. After birth, however, myocardial growth is mainly due to hypertrophy[1]. In this regard, no biopsies are available to study cardiomyocytes in TF directly after birth, as we were only able to sample biopsies at corrective cardiac surgery. In TF the RV remodeling is a combination of myocardial

hypertrophy and fibrosis. Dilatation may occur later in life when (volume) overload is sustained. Remodeling continues until there is a balance between the RV pressure and the mechanical stretch and strength. TF patients without corrective cardiac surgery develop pressure overload where the RV pressure is equal to the left ventricular pressure (table 4.1). This will increase the myocardial wall stress and result in pathological concentric hypertrophy of the myocytes, with characteristic myocardial wall thickening. The haemodynamic stress is generally considered to be the major cause of hypertrophy with myocyte disarray and myofibrillar disorganization[2].

The RV myocyte hypertrophy is believed to be a result of increased mechanical forces like pressure overload and shear stress[1]. Jones *et al*. reported that RVH was correlated with the systolic outflow gradient and a high RV end systolic pressure[3]. In our study we could not find such a correlation between the RV pressure and myocyte cross sectional area within the respective groups. The myocyte cross sectional area however, was found to have a linear correlation with age in TF-1 (Fig. 4.4). This is in agreement with others who found that the RVH in TF has its onset immediately after birth, with increasing myocyte diameters correlating with age but not with the oxygen saturation of the arterial blood or cyanotic spells[2,4]. This implies that until hypertrophic stimuli are removed, at least in the first year, the pathological hypertrophy is an ongoing process. Our further findings of a positive correlation between the myocyte cross sectional area with the age ($r=0.90$, $p<0.05$; age range of 0-7 year) in normal hearts confirm the data of Kawai *et al.* who found a tendency of increased myocyte size with the age[2].

Rakusan *et al.* reported a myocyte radius of 2.5 μm in neonates, in both normal and TF-myocardium[5]. In our study the radius of TF myocytes increased form 3.7 μm at the age of 5 months to 5.8 μm at the age of 1.8 years. The increase in myocyte hypertrophy is believed to be irreversible when exceeding a radius of 7-8 micron at an age of four years or more. The results clearly show that there is myocyte hypertrophy in all stages of TF, with an increase in average myocyte cross sectional area of: 3.2, 2.0 and 3.5 fold for TF-1, PA-VSD and TF-2 respectively, as compared to the age matched controls. Based on these data, it is considered that the optimal time for corrective

surgery for TF, to prevent an irreversible alteration of the RV muscle fibers, should be at least before the age of three years[4].

The largest increase in myocyte cross sectional area was found in TF-2 patients. Those patients faced haemodynamic overload, first at a young age as a result of the TF anomalies and secondly due to pulmonary regurgitation after primary correction for TF, later in life. The pulmonary regurgitation will cause volume overload with consequently pathological hypertrophy. Furthermore, myocyte disarray is considered to require more energy for contraction and may act as a generator of cardiac hypertrophy[2]. Our histological observations showed that TF-2 patients already faced myocyte disarray as well as 3.2 fold increase in the myocyte cross sectional area at young age as compared to normal myocytes. Pulmonary regurgitation later in life results in an additional increase of cardiomyocyte hypertrophy, that sustains the RV performance but is assumed to further deteriorate the RV compliance.

Myocardial fibrosis

Initially, myocardial fibrosis is an adaptive response to the haemodynamic overload. The RV pressure overload in TF patients remodels the extracellular matrix scaffold, finally allowing (pathological) RV expansion. To restore the tensile strength and to resist the distending forces the myocardial cells, mainly fibroblasts, enhance the collagenous fiber production until enough new fibers have been produced to prevent further dilatation[6,7]. In this regard, our data (chapters 2, 3, 4 and 5) is in agreement with the histopathologic findings from the RV myocardium in pre-operative TF that show interstitial fibrosis, myofibrillar disorganization, disarray and degenerative changes in addition to myocardial cell hypertrophy[8,9]. Significantly increased interstitial total collagen, collagen subtypes and fibronectin levels, were found in almost all TF-groups indicating an ongoing fibrosis to restore the mechanical myocardial strength. The collagen levels in the peri-vascular area of most TF patients however, were not increased suggesting that no extra support to the vessels is provided.

The apparent development of cardiac fibrosis is induced by changes in cardiac gene expression that provide means of compensation for increased haemodynamic load. The neonatal myocardium will increase the collagen mRNA expression and synthesis[6].

Upregulation of fibronectin and collagen expression has also been shown during congestive heart failure[10]. Our DNA micro-array data (table 4.2) from TF-1 patients show similar patterns of up- or down-regulation of collagen subtype Iα and III and fibronectin. At the same time the extracellular matrix was further remodeled by the down regulation of TIMPs (tissue inhibitors of metalloproteinases) and up regulation of MMP-9 gelatinase (matrix metalloproteinases), which are known to favor extracellular matrix degradation and turnover. Our findings are in agreement with others[11] that the extracellular matrix degradation with collagen fiber disruption may result in myocardial dilatation, myocyte disarray and myocardial remodeling[11,12].

At protein level the interstitial staining levels for total collagen and fibronectin in TF-1 patients were increased 1.5 fold. Doubled fibrosis levels have been reported for 8 year old TF patients compared to normal hearts[2], which suggest an ongoing fibrosis in young TF patient with the age. A correlation was found between the myocyte diameter in older TF-1 patients with the increase in fibrosis in areas of disarray and with age[2]. In our study however, fibrosis only increased with age but no correlation was found between fibrosis, RV pressure, myocyte size or age.

The degree of fibrosis in our study was higher in the adult TF as compared to the adult normal heart, whereas TF-1 values were already higher as compared to the normal adult myocardial levels. This information suggests that the pressure overload and stress in the young heart are more severe and therefore needs more extracellular matrix support to prevent myocardial dilatation. In adult TF-2 patients however, excessive collagen (4.4 fold) and fibronectin (2.6 fold) contents are far above normal staining values. At a young age TF-2 patients already got primary corrective surgery which is believed to regress the myocyte hypertrophy, but most likely will not restore the myocyte alignment and myofibrillar organization. When later in life, pulmonary regurgitation with accompanied volume overload is becoming a problem, the myocyte disarrayed RV compensates again by additional hypertrophy and expression of collagenous fibers to restore the mechanical myocardial strength, with excessive fibrosis as a result.

The myocardial fibrosis mainly consists of increased accumulation of collagen subtype Iα and III fibers, where collagen type Iα provides myocardial rigidity and type III elasticity[13]. The collagen type Iα/type III ratio appeared to be very high in the young hearts, whereas the ratio was decreasing and stabilizing with age. These findings suggest a rigid, less compliant heart in neonates[13]. Higher collagen type Iα/type III ratios were also found in hearts with dilated cardiomyopathy[14]. Our additional RT-PCR data indeed showed a slightly higher collagen type Iα/type III ratio for the normal young myocardium with a decreasing ratio with age. However, the ratios remained the same in TF patients (chapter 4). The RT-PCR data was confirmed by the DNA micro-array hybridization signals, although the collagen type Iα/type III ratio was slightly higher in TF-1. The staining data showed similar patterns for the young controls, but collagen type Iα/type III ratios were lower in all TF patients, with already very high collagen Iα levels in TF-1 and TF-2 as compared to normal hearts. These changes in the collagen subtype composition and rearrangements of the collagen matrix may have a negative impact on the diastolic function[14]. The growth of a collagen type Iα diameter is limited by type III, as the latter is laid down onto the fiber core of type Iα, thus inhibiting further growth. A change in the collagen type Iα/type III ratio therefore can regulate collagen growth and thickness of the collagen fibers[14]. The observation of thicker uncoordinated collagen fibers in TF may represent a imbalance of the collagen type Iα/type III ratio, in order to support RV mechanical strength together with the preservation of the myocardial compliance without further dilatation. Because the cardiac compliance is already reduced due to the increased myocardial fibrosis in TF, preservation of contractility is achieved by reducing the collagen type III degradation and increasing the collagen III transcription. This might indicate that the hypertrophic non-dilating heart preserves its contractility by increasing the amount of collagen type III fibers as compared to normal or dilating hearts. Patients with PA-VSD (chapter 5) showed increased fibrosis levels mainly by a significant increased collagen III and fibronectin expression, with lower collagen type Iα/type III ratios both at mRNA and protein level.

An unexpected finding of our studies was the increased amount of collagen in the RV of patients operated for a pulmonary autograft root replacement (PAG; chapter 3) as

compared to control biopsies obtained from heart valve donors. However, the fibronectin levels remained unchanged in PAG as compared to normal values. These findings lead us to the conclusion that the PAG group of patients could not serve as controls for our studies. Most probably the haemodynamic overload in the left ventricle of those patients leads to remodeling of the RV as well, with consequently an increase in collagen content and myocyte disarray.

Myocardial angiogenesis

Our data on the myocardial angiogenesis (chapter 7) revealed increased vascularization of the RV myocardium at all stages of TF. The activated myocardial angiogenesis in patients with TF might represent the hypoxic state of the pathologically hypertrophied heart. In the normal young growing heart, there is an increased demand for oxygen and energy supply. In the young TF hearts the demands are even higher due to myocyte hypertrophy. At the same time the mechanical myocardial strength of the RV is restored by the accumulation of more collagenous fibers. This remodeling process increases the myocyte disarray and myocardial stiffens and reduces the RV compliance. The remodeled heart is considered to require more energy for each contraction[2]. This and the increasing capillary-myocyte diffusion distance, due to the increasing myocyte cross sectional area could stimulate the myocardial angiogenesis. The extracellular matrix degradation is not only important for the cardiac remodeling but may also allow the formation of new vessels in-between the myocytes[15]. Our findings described in this thesis support this observation.

To overcome a hypoxic and hypo-glycemic condition during the RV remodeling, myocytes express angiogenic factors like VEGF (chapter 7), required for the initiation of neoangiogenesis. RV haemodynamic overload induced by pulmonary banding (without effect on blood oxygenation) in experimental animals result in rapid increase of VEGF expression (2 fold) in the heart. After one day, however, the mRNA levels declined to normal values[16]. For the VEGF receptor, flk-1, the mRNA expression increases till 24 hours after banding, decreases after day 3 and returns to baseline levels after one week[16]. In our study, the ongoing angiogenesis in the growing hearts becomes apparent in both TF-1 as well as in the controls with detection of immunoreactive VEGF. The VEGF expression, at mRNA level, was increased in TF

patients, at the time of operation, as compared to the normal hearts (chapter 7). It is known that during hypoxia the half-life of VEGF can be prolonged from 30 minutes to 8 hours[16]. It might be that the long lasting RV outflow tract obstruction and cyanosis in TF from birth onward reduce the mRNA degradation for VEGF, rather than the increase of VEGF expression during an acute ventricular overload as observed during pulmonary banding. In this way, the decreased turnover results in VEGF accumulation at a protein level and will stimulate the angiogenic processes[16]. Similarly the upregulated trend of flk-1 expression in TF, as found in our micro-array and RT-PCR data (chapter 7), might be a result of prolonged flk-1 turnover during longstanding stress, like in VEGF. Lower VEGF mRNA expression profiles in this regard may be responsible for higher degrees of angiogenesis in TF. This might explain the increased vascular density in TF-2, with lower VEGF staining values as compared to TF-1 (Fig. 7.3). The vascular density in TF patients was already high at a very young age and remains high later in life (TF-2).

Increased vascularization and capillary density after long-term pressure overload was also found after pulmonary artery banding in animal studies[17,18], although other studies report an unchanged capillary to myocyte ratio[19]. In patients with left ventricular hypertrophy the capillary density was normal, with an increased capillary supply per myocyte, proportional to the increased myocyte size[20]. Although capillary density in TF patients remained unchanged, the capillary segment length (distance between two branching points), however, was found to be increased[21]. In the hypertrophied heart this will increase the capillary to myocyte ratio with an increased surface for oxygen and nutrient diffusion. The enhanced vascular density in TF patients, mainly due to the increased number of small vessels (Fig. 7.4), indicates for an improved nutrient supply to serve the hypertrophied myocytes in their metabolic and oxygen need, avoiding anaerobic metabolism. As yet, it is not clear if the increase in vascular density is representative for the whole of the RV, as RV outflow tract is thought to have an increased workload compared to other parts of the heart[22]. This might lead to excessive shear stress during pressure and volume overload with higher vascular densities as compared to the rest of the RV.

Right ventricular remodeling in tetralogy of Fallot

Data presented in this thesis showed that the RV remodeling in TF was associated with myocyte hypertrophy as well as with increased myocardial fibrosis, myocyte disarray and myofibrillar disorganization. The increased amount of collagen fibers in the interstitium during cardiac hypertrophy by pressure-overload is thought to be a result of a decreased collagen destruction rate and a higher collagen synthesis rate by the fibroblast, to increase the myocardial stiffness and to stop further RV expansion[23,24]. This is in accordance with the findings in our TF-study. Although RVH is initially a compensating mechanism to pressure overload, over time it tends to become more complicated by an increase of accumulated interstitial fibrous tissue reducing the cardiac compliance and eventually it might result in RV dysfunction. Both pressure overload and myocardial ischemia associated with cyanosis contribute to RVH. Depending on the importance and duration of overload and concomitant pathology, the RV compliance and the ejection fraction may be decreased[25]. Also the left ventricular contractile reserve and compliance can be depressed in TF patients, when undergoing repair older than 2 years[26]. A problem that most likely will remain after the surgical correction is the disarray of the myocytes. As a consequence, the increased interstitial space, after myocyte regression, might accumulate more extracellular matrix proteins. Furthermore the disarray of the myocytes, among other factors, will decrease the efficiency of the myocardial contractility and cardiac conductance.

8.3 Clinical implications in tetralogy of Fallot

Correlation with molecular data

Our working hypothesis was that molecular and cellular characteristics of the RV myocardium at corrective and redo surgery may provide information, relevant for the assessment of the clinical condition of the patient and important for cardiac prognosis. Although we have compared the molecular and cellular data of this study with the age at operation, right and left ventricular pressure, oxygen saturation, haemoglobin content and gender, we did not find any significant correlation.

We only found a linear correlation between the time of corrective surgery and the myocardial cross sectional area that is referred as cellular hypertrophy. The correlation of the myocyte diameter with age, in areas with increased fibrosis and myocyte disarray, in young TF patients is confirmed by others[2,4]. Furthermore, the myocyte diameter was not affected by the presence of cyanotic spells[2] and there was no correlation between the myocyte diameter and the oxygen saturation of the arterial blood or the pulmonary trunk/aorta diameter (PA/Ao) ratio [4]. Kato *et al.* however found a correlation between myocyte diameter and the haemoglobin level[4]. We found a trend of increasing fibrosis with the age and hypertrophy in most TF patients. This finding is in accordance with the studies of others[2,6,14]. Furthermore, Jones *et al.* found that RVH was correlated with the systolic outflow gradient and a high RV end systolic pressure but not with the age[3]. Our results however did not show any correlation with the right or left ventricular pressure. The pulmonary regurgitation in TF-2 is often responsible for RV dysfunction with increased fibrosis but also complete disarray of the myocytes. Earlier studies showed a linear relationship between the degree of pulmonary regurgitation and RV volume[27].

Clinical implications

Our studies demonstrate that TF patients compensate for haemodynamic overload by myocyte hypertrophy and accumulation of collagen and fibronectin in the extracellular matrix. This is supposed to increase the myocardial stiffness and mechanical strength, thereby preventing further myocardial dilatation[6,7]. As a consequence the cardiac compliance may decline and result in a decrease of tensile contractility represented by decreased diastolic performance. The RVH with increased myocardial fibrosis and myocyte disarray is assumed to lead to arrhythmias later in life[28,29].

Several studies, including ours, report a correlation of the myocyte cross sectional area with the age for young patients with TF[4] (chapter 4). At the same time, we found myocardial fibrosis and myocyte disarray. It is believed that the RVH in TF has its onset immediately after birth and that hypertrophy becomes irreversible when the diameter of the myocytes exceeds 15 μm around the age of 4 years[4]. Therefore, Kato *et al.* proposed that corrective surgery should be performed before the age of three

years[4]. Although there are some indications that the myocyte hypertrophy will regress after primary surgery, most likely the myocyte disarray is irreversible. The disarray will require more energy for each contraction with decreased myocardial performance as compared to normal hearts. Therefore, from a molecular point of view, it is not only important to remove the stimuli but also to do this at an early stage in life to limit the irreversible effects. This, together with good survival after primary correction, support the present policy of surgical correction in infancy to prevent or limit the irreversible alteration and to reduce the risk for cardiac complications later in life. Studies by Rabinovitch *et al*. demonstrated that early correction for TF restores the normal haemodynamics, with normal blood pressures, which may be desirable for normal structural development of the lungs[30].

The PA-VSD patients in our study already have an average myocyte diameter of 19 μm, at the average surgical age of 2.5 years (range 0.8-5.5 years). It might be advisable, at least from an cellular point of view, to correct those patients at an earlier age before the myocyte hypertrophy becomes irreversible.

8.4 Limitations of the study

Patients

Although our study provides further information about the compensatory mechanisms involved in the remodeling of the RV myocardium in patients with TF, the conclusions cannot be drawn for individual patients.

The biopsies examined were obtained from different patients with TF. We classified them in 3 main groups: TF-1, TF-2 and PA-VSD, according to the time point and procedure of the surgical intervention. Those patients as such form heterogeneous groups with a variable degree of hypertrophy, aortic overriding, size of VSD or pulmonary stenosis and oxygen saturation. But also indirectly related factors such as further medical history, ethnical identity, genetical background and other (congenital) complications might influence our findings.

Although our classification of patients was simple, variations in our results were limited as can be observed by the linear correlation of the myocyte cross sectional area with the age, at time of primary corrective surgery in TF-1 patients. However, the variation in cell size was wider and less predictable in the other groups. The limited number of biopsies prohibits a more detailed analysis of patient subgroups. Within the TF-1 group for example, there are patients with and without palliative Blalock-Taussig shunt before corrective surgery. Although the clinical situation might be different at the time of birth, we could not find any significant difference in the levels of fibrosis or hypertrophy at time of corrective operation in those sub-groups. The same holds for the subdivision of PA-VSD patients with or without SPCAs. No differences in the level of fibrosis could be observed.

In addition, the control group, especially young donors, remains a point of concern. As the biopsies of the patients who got a pulmonary autograft root replacement appeared to have higher collagen levels and altered myocardial architecture as compared to normal hearts, we started to collect RV biopsies from heart valve donors and of autopsies. It may be added here that due to obvious reasons, it is very difficult to obtain any young age matched myocardial control biopsies. Furthermore, the lack of data on normal myocardium in young patients and adult patients limits the interpretation of our findings.

Biopsies

All the biopsies were taken from the free wall of the RV outflow tract. This might limit the interpretation of our results for the whole RV, although we assume that those biopsies are representative for the rest of the myocardium. Some reports state that the level of RV fibrosis is higher in the RV outflow tract[6,22]. The same might be true for the RVH and vascularization, although from previous studies it is known that cellular disorganization and hypertrophy is also present in other parts of the ventricle[31]. Therefore, both TF and normal biopsies were taken form the same position, and they are representative to compare with each other. More biopsies of different positions of the myocardium and at different stages of TF would improve our tissue sampling and the knowledge into the pathogenesis of TF. However, due to obvious reasons, it was not possible for us to obtain those biopsies. Especially human biopsies after corrective

surgery could elucidate whether the removal of the pathological stimuli will stop or even regress the morphological changes.

mRNA expression studies

All biopsies of TF patients were immediately snap frozen in liquid nitrogen or preserved in paraformaldehyde. As we had no direct access to the control donors there is a time span between the time of death and the time of preservation of the control biopsies. Especially the use of autopsy biopsies for the use of mRNA-expression studies remains a point of concern, because the normal mRNA breakdown might have continued before final preservation. Donor hearts are obtained in preserving conditions and therefore might be more useful for our experiments. At least our DNA micro-array data revealed that the donor heart mRNA used for the chip hybridization experiments was of good quality without significant mRNA breakdown.

Video image analysis & corrections

Our study provides further evidence that myocardial architecture in patients with TF depicts increased fibrosis at the expression level of extracellular matrix components. Visual analysis of microscopy sections is a good tool to observe the morphological changes and localization of stained proteins, but is less useful for the objective comparison of larger number of sections and for morphometric measurements. Video image analysis proved to be more useful and objective in this regard, where even small differences, e.g. in the peri-vascular accumulation of collagen and fibronectin, could be detected. An additional advantage is the possibility to quantify the staining patterns in specific tissue compartments, e.g. interstitial and peri-vascular staining, at the same time.

To get a more objective comparison of different sections, video image analysis has the possibility to correct the measurements for the morphological changes, e.g. correction for peri-vascular staining (chapter 3, 4 and 5) and hypertrophy (chapter 4 and 5). The increase in myocardial hypertrophy as detected in TF will influence the staining data as the enlarged cells will increase the total tissue area per digital image and consequently decrease the staining ratio. Because of this, an increased myocardial fibrosis in a hypertrophied heart may not be noted. This is confirmed by others who reported that

clearly visible myocardial fibrosis by eye in TF did not reveal a significant increase in collagen levels after computerized analysis[6]. The correction for the increase in myocyte cross sectional area therefore seems to be valid in this detection method, which is supported by the comparable data obtained by visual scoring[32] (chapter 2).

DNA micro-array analysis

The DNA micro-array experiments are a powerful tool to analyze the expression pattern of a large group of genes in one go. In our study, due to practical purposes, we only analyzed a limited number of pooled RNA samples from TF and age matched heart valve donors. This, together with the limited number of chips makes the interpretation for gene clustering and statistical analysis difficult. Furthermore, for the low copy number genes, more DNA micro-array experiments would be advisable. Additional validation experiments e.g. with quantitative (real time) PCR, also could support our data.

8.5 Implications for future research

Although surgical techniques are improving to the beneficial treatment of patients with TF, still little is known about the underling molecular mechanisms causing the malformations. With the studies described in this thesis we made a start with the assessment of the molecular phenotype in the RV of patients with TF. Still many dilemmas remain to be unraveled. Several areas of research involved in the cardiac remodeling still need a lot of attention e.g. cardiac (mall)development, genetics, hypertrophy, regression of the pathological myocardial remodeling and implication for clinical treatment. Further studies with a larger number of patients and the examination of the biopsies with new techniques are necessary in this regard.

Molecular analysis of expression profiles

The innovation in the molecular biological research is developing rapidly. The development of new techniques to study pathological conditions at a molecular and cellular level has rapidly increased our knowledge in the last decade. One powerful technique is the DNA micro-array analysis. A big advantage of this technique is the

possibility to study the expression profile of several thousands of genes at the same moment. The application of this technique in the study on the molecular phenotype of TF would give a kind of fingerprint of the RV expression pattern at time of operation. The analysis of this pattern would enhance the knowledge about the large number of genes involved in cardiac remodeling.

Analysis of the gene expression pattern at more time points would even increase the impact of this technique, as the expression profile at different stages of TF could be used for genes clustering. Novel genes or new cell signaling pathways involved in the cardiac remodeling could be elucidated in this way. A proper animal model which would mimic the TF condition, could be of great use for such mRNA expression study of the cardiac development and remodeling. In the same way myocyte cultures could be stimulated with different factors to unravel the molecular mechanisms behind the phenotypic changes. Furthermore, the genomics information on the RV could be extended to proteomics where the differently expressed proteins can be identified by mass spectrophotometry. This would improve our knowledge about differently expressed or differently processed proteins during the different stages of TF.

The study of altered expression levels of proteins and genes known to be involved in the RV outflow tract anomalies and TF, like Connexin 43[33] and the GATA transcription factors, involved in cardiac hypertrophy, might be interesting. Also the assessment of the transcription levels of the cardiac specific genes, stimulated by the GATA transcription elements which have been identified within the promoters of atrial naturetic factor (ANF), b-type natriuretic factor (BNP), α-myosin heavy chain, β-myocin heavy chain, angiotensin II type 1a receptor and cardiac troponin C would contribute to the elucidation of the molecular pathways in TF[34,35]

Role of apoptosis in myocardial remodeling in tetralogy of Fallot

The compensatory hypertrophy in TF is a result of a number of intrinsic and extrinsic mechanisms of the cardiac myocytes, including alterations in cardiomyocyte contractility and structural proteins together with apoptosis, necrosis, and extracellular matrix and myocardial remodeling[36,37]. The myocyte dropout, due to myocardial cell

death and hypertrophy, of the remaining viable myocytes has been proposed to account for impaired function and failure during ageing and hypertension[1,38-40]. Apoptosis also plays an important role in the cardiac and vascular remodeling in response to pathologic stimuli[41,42]. In a preliminary study, we detected apoptotic cells by *in situ* staining of terminal deoxynucleotidyl transferase mediated-nick end labeling with fluorecein-12-dUTP (TUNEL). The number of apoptotic cells was found to be significantly increased in TF-1; 0.5±0.2% and TF-2 1.0±0.6% *vs*. normal 0.04±0.01% of the total number of cells[43]. This indicates myocyte loss during RV remodeling in TF. A more detailed study with an increased number of patients and more apoptotic markers would improve the information about the role and consequences of myocardial apoptosis in TF.

Animal models for tetralogy of Fallot

Until now no good animal model is available which approach the TF pathogenesis. Transgenic attempts did reveal puppies with the TF features but those were not viable[44]. A transgenic viable model would not only improve our knowledge on the cardiac maldevelopment but would also allow to study the cellular and molecular mechanisms of cardiac congenital diseases at different pathological stages and perhaps during follow-up after surgical correction.

An appropriate experimental TF animal model would also allow experimental intervention studies, both medical, percutaneous and surgical. In this way TF could be studied at different time points and the molecular and cellular changes could be followed in all stages of treatment.

References

1. Walsh R, Dorn G. Growth and hypertrophy of the heart and blood vessels. In: Alexander W, Schlant R, Fuster V, eds. *Hurst's The Heart, arteries and veins*. 9th edition: The McGraw-Hill Companies; 1998:155-168.
2. Kawai S, Okada R, Kitamura K, et al. A morphometrical study of myocardial disarray associated with right ventricular outflow tract obstruction. *Jpn Circ J*. 1984;48:445-456.
3. Jones M, Ferrans VJ, Morrow AG, et al. Ultrastructure of crista supraventricularis muscle in patients with congenital heart diseases associated with right ventricular outflow tract obstruction. *Circulation*. 1975;51:39-67.
4. Kato M, Kawashima Y, Fujita T, et al. Right ventricular hypertrophy in tetralogy of Fallot. *Recent Adv Stud Cardiac Struct Metab*. 1976;12:149-55.
5. Rakusan K. Cardiac growth, maturation and ageing. In: Zak R, ed. *Growth of the heart in health and disease*. New York: Raven press; 1984:131-164.
6. Schwartz SM, Gordon D, Mosca RS, et al. Collagen content in normal, pressure, and pressure-volume overloaded developing human hearts. *Am J Cardiol*. 1996;77:734-738.
7. Vikstrom KL, Bohlmeyer T, Factor SM, et al. Hypertrophy, pathology, and molecular markers of cardiac pathogenesis. *Circ Res*. 1998;82:773-778.
8. Brand T, Sharma HS, Fleischmann KE, et al. Proto-oncogene expression in porcine myocardium subjected to ischemia and reperfusion. *Circ Res*. 1992;71:1351-1360.
9. Brand T, Sharma HS, Schaper W. Expression of nuclear proto-oncogenes in isoproterenol-induced cardiac hypertrophy. *J Mol Cell Cardiol*. 1993;25:1325-1337.
10. Boluyt MO, L. O, Meredith AL, et al. Alterations in cardiac gene expression during the transition from stable hypertrophy to heart failure. Marked upregulation of genes encoding extracellular matrix components. *Circ Res*. 1994;75:23-32.
11. Li YY, Feldman AM, Sun Y, et al. Differential expression of tissue inhibitors of metalloproteinases in the failing human heart. *Circulation*. 1998;98:1728-34.
12. Mann DL, Spinale FG. Activation of matrix metalloproteinases in the failing human heart: breaking the tie that binds. *Circulation*. 1998;98:1699-702.
13. Marijianowski MM, van der Loos CM, Mohrschladt MF, et al. The neonatal heart has a relatively high content of total collagen and type I collagen, a condition that may explain the less compliant state. *J Am Coll Cardiol*. 1994;23:1204-8.
14. Marijianowski MM, Teeling P, Mann J, et al. Dilated cardiomyopathy is associated with an increase in the type I/type III collagen ratio: a quantitative assessment. *J Am Coll Cardiol*. 1995;25:1263-72.
15. Tsurumi Y, Murohara T, Krasinski K, et al. Reciprocal relation between VEGF and NO in the regulation of endothelial integrity. *Nat Med*. 1997;3:879-86.
16. Bauer EP, Kuki S, Arras M, et al. Increased growth factor transcription after pulmonary artery banding. *Eur J Cardiothorac Surg*. 1997;11:818-23.
17. Kassab GS, Imoto K, White FC, et al. Coronary arterial tree remodelling in right ventricular hypertrophy. *Am J Physiol*. 1993;265:H366-75.
18. Olivetti G, Lagrasta C, Ricci R, et al. Long-term pressure-induced cardiac hypertrophy: capillary and mast cell proliferation. *Am J Physiol*. 1989;257:H1766-72.
19. Bache RJ. Effects of hypertrophy on the coronary circulation. *Prog Cardiovasc Dis*. 1988;30:403-440.
20. Rakusan K, Flanagan MF, Geva T, et al. Morphometry of human coronary capillaries during normal growth and the effect of age in left ventricular pressure-overload hypertrophy. *Circulation*. 1992;86:38-46.
21. Rakusan K, Cicutti N, Spatenka J, et al. Geometry of the capillary net in human hearts. *Int J Microcirc Clin Exp*. 1997;17:29-32.
22. Armour JA, Pace JB, Randall WC. Interrelationship of architecture and function of the right ventricle. *Am J Physiol*. 1970;218:174-9.

23. Samuel JL, Barrieux A, Dufour S, et al. Accumulation of fetal fibronectin mRNAs during the development of rat cardiac hypertrophy induced by pressure overload. *J Clin Invest*. 1991;88:1737-1746.
24. Bishop JE, Rhodes S, Laurent GJ, et al. Increased collagen synthesis and decreased collagen degradation in right ventricular hypertrophy induced by pressure overload. *Cardiovasc Res*. 1994;28:1581-1585.
25. Leeuwenburgh BP, Steendijk P, Helbing WA, et al. Indexes of diastolic RV function: load dependence and changes after chronic RV pressure overload in lambs. *Am J Physiol Heart Circ Physiol*. 2002;282:H1350-8.
26. Deanfield JE, McKenna WJ, Presbitero P, et al. Ventricular arrhythmia in unrepaired and repaired tetralogy of Fallot. Relation to age, timing of repair, and haemodynamic status. *Br Heart J*. 1984;52:77-81.
27. Redington AN. Determinants of short- and long-term outcome in the surgical correction of tetralogy of Fallot. *Curr Opin Pediatr*. 1993;5:619-22.
28. Deanfield JE. Late ventricular arrhythmias occurring after repair of tetralogy of Fallot: do they matter? *Int J Cardiol*. 1991;30:143-50.
29. Bricker JT. Sudden death and tetralogy of Fallot. Risks, markers, and causes. *Circulation*. 1995;92:158-9.
30. Rabinovitch M, Herrera-deLeon V, Castaneda AR, et al. Growth and development of the pulmonary vascular bed in patients with tetralogy of Fallot with or without pulmonary atresia. *Circulation*. 1981;64:1234-49.
31. Maron BJ, Bonow RO, Cannon RO, 3rd, et al. Hypertrophic cardiomyopathy. Interrelations of clinical manifestations, pathophysiology, and therapy (1). *N Engl J Med*. 1987;316:780-9.
32. Peters THF, Sharma HS, Yilmaz E, et al. Quantitative analysis of collagens and fibronectin expression in human right ventricular hypertrophy. *Ann N Y Acad Sci*. 1999;874:278-285.
33. Kolcz J, Rajwa B, Drukala J, et al. Three-dimensional Visualization of Connexin 43 on the Human Cardiomyocytes. *Appl Immunohistochem Mol Morphol*. 2002;10:247-252.
34. Liang Q, Molkentin JD. Divergent Signalling Pathways Converge on GATA4 to Regulate Cardiac Hypertrophic Gene Expression. *J Mol Cell Cardiol*. 2002;34:611-6.
35. McFadden DG, Olson EN. Heart development: learning from mistakes. *Curr Opin Genet Dev*. 2002;12:328-35.
36. Teiger E, Than VD, Richard L, et al. Apoptosis in pressure overload-induced heart hypertrophy in the rat. *J Clin Invest*. 1996;97:2891-7.
37. Cheng W, Li B, Kajstura J, et al. Stretch-induced programmed myocyte cell death. *J Clin Invest*. 1995;96:2247-59.
38. Anversa P, Hiler B, Ricci R, et al. Myocyte cell loss and myocyte hypertrophy in the aging rat heart. *J Am Coll Cardiol*. 1986;8:1441-1448.
39. Engelmann GL, Vitullo JC, Gerrity RG. Morfphometric analysis of cardiac hypertrophy during development, maturation, and senscence in spontaneously hypertensive rats. *Circ Res*. 1987;60:487-494.
40. Capasso JM, Palackal T, Olivetti G, et al. Left ventricular failure induced by long-term hypertension in rats. *Circ Res*. 1990;86:1400-1412.
41. Thompson CB. Apoptosis in the pathogenesis and treatment of disease. *Science*. 1995;267:1456-62.
42. Vaux DL, Strasser A. The molecular biology of apoptosis. *Proc Nat Acad Sci U S A*. 1996;93:2239-44.
43. Peters THF, Sharma HS, Saxena PR, et al. Right Ventricular Fibrosis and Apoptosis in Patients with Tetralogie of Fallot. *J Mol Cell Cardiol*. 2001;33:A93.
44. Tullio AN, Accili D, Ferrans VJ, et al. Nonmuscle myosin II-B is required for normal development of the mouse heart. *Proc Nat Acad Sci U S A*. 1997;94:12407-12.

List of abbreviations

ANF	atrial natriuretic factor
Ang-1	angiopoietin 1
bp	base pairs
BSA	bovine serum albumin
cDNA	complementary DNA
CHD	congenital heart disease
DAB	3,3-diaminobenzidine
DNA	deoxyribonucleic acid
ECM	extracellular matrix
EGF	epidermal growth factor
FGF	fibroblast growth factor
GAPDH	glyceraldehyde-3-phosphate dehydrogenase
GTC	guanidinium thiocyanate
Ig	immunoglobulin
IGF	insulin like growth factor
LA	lumen area
MHC	myosin heavy chain
MMP	matrix metalloproteases
mRNA	messenger ribonucleic acid
NL	normal
PAG	group of patients operated for pulmonary autograft root replacement
PA-VSD	pulmonary atresia with ventricular septal defect
PBS	phosphate buffered saline
PCR	polymerase chain reaction
PDGF	platelet derived growth factor
PlGF	placenta growth factor
PVCA	peri-vascular collagen (stained) area
PVFA	peri-vascular fibronectin (stained) area
RAS	renin-angiotensin system
RT-PCR	reverse transcriptase polymerase chain reaction
RV	right ventricle
RVH	right ventricular hypertrophy
RVOT	right ventricular outflow tract
SEM	standard error of mean
SPCAs	systemic pulmonary collateral arteries
TF	tetralogy of Fallot
TF-1	group of TF patients operated for primary correction
TF-2	group of TF patients re-operated for pulmonary regurgitation
TGF-β	transforming growth factor-β
TIMP	tissue inhibitor of matrix metalloproteases
TNF-α	tumor necrosis factor-α
VEGF	vascular endothelial growth factor
VEGFR	VEGF receptor
VSD	ventricular septal defect

Summary

Tetralogy of Fallot (TF) is one of the most common congenital heart disease which can cause cyanosis. **Chapter 1** provides a short overview about the main features and the treatment of TF. Patients with TF suffer from pressure overload in the right ventricle (RV) due to a (sub)pulmonary stenosis and a ventricular septal defect (VSD). As an adaptive response the RV mass increases, known as right ventricular hypertrophy (RVH). To reduce the chronic RV stress, primary corrective surgery at young age (TF-1), nowadays is the treatment of choice. Correction is aimed at prevention of the complications such as ventricular dysfunction and arrhythmias as a result of long standing RVH. Despite adequate surgery, some patients develop RV failure due to volume-overload (pulmonary regurgitation) and may require redo surgery later in the life.

It is not yet established how the different adaptations of the RV in patients with TF take place at a cellular and molecular level. This study aimed at getting a better understanding of the pathogenesis in those patients in order to improve the timing of surgical intervention and post-operative prognosis of those patients. By the examination of RV biopsies obtained during corrective surgery of patients with TF an attempt was made to correlate the RV overload with the phenotypic changes at a cellular, protein and mRNA level. The study focussed on: myocardial fibrosis (synthesis of connective tissue) (**chapter 2-5**), myocyte hypertrophy (**chapter 4 and 5**) and myocardial angiogenesis (vascularization of the RV) (**chapter 6 and 7**).

Chapter 2 describes a microscopic study of RV biopsies of TF patients, to examine the degree of myocardial fibrosis as an adaptive response to the RV pressure overload. After the immuno-histological staining of the fibrotic markers, collagen and fibronectin, TF-1 and TF-2 patients were compared with patients who underwent a pulmonary autograft root replacement (PAG). The results showed an increased level of myocardial fibrosis in the extracellular space and peri-vascular regions and in some cardiomyocytes.

In **chapter 3** the content of fibrotic markers was quantified, with specific video image analysis software, in digitalized microscopical pictures in the interstitial space and peri-vascular area of different patients. This quantification revealed that the PAG patients, which were used as a control, can not be regarded as such, despite clinically normal RV function. Like TF patients they had increased levels of fibrosis markers in the extracellular matrix (ECM) of the RV. The TF patients appeared to have higher contents of interstitial collagens, but less peri-vascular collagen was found in patients who got re-do surgery. This was accompanied by a lower amount of interstitial fibronectin and increased levels of peri-vascular fibronectin.

In **chapter 4** the total collagen, collagen type I, collagen type III and fibronectin content in TF patients were quantified. Also the mRNA expression patterns of the RV myocardium were quantified by DNA micro-array hybridization analysis. The image analysis data revealed an increased total collagen, collagen type I, collagen type III and fibronectin content in the interstitial space as well as in the peri-vascular area in TF-1 and TF-2 patients as compared to the control group. This increase is confirmed by the gene upregulation as found by micro-array hybridization analysis. Also the gene-expression profile of genes encoding for proteins involved in the ECM homeostasis (MMPs, TIMPs, PAI, PA etc.) supported the finding of an ongoing fibrosis. Furthermore the increase of the myocyte cross sectional area with the age, indicated for myocardial hypertrophy in patients with TF.

Chapter 5 describes a study of a sub-group of TF patients. Tetralogy of Fallot is a generic name for patients with different degrees of anomalies. Pulmonary atresia combined with a VSD is an extreme form of TF where the RV outflow tract is completely blocked or absent. The myocardial hypertrophy in those patients is accompanied by increased myocardial fibrosis in the interstitial space, although the content is limited as compared to TF patients. At the same time the collagen support of the blood vessels decreased, although there is an increased synthesis of collagen III (at mRNA level) as compared to the control group.

In **chapter 6** and **7** the level of angiogenesis was studied by assessing the growth factors (e.g. VEGF) which stimulate the vascularization of the heart and the vascular density. The gene-expression profile assessed with DNA-micro-array hybridization

revealed the pattern that supports the observed angiogenesis in patients with TF. Further examination showed that the increased VEGF gene expression in the RV of TF patients resulted in an increased RV vascularization, especially represented by small vessels without vascular remodeling. The myocardial remodeling in TF patients appears to be associated with an increased number of blood vessels to serve the RV in oxygen and nutrient demand.

In **chapter 8** the data represented in this thesis is evaluated in a general discussion. Furthermore it describes proposals for future research.

Samenvatting

Tetralogie van Fallot (TF) is een van de meest voorkomende aangeboren hartafwijkingen die tot blauwzucht kan leiden. In **hoofdstuk 1** wordt een kort overzicht gegeven van de kenmerken van TF met een beschrijving van de huidige behandeling. De hartafwijking wordt gekenmerkt door overbelasting van de rechter hartkamer (RV; rechter ventrikel) die veroorzaakt wordt door een vernauwing in de longslagader en een open verbinding tussen beide hartkamers (VSD; ventrikel septum defect). Het hart past zich hieraan aan door de hartspier te verdikken (RVH; rechter ventrikel hypertrofie). Om de nadelige gevolgen van langdurige overbelasting van de RV te voorkomen, is tegenwoordig een correctieve operatie in het eerste levensjaar (TF-1) de behandeling van keuze. Door middel van deze operatie wordt onder andere geprobeerd om hartfalen en hartritmestoornissen op lange termijn te voorkomen. Desondanks ontwikkelen sommige patiënten op volwassen leeftijd weer een RV volume overbelasting als gevolg van een disfunctionerende pulmonalisklep. Deze kan operatief worden vervangen om de opnieuw ontstane overbelasting van de RV te verhelpen (TF-2).

De wijze waarop de aanpassingen in de hartspier bij de mens wordt gereguleerd op cellulair en moleculair niveau is nog grotendeels onbekend. Het doel van deze studie is om een beter inzicht te verkrijgen in het verloop van de pathogenese bij deze patiënten, om zo nauwkeuriger het tijdstip van operatie te bepalen en om een beter post-operatieve prognose te geven in de diverse stadia en vormen van TF. Met name door bestudering van stukjes menselijk hartweefsel, verkregen tijdens de correctieve operatieve, is geprobeerd om een verband te leggen tussen de mate van rechter kamerbelasting en de mate waarin de expressie-patronen, die het moleculaire fenotype bepalen, op mRNA-, eiwit- en cellulair niveau veranderd zijn. Er is bij de bestudering van deze stukjes hartweefsel vooral gekeken naar: de mate van fibrose (bindweefsel vorming) (**hoofdstuk 2-5**), de mate van hartspiercel hypertrofie (vergroting) (**hoofdstuk 4 en 5**) en de mate van vascularisatie (bloedvatvorming) van de RV (**hoofdstuk 6 en 7**).

De overbelasting in de rechter hartkamer van patiënten met TF, wordt o.a. gecompenseerd door een toename van de concentratie van de fibrose markers collageen en fibronectine. In **hoofdstuk 2** worden deze aanpassingen microscopisch bestudeerd na (immuno)histologische aankleuring van deze markers in de hartspierweefsel-preparaten van de RV van TF-1 en TF-2 patiënten en vergeleken met preparaten van patiënten die een "pulmonary autograft root replacement" (PAG) hebben ondergaan. Hieruit kwam naar voren dat er een verhoogde mate van fibrose plaats vind met name in de intercellulaire ruimte en rond de bloedvaten.

Door gebruik te maken van speciale beeldverwerkingsoftware kunnen de fibrose markers in gedigitaliseerde microscopische opnamen in de interstitiële ruimte en rond de bloedvaten, van de verschillende preparaten apart worden geanalyseerd. In **hoofdstuk 3** wordt hier nader op ingegaan. Hierbij kwam onder andere naar voren dat de groep van PAG-patiënten, die als controle werden gebruikt, geen normale morfologie had, ondanks een normale klinische RV functie. Net als de patiënten met TF hadden ze een verhoogde afzetting van de fibrose markers in de extra-cellulaire matrix (ECM). De patiënten met TF bleken een hogere concentratie interstitiële collagenen te hebben maar een minder peri-vasculaire collageen. Tegelijkertijd hadden ze een lagere concentratie interstitiële fibronectine en meer peri-vasculair fibronectine.

In een de studie, beschreven in **hoofdstuk 4**, worden naast de beeldanalyse van totaal collageen en fibronectine ook de veranderingen in de hoeveelheid collageen subtypen I en III bepaalt. Daarnaast zijn ook de expressie patronen van deze fibrose markers op mRNA niveau geanalyseerd met behulp van DNA micro-array hybridisatie experimenten. Met behulp van de beeldanalyse werd er een significante toename van de fibrose markers totaal collageen, collageen subtype I en III en fibronectine in zowel de interstitiële ruimte als rond de bloedvaten waargenomen bij zowel TF-1 als TF-2 patiënten, ten opzichte van de controle groep. Deze toename wordt bevestigd door de bevindingen dat de genen die coderen voor extracellulaire matrix eiwitten in TF-1 patiënten zijn opgereguleerd. Het gen-expressie profiel laat verder zien dat de genen die coderen voor eiwitten die de ECM homeostase reguleren, de fibrose te ondersteunen. Verder bleek de mate van hypertrofie van de hartspiercellen in de RV van patiënten met TF te zijn toegenomen en in het eerste levensjaar gecorreleerd te zijn met de leeftijd.

In TF kan de obstructie van de RV ook compleet zijn. Er is een groep patiënten met pulmonales atresia in combinatie met een VSD. In **hoofdstuk 5** blijkt dat de fibrose in deze patiënten samen gaat met hypertrofie van de hartspiercellen, maar in mindere mate in vergelijking met andere TF patiënten. Daarnaast is er microscopisch een afname in de collageen ondersteuning van de bloedvaten in vergelijking met de controle groep waar te nemen, ondanks een verhoogde expressie collageen III (op mRNA niveau).

De remodelering van het hart gaat ook gepaard met een verhoogde aanmaak van bloedvaten om in de zuurstof behoefte van de RV te blijven voorzien. In **hoofdstuk 6 en 7** wordt de mate van angiogenese in patiënten met TF bestudeerd, door de aanmaak van groeifactoren die aanzetten tot vascularisatie van het hart (o.a. VEGF) en de bloedvat-dichtheid te bepalen. Uit het gen-expressie profiel, bepaald met behulp van DNA-micro-array hybridisatie analyse, bleek duidelijk het dat de genen die betrokken zijn bij de vorming van bloedvaatjes een verhoogde gen-expressie vertoonde. Verder onderzoek wees uit dat de verhoogde VEGF expressie in de RV van patiënten met TF resulterende in een toegenomen bloedvatdichtheid van de rechter hartkamer met voornamelijk kleine bloedvaatjes, zonder dat er spraken is van bloedvat remodelering.

In **hoofdstuk 8** worden de resultaten zoals beschreven in dit proefschrift in een algemene discussie geëvalueerd en worden er aanbevelingen gedaan voor vervolg onderzoek.

Dankwoord

Aan het eind gekomen van dit proefschrift kom ik aan bij één van de meest gelezen pagina's. Waar de inhoud van de voorgaande bladzijden voor sommigen een aanvulling op hun kennis zal zijn, zal dit voor anderen altijd een ondoorgrondelijke materie blijven. Maar ik hoop dat we met dit onderzoek naar tetralogie van Fallot weer een stukje in de goede richting zijn opgeschoven met als uiteindelijk doel de patiënten beter te kunnen behandelen.

Gelukkig doe je zo'n onderzoek niet alleen. Veel mensen van zowel binnen als buiten de universitaire wereld hebben mij hierbij geholpen. Ik wil hen allen hiervoor bedanken. Maar enkele mensen die het nemen van de hobbels de afgelopen jaren van dichtbij hebben meegemaakt wil ik toch graag met name noemen.

Als eerste wil ik de twee drijvende krachten achter het TF-project, Prof. dr. A. Bogers en Dr. H. Sharma, bedanken voor het feit dat ik ondanks mijn afwezigheid op het eerste sollicitatiegesprek toch als AIO ben aangenomen bij de vakgroepen Farmacologie en Thoraxchirurgie.
Hari, als mijn dagelijkse begeleider en co-promotor, zijn we samen over pieken en door dalen gegaan. Ik wil je bedanken voor alle raad en ondersteuning, leuke congresbezoeken, je gedrevenheid en de vele uren die je in het onderzoek stak (Hari, *Dhanyavad*).
Ad, als promotor en mede-initiator van het project wil ik ook jou bedanken voor de prettige samenwerking, voor je kritische kijk, je onaflatende steun en de tijd die je voor mij, ondanks je drukke werkzaamheden, toch steeds weer vrij wist te maken.
Daarnaast kon ik ook altijd bij mijn tweede promotor, Prof. dr. Saxena, terecht. Pramod, ik wil je bedanken voor de getoonde interesse (ook al stond mijn promotieonderwerp ver van de farmacologie af), de wetenschappelijke discussies en niet te vergeten het wijzen op de tijdsplanningen.

Terugkijkend op de leuke momenten van mijn promotie kom ik ook zeker bij mijn kamergenoten terecht. Emine, jij was nauw bij mijn onderzoek betrokken en hebt er bergen werk voor verzet. Helaas was je er niet tot het einde bij maar mijn dank voor de leuke samenwerking is er niet minder om. Ik wens je het beste voor de toekomst!

Sue, schip ahoi! Het wordt weer drukker in de haven der promovendi. Bedankt voor de leuke tijd, opbeurende verhalen en alle hulp op het lab. De *didi's* Marieke, Mechteld en Inge wil ik niet alleen bedanken voor de leuke tijd op de afdeling, maar ook voor de zeer geslaagde reis naar het dak van de wereld. Maar ook met Marion, Wenxia en Wendy was het uitstekend op één kamer, op "grote hoogte" boven Rotterdam, uit te houden. Jullie allen bedankt voor alle hulp, vriendschap, de gezellige momenten binnen en buiten de afdeling en natuurlijk de vele kilo's snoep.

Edwin (Eddyman), Andor en Mark wil ik bedanken voor de ontspannende uurtjes buiten werktijd. Maar ook mijn mede (CMBL) lab-genoten; Pankaj, Anna, Vijay, Suneet, Joy, Oka en Sherif en de andere medewerkers van *De Farma;* Uday, Jan H, Martin, Ingrid, Jasper, Richard, Peter, Beril, Antoinette, Saurabh, Ria, Roeland, Magda, Rémon, Kapil, Larissa, Toos, Jeanette, Aloys, René, Wiro, Birgitte, Regien, Corné, Freek, Jan D, Carlos en alle studenten wil ik bedanken voor de interesse, de adviezen, de thee- en koffie-pauzes in de bibliotheek zonder boeken, de gezellige (evaluerende) lunches, (de FECO) voor de zeer geslaagde labuitjes en de terrasbezoeken (meestal) na werktijd. And for all of you who are still learning Dutch, many thanks for the nice time in- and outside the department.

"Mijn" studenten Chantal en Lennart mogen ook zeker niet in dit dankwoord ontbreken. Ik wil jullie bedanken voor de prettige samenwerking en jullie bijdrage aan dit proefschrift (en de ontdekkingstocht door Canada). Inmiddels zijn jullie artsen, maar ik hoop dat jullie nog niet helemaal van het onderzoeksvirus genezen zijn.

Buiten mijn standplaats bij de vakgroep Farmacologie hebben er ook verschillende mensen bijgedragen aan de voortgang van mijn onderzoek. Zo hebben de secretaresses van de afdeling Thoraxchirurgie, Saskia, Petra en Simone er voor gezorgd dat de coördinatie tussen de twee locaties prima verliep en wij allen tijdig werden opgetrommeld voor de werkbesprekingen. Ik zou geen resultaten hebben gehad zonder het humane materiaal dat me ter beschikking werd gesteld door de medewerkers van de Thorax-OK, de Hartkleppenbank en Dr. R. de Krijger. Jullie hebben mij allen geholpen bij het verkrijgen van de juiste (controle) biopten. Deze biopten werden verder "geprocessed" in het Cytologisch lab van de afdeling Pathologie die mij ook regelmatig van advies voorzag. Daarnaast was Alex Nigg mij altijd behulpzaam bij het ontwikkelen van de juiste beeldanalyse-programmatuur die

ik kon gebruiken na de dagenlange opnamens achter de microscoop bij de afdeling Longziekte. Ik wil jullie allen bedanken voor de ondersteuning en prettige samenwerking.

Naast de praktische ondersteuning hebben anderen mij met hun vakkennis bijgestaan. Hiervoor gaat mijn dank uit naar Rolf Berger en Peter de Jong voor hun bijdragen in de discussies en het tot stand komen van het "PA-VSD" onderzoek, Walter Mooi voor het beoordelen van de biopten en Adriana Gittenberger de Groot, Rob Poelmann en Margo Bartelings die altijd bereid waren hun licht te laten schijnen op mijn experimenten en bevindingen.

Het leven van een AIO speelt zich niet alleen af op de universiteit. Daarom wil ik ook mijn familie en vrienden bedanken voor alle interesse en het aanhoren van m'n klaagzangen als het (weer) eens fout ging. Zij hebben mij de afgelopen jaren af en toe eens van het werk vandaan getrokken, mee naar een feestje of een gezellig weekendje weg zodat ik weer met frisse moed verder kon.

De bewoners van *het Boezemhuis* wil ik ook in mijn dankwoord betrekken. Jullie hebben mijn verblijf in Rotterdam zeker veraangenaamd. Bedankt daarvoor. Veel succes in het afronden van jullie studies en op naar glansrijke carrières.

Conny, Dirk, Saskia en Rodolfo, bedankt voor de belangstelling en voor al het geduld dat jullie voor me hebben gehad. Dat het promotieonderzoek niet altijd even gemakkelijk ging hadden jullie al snel door maar toch hebben jullie me altijd gesteund.

En natuurlijk "*ons Pap en ons Mam*". Bedankt dat jullie me altijd hebben gesteund en gestimuleerd om die dingen te doen die ik leuk vond. De deur in Sambeek stond altijd voor me open. Bedankt voor alles!

Rotterdam, november 2003.

Curriculum vitae

Erik (Theodorus Henderikus Fransiscus) Peters, werd op 29 januari 1969 geboren te Sambeek waar hij tevens zijn hele jeugd doorbracht. Na het behalen van het MAVO en HAVO-diploma op de Scholengemeenschap Stevensbeek te Stevensbeek en zijn VWO-diploma aan het Elzendaal College te Boxmeer ging hij in 1989 Moleculaire Wetenschappen studeren aan de Landbouw Universiteit te Wageningen. Daar oriënteerde hij zich op het dierlijke (cel) biotechnologie profiel. Na zijn afstudeer-onderzoeken bij de sectie Moleculaire Cel Genetica (vakgroep Erfelijkheidsleer) onder de dagelijkse begeleiding van Dr. M. Schalk en Prof. dr. C. Heyting en bij de sectie Celbiologie en Immunologie (vakgroep Experimentele diermorfologie en celbiologie) onder supervisie van Dr. M.J. van Lierop en Dr. R. Stet, mocht hij in juni 1996 zijn ingenieursdiploma in ontvangst nemen. Een half jaar later begon hij in maart 1997 aan zijn promotie-onderzoek bij de vakgroepen Cardiothoracale Chirurgie en Farmacologie aan de Erasmus MC, te Rotterdam, onder begeleiding van promotoren Prof. dr. A.J.J.C. Bogers en Prof. dr. P.R. Saxena en co-promotor Dr. H.S. Sharma. Het door de Nederlandse Hartstichting gefinancierde onderzoek richtte zich op de "*Molecular phenotype of right ventricular hypertrophy in patients with tetralogy of Fallot*". De resultaten van dat onderzoek zijn vast gelegd in dit proefschrift.

Publications

Full papers:

Schalk JAC, Offenberg HH, Peters E, Groot NPB, Hoovers JMN and Heyting C. Isolation and characterization of the human SCP2 cDNA and chromosomal localization of the gene. *Mamm Genome* 1999; 642-644.

Peters THF, Sharma HS, Yilmaz E and Bogers AJJC. Quantitative analysis of collagens and fibronectin expression in human right ventricular hypertrophy. *Ann N Y Acad Sci* 1999; 874: 278-285.

Opgaard OS, Adner M, Peters THF, Xu CB, Stavenow L, Gulbenkian S, Erlinge D, Edvinsson L and Sharma HS. Endocardial expression and functional characterization of endothelin-1. *Mol Cell Biochem* 2001; 224: 151-158.

Klompe L, Peters THF, de Jong PL, Sharma HS and Bogers AJJC. Myocardial characteristics in patients with pulmonary atresia and ventricular septal defect. *Thoraxcenter J* 2002; 14:2, 33-36.

Peters THF, Sharma HS and Bogers AJJC. Computerized image analysis in the quantitative assessment of interstitial fibrosis late after correction of tetralogy of Fallot. *Cardiovasc Eng* 2003; 8: 114-120.

Peters THF, de Jong PL, Klompe L, Saxena PR, Berger RMF, Sharma HS and Bogers AJJC. Right ventricular collagen and fibronectin levels in patients with pulmonary atresia and ventricular septum defect. *Mol Cell Biochem 2003; 251: 27-32*.

Peters THF, Sharma HS, Yilmaz E, Saxena PR, and Bogers AJJC. DNA micro-array and quantitative analysis reveal up-regulation of genes encoding extracellular matrix proteins in patients with tetralogy of Fallot. (*Submitted*).

Peters THF, Bogers AJJC, Saxena PR and Sharma HS. Right ventricular hypertrophy in human tetralogy of Fallot is associated with enhanced vascularization and expression of vascular endothelial growth factor. (*Submitted*).

Chapters:

Bogers AJJC, Peters THF, Hokken RB, Saxena PR and Sharma HS. Myocardial phenotype of right ventricular hypertrophy in human tetralogy of Fallot. In: Imai Y, Momma K. eds*: Proceedings of 2nd World Congress of PCCS* 1998; 746-749: Futura, Armonk, New York, USA (ISBN: 0879936991).

Peters THF, Sharma HS, Yilmaz E, Saxena PR and Bogers AJJC. Quantitative evaluation of interstitial fibrosis in patients with tetralogy of Fallot. In: Bogers AJJC, Bartelings MM. Eds.: *The Rotterdam-Leiden seminars on cardiovascular anatomy and tetralogy 1997/1998/1999,* 1999: 53-58, Erasmus University Rotterdam, Rotterdam.

Bogers AJJC, Peters THF and Jong de PL. Tetralogy of Fallot, surgical aspects. In: Bartelings MM, Wenink ACG eds: *Congential Heart Disease.* Boerhaave Committee for Postgraduate Medical Education. 1999; 59-65: Leiden (ISBN 90-6767-411-7).

Sharma HS, Peters THF and Bogers AJJC. Angiogenesis and fibrosis during right ventricular hypertrophy in human tetralogy of Fallot. In: Takeda N, Nagano M, Dhalla NS eds: *The hypertrophied heart*. 2000; 227-241, Kluwer Academic Publishers, Boston, USA (ISBN: 0-7923-7741-9).

Peters THF, Klompe L, Bogers AJJC and Sharma HS. Molecular phenotype of the developing heart with a congenital anomaly. In: Ostadal B, Nagano M and Dhalla NS eds.: *Cardiac Development* 2002; 195-212: Kluwer Academic Publishers, Boston, USA (ISBN 1-40207-052-7).

Abstracts:

Sharma, HS, Peters THF, Yilmaz E, Hokken RB and Bogers AJJC. Right ventricular hypertrophy in human tetralogy of Fallot is associated with increased myocardial fibrosis and vascularization. *Circulation* 1997; 96 (8): I.17-18.

Peters THF, Sharma HS, Yilmaz E and Bogers AJJC. Quantitative analysis of collagens and fibronectin expression in human right ventricular hypertrophy. *Pathophysiol* 1998; 5 (1): 5.

Sharma HS, Yoshida T, Maulink G, Peters THF and Dipack K. Increased myocardial tolarance to ischemia-reperfusion injury in coenzyme Q_{10}-fed pigs is associated with induced expression of heme oxygenase-1 and ubiquitin. *Pathophysiol* 1998; 5 (1): 5.

Peters THF, Sharma HS, Yilmaz E, Saxena PR and Bogers AJJC. Right ventricular hypertrophy in human tetralogy of Fallot is accompanied with the expression of fibrosis markers. *Fundam Clin Pharmacol* 2000; 14: 54.

De Jong PL, Peters THF, Klompe L, Sharma HS and Bogers AJJC. No difference in right ventricular myocardial fibrosis at correction of PA-VSD with or without SPCAs. *Cardiol Young* 2001; 11 (3) supl. 1: 385.

Peters THF, Sharma HS, Saxena PR and Bogers AJJC. Right ventricular fibrosis and apoptosis in patients with tetralogie of Fallot. *J Mol Cell Card* 2001; 33, (6) A93.

Klompe L, Peters THF, de Jong PL, Bogers AJJC and Sharma HS. Myocardial collagen and fibronectin levels in patients with pulmonary atresia and ventricular septal defect. *J Mol Cell Card* 2001; 33 (6) A60.

Sharma HS, Peters THF and Bogers AJJC. Right Ventricular failure in human tetralogy of Fallot: micro-array and expression analysis. *J Mol Cell Card* 2002; 34 (6) A89.

Peters THF, Bogers AJJC, Saxena PR and Sharma HS. DNA micro-array and quantitative analysis revealed upregulation of genes encoding extracellular matrix proteins in patients with tetralogie of Fallot. *Circulation* 2002; 106 (19): II-450.

Sharma HS, Peters THF and Bogers AJJC. DNA micro-array and quantitative expression analysis of genes involved in human right ventricular hypertrophy. *J Mol Cell Card* 2003; 35 (6) A53.

Sharma HS, Peters THF, Verdouw PD and Bogers AJJC. Genetic reprogramming during ischemia/reperfusion induced myocardial cytoprotection. *Exp Clin Cardiol* 2003; 8 (1) A49.